Agonist-Selective Signaling and MOR

A DISSERTATION
SUBMITTED TO THE FACULTY OF THE GRADUATE SCHOOL
OF THE UNIVERSITY OF MINNESOTA
BY

HUI ZHENG

IN PARTIAL FULFILLMENT OF THE REQUIREMENTS
FOR THE DEGREE OF

DOCTOR OF PHILOSOPHY

Dr. PING-YEE LAW, Advisor

DECEMBER, 2009

Acknowledgements

This thesis presents the results of my four-year studies whereby I have been accompanied and supported by many people.

I would like to acknowledge the guidance of my supervisor, Dr. Ping-Yee Law. I would also like to thank the other members of my Ph.D committee who took effort in reading the reports of my works and providing me valuable comments: Dr. Timothy F. Walseth (chair), Dr. Esam EL-Fakahany, Dr. Jonathan Marchant, and Dr. Yan Zeng. I would like also to thank Dr. Horace H. Loh for his advise and leadership.

I would like also to thank the researchers in the laboratory of Dr. Horace H. Loh and Dr. Ping-Yee, especially Ji Chu, Xiaohong Guo, Vida Gavino, Yongjiao Zhai and Yuhan Zhang. Without their help, I would not have been able to accomplish all the things that I did.

Finally, I would like to thank my parents, Qixiang Zheng and Hui Su.

Dedication

This work is dedicated to the human being's suffered from the tolerance and addiction of opioids. With the understanding of the functional mechanisms of opioids, I hope human beings will never experience this kind of torture any more in the near future.

Abstract

Opioids are potent analgesics, but their application is limited by the development of tolerance (the increase in doses required to achieve the same effect) after chronic or repetitive usage. Because tolerance developed much more easily for the analgesia effect than for side effects (e.g. respiration depression), it is difficult to be overcome by simply increasing the doses of opioids. On the other hand, the identification of opioid receptors and endogenous agonists suggests the involvement of opioid pathways in the central nervous system. Thus exploring the mechanisms of tolerance development has been the focus of a vast number of laboratories for decades.

Several hypotheses on tolerance development have been proposed. For example, because of the correlation between receptor internalization and tolerance development, receptor internalization has been considered as an inhibitor of tolerance. In addition, the involvement of δ-opioid receptor preproenkephalin, Ca^{2+}/calmodulin-dependent protein kinase II, Protein Kinase C and β-arrestin2 has been suggested by knockout experiments. However, there is no universal explanation for tolerance development.

The long-term goal of my studies is to understand the mechanism of tolerance development. Taking advantage of the observations that opioids have different abilities to induced tolerance and signaling events, I have proposed is that agonists induce different levels of tolerance by inducing different signaling events (agonist-selective signaling). Because of the inconsistency between the time courses of signaling cascades (usually seconds to hours) and the tolerance development (usually hours to days), It is suggested

that the agonist-selective regulation on gene expression transduces the signals from the agonist-selective signaling to agonist-selective tolerance development.

Hence, in my studies, the different abilities of agonists to initiate signaling events (ERK phosphorylation, receptor desensitization on intracellular calcium release) were compared. Then several determinants (receptor phosphorylation, cholesterol-rich lipid raft microdomain, receptor palmitoylation) for the agonist-selective signaling were identified. The final portion of my studies is to explore how agonist-selective regulation on gene expression (NeuroD and miR-190) results from the agonist-selective signaling and to determine whether the agonist-selective regulation on gene expression can contribute to the different levels of tolerance induced by agonists.

Table of Contents

List of Figures

List of Tables

Abbreviation

2-BP: 2-bromopalmitate

3A: mutant of MOR (S363A, T370A and S375A)

90RSK: 90 kD ribosomal S6 kinase

btn-BMCC: 1-biotinamido-4-[4′-(maleimidomethyl) cyclohexane carboxamido] butane

CaMK: Ca^{2+}/calmodulin-dependent protein kinase

ChIP: chromatin immunoprecipitation

CREB: cAMP response element binding protein

CT-B: cholera toxin subunit B

CTOP: D-Pen-Cys-Tyr-D-Trp-Orn-Thr-Pen-Thr-NH_2

DAMGO: [D-Ala^2, *N*-Me-Phe^4, Gly^5-ol]-enkephalin

DOR: δ-opioid receptor

ERK: extracellular signal-regulated Kinase

HEK: human embryonic kidney

HEKC170A: HEK cells stably expressing HA tagged MOR with C170A mutation

HEKC346A: HEK cells stably expressing HA tagged MOR with C346A mutation

HEKC351A: HEK cells stably expressing HA tagged MOR with C351A mutation

HEKHM: HEK cells stably expressing HA tagged MOR

I35: mutant of MOR (lacking the last five amino acid of the third intracellular loop)

ICaR: intracellular calcium release

GIRK: G protein-coupled inwardly rectifying potassium channel

GPCR: G protein coupled receptor

GRK: G protein-coupled receptor kinase

HMG-CoA: 3-hydroxy-3-methylglutaryl CoA

KOR: κ-opioid receptor

MβCD: methyl-β-cyclodextran

MEF: mouse embryonic fibroblast

MEK: mitogen-activated protein kinase

miRNA: microRNA

MOR: μ-opioid receptor

N2A: neuroblastoma neuro2A

NEM: N-ethylmaleimide

NeuroD: neurogenic differentiation 1

ORL1: opioid receptor-like 1

pAAs: phosphorylated amino acids

PKA: Protein Kinase A

PKC: Protein kinase C

pS^{375}: phosphorylated Ser^{375} of MOR

PTX: pertussis toxin

TIPPψ: H-Tyr-Ticψ[CH2NH]-Phe-Phe –OH

TR: transferring receptor

UTR: untranslated region

YY1: Yin Yang 1

1. Introduction

1.1 G protein coupled receptor (GPCR)

G protein coupled receptors (GPCRs) are a large family of membrane receptor with seven trans-membrane domains. They respond to a diverse array of sensory and chemical stimuli, such as light, odor, taste, hormones, and neurotransmitters, and play critical role in a variety of physiological processes (1, 2). They represent more than fifty percent targets of market drugs. The signaling mechanisms of GPCRs, therefore, are subjects of interests in cellular and molecular research and the development of new drugs. GPCR transduces the signal from outside the cell to intracellular second messengers, and then to downstream effectors. This process involves the coupling between agonist-GPCR complex to the heterotrimeric guanine nucleotide binding protein (G protein) (1, 3). The binding of agonist promotes the exchange of GDP for GTP on the G protein α-subunit and leads to the dissociation of the G protein Gα- and Gβγ subunits. Subsequently, the activated subunits of G protein positively and/or negatively regulate the activity of effecter enzymes and ion channels (3, 4). GPCR signaling is affected by various factors in addition to the G proteins. For example, β-arrestin influences the signaling by uncoupling the G protein from GPCR complex (5). The internalization of receptor also influences GPCR signaling by two means. It decreases the availability of GPCR on cell membrane and also enables GPCR to recycle to cell membrane after being processed in intracellular vesicles (1, 6). Factors that affect receptor internalization, e.g. dynamin (7), Src Kinase (7), arrestin (8) and adaptor protein 2 (9), influence the signaling of GPCR. In addition, the agonist-induced desensitization (10-12) and changes in gene expression (13-15) modulate GPCR signaling.

1.2 Opioids

Opioids have been considered as the most potent analgesics in clinic. Morphine is one of the opioids and has been used for thousand years. After the purification of morphine, functional mechanisms of opioids, especially morphine, has been studied in depth. In addition, the purification of morphine has enabled and extended the usage of

morphine in modern medical care. Due to its outstanding analgesic effects and serious unwanted side effects (e.g. respiratory suppression), morphine-like molecules have been synthesized and studied. Currently, the opioids are divided into several categories include alkaloids, synthetic opioids and endogenous opioids depending on their molecular structures. Usually, alkaloid opioids are the natural opioids or their derivatives, such as morphine, heroin or etorphine. Synthetic opioids include [D-Ala^2, *N*-Me-Phe^4, Gly^5-ol]-enkephalin (DAMGO) and fentanyl. Endogenous opioid peptides include enkephalins, β-endorphine and dynorphine (16). Although opioids have different molecular structures, they bind to the opioid receptors and execute their functions through opioid receptor-activated G-proteins.

1.3 Opioid receptors

The discovery of opioid receptors greatly advances the understanding of opioids (17-20). There are three subtypes of opioid receptors: mu (μ)-opioid receptor (MOR), delta (δ)-opioid receptor (DOR) and kappa (κ)-opioid receptor (KOR) (21-28). As reviewed (29, 30), these opioid receptors have a putative structure of seven transmembrane domains, extracellular N-terminus with multiple glycosylation sites, third intracellular loop with multiple α-helixes, and fourth intracellular loop formed by putative palmitoylation sites at the carboxyl tail (21, 24-27). The three subtypes are about 60% identical, with the greatest identity found in the seven transmembrane domains (73–76%) and intracellular loops (86–100%). The greatest divergent areas were found in the N terminus (9–10%), extracellular loops (14–72%), and C terminus (14–20%) (25). In addition, there are two other receptors suggested to be related to opioid receptors. One of them is sigma (σ)-receptor (31, 32). However, because of the inability of σ-receptor to be activated by endogenous opioid peptides and its structural difference from other opioid receptors, it is not classified as an opioid receptor (31). Several groups also isolated a cDNA that encoding an opioid receptor-liked protein (33-39). This GPCR protein was named as opioid receptor-like 1(ORL1). ORL1 is involved in opioid analgesic, opioid dependence and tolerance development (40-46).

1.4 Opioid receptor functions

Studies using subtype-selective agonists/antagonists and opioid receptor subtype knockout mice revealed that opioids induce analgesia effects primarily through MOR (47-49). MOR also mediates the majority of opioid functions, including hyperlocomotion, respiratory depression, constipation, immuno-suppression and opioid reward/withdrawal (47-49). DOR is suggested to be essential for the development of morphine tolerance (50-52) and to contribute to the emotional and rewarding responses (53, 54). In contrast, KOR is shown not to be involved in the analgesia effect; however, it participates in withdrawal symptoms after morphine and antagonist treatment (55-57), opioid-mediated dysphoria effect (57) and stress-induced emotional response (58).

Opioid receptor-mediated signaling can be abolished by pertussis toxin (PTX) pre-treatment, indicating that opioid receptors couple to the Gi/Go α subunits, which are PTX sensitive (59, 60), even through MOR can associate with a PTX-insensitive G protein Gz to execute its analgesia function both *in vivo* and *in vitro* (61-64). For *in vitro* signaling transduction, all three subtypes of opioid receptors initiate similar spectra of downstream signaling events, which include regulation of adenylyl cyclase, the N-type (65) and L-type (66, 67) Ca^{2+} channels, phospholipase C (36), inward rectifying K^{+} channels (68, 69), and extracellular signal-regulated kinase (ERK) (70, 71). Recently, Src family nonreceptor tyrosine kinases have been implicated in GPCR functions (72-76); and all three major subtypes of opioid receptor have been reported to activate Src kinase(77-79). Although the exactly mechanism of Src kinase activation by opioid receptors is still under investigation, Src kinase activation has been strongly suggested to contribute to MOR-mediated adenylyl cyclase super-activation *in vitro* (78), which is the molecular model for morphine withdrawal *in vivo* (80-82).

1.5 MOR

MOR contains four exons (83, 84). The first three exons encode the N-terminus and the seven transmembrane domains, with the fourth corresponding to the intracellular carboxyl-terminus of the receptor. Similar to other GPCRs, MOR undergoes alternative splicing downstream of exon 3 (83-86). In MOR-1A, exon 4 is absent and there are four additional amino acids encoded at the end of exon 3. Five other variants identified in the mouse have different combinations of exon 5-10 replacing exon 4 (87). All of these variants contain exons 1, 2 and 3 and have the predicted amino acid sequences identical to MOR-1 through the transmembrane regions, differing only at the intracellular carboxyl tail. The variants also display distinct regional distributions within the central nervous system, indicating possible differences in their functions. Without studying mice which deficient in expressing individual variants, the functions of different variants are difficult to be predicted. However, MOR-1 has been suggested to be the major variant that mediates the functions of morphine. And many studies on MOR have been focused on MOR-1. Thus, in the current projects, MOR-1 was studied and referred to "MOR".

2. Agonist-selective signaling

2.1 Agonist-selective signaling through GPCR

Agonist-selective signaling is an emerging theory used to interpret GPCR signaling The reports on the agonist-selective signaling have been published with many GPCRs and the volume of literature is increasing.

2.1.1 The “intrinsic efficacy” concept

GPCRs transduce signals via a variety of signaling pathways, and each GPCR has multiple agonists. To understand the relation between agonists and signaling pathways activation under one particular GPCR, scientists have tried to categorize both agonists and signaling pathways. The “intrinsic efficacy” concept is a hypothesis that has been used for decades (88). According to this concept, signaling pathways under a single GPCR are similar to each other. On the other hand, there are two important properties of an agonist, the affinity to interact with the receptor (potency) and the ability to activate the receptor (intrinsic efficacy). Because low potency can be overcome by using higher concentration of the agonist, intrinsic efficacy has been used to categorize agonists. Intrinsic efficacy is defined as the maximum activation of receptor that can be induced by an agonist. Depending on the intrinsic efficacies, agonists have been divided into full agonists (inducing 100% activation of the receptor), partial agonists (inducing receptor activation but less than 100%), neutral antagonists (antagonist which binds, but do not activate, receptor) and inverse agonists (decreasing the activation of receptor to the level below basal level) (89). This concept does not highlight the differences among signaling pathways and suggests that one agonist activates all the signaling pathways under one particular receptor similarly, and that the agonists activate signaling pathways depending on their intrinsic efficacies.

However, as reviewed by Urban et. al., the insufficiency of the “intrinsic efficacy” concept has been noted in recent years (90). Agonist can activate signaling pathways differentially, which has been observed with various GPCRs, including 5-HT_2 serotonin

receptors, adrenergic receptors, dopamine receptors and opioid receptors. The observations are summarized and abstracted in Fig. 2-1. Agonist I and agonist II activate the same receptor, which transduces the signal to two pathways, pathway A and pathway B. But Agonist I can be a full agonist on pathway A, yet a neutral antagonist on pathway B. Agonist II can be just the opposite: full agonist on pathway B, while neutral antagonist on pathway A. Here lies the major shortcoming of "intrinsic efficacy" concept: agonists can activate signaling pathways differentially. Therefore the "intrinsic efficacy" concept which suggests an agonist have the same efficacy on different signaling pathways can not be applied in these cases. An agonist-selective signaling (ligand-biased signaling or others) theory has been proposed to interpret the signaling of GPCRs.

2.1.2 "Agonist-selective signaling" theory

The biggest difference between the "agonist-selective signaling" theory and the "intrinsic efficacy" concept is on categorizing the signaling pathways. The "agonist-selective signaling" theory suggests there are large differences among the activation of the signaling pathways, even though the activation of some signaling pathways are similar. Thus the activation of signaling pathway is not only dependent on the potency and intrinsic efficacy, but also dependent on which signaling pathway is involved. The "agonist-selective signaling" theory does not categorize signaling pathways, but analyzes them individually.

As indicated in Fig.2-2, the "intrinsic efficacy" concept tries to correlate agonists to all the signaling pathways. The "agonist-selective signaling" theory tries to correlate agonists to individual signaling pathways. To distinguish the agonist-selective signaling theory from the "intrinsic efficacy" concept, the "ability" of agonist was used rather than its "efficacy" hereafter.

Fig. 2-1 Schematic of agonist-selective signaling

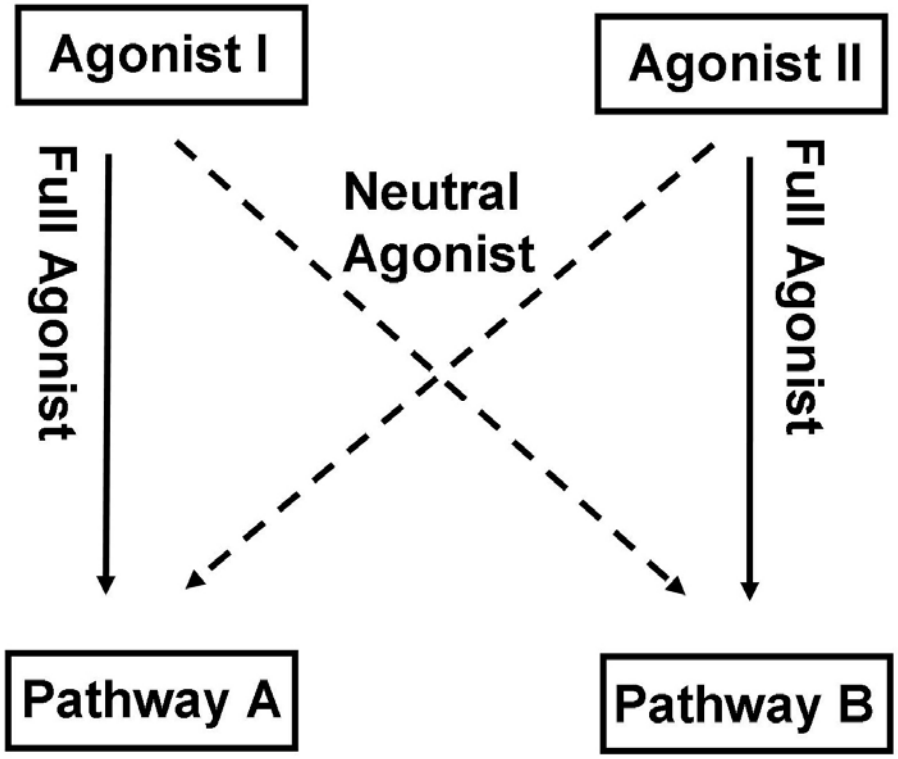

Fig. 2-1 Schematic of agonist-selective signaling

Agonist I is a full agonist on Pathway A, while a neutral agonist (antagonist) on Pathway B. In contrast, agonist II is a full agonist on Pathway B, while a neutral agonist (antagonist) on Pathway A. Although the abstracted schematic can not present all conditions of agonist-selective signaling, it indicates the pathway selection of agonists.

Fig. 2-2 Schematic comparison of the two hypotheses

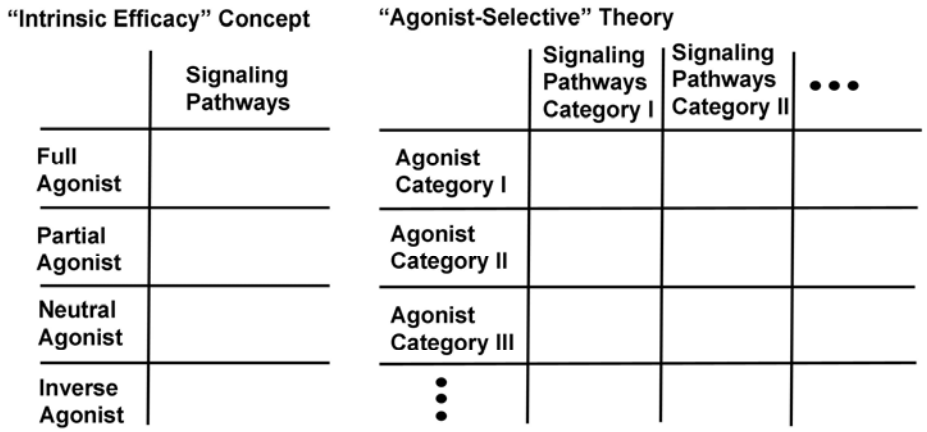

Fig. 2-2 Schematic comparison of the two hypotheses

The “Intrinsic Efficacy” concept categorizes the agonists but not the signaling pathways, and suggests a multiple-to one correlation. The “Agonist-selective” theory categorizes both the agonists and the signaling pathways, and suggests a multiple-to multiple correlations.

In addition, there is "receptor trafficking" theory has been suggested (89, 91), which suggests that different conformation changes induced by agonists can lead to the activation of distinct G proteins. This theory also attributes the differential signaling induced by agonists to which level of the signaling events locates in the signaling cascade. Although, this theory is not accurate under many conditions, it has implications on the developing of agonist-selective signaling theory.

2.1.3 Agonist-selective ERK phosphorylation

ERK phosphorylation may be the best-studied phenomenon of agonist-selective signaling. Two pathways can be used by GPCRs to mediate ERK phosphorylation, the PKC/PKA pathway and β-arrestin pathway (5, 8, 92). The existence of the two pathways were demonstrated by blocking PKC/PKA activities with specific inhibitors and by downregulating β-arrestin with siRNAs (92, 93). The selectivity of agonists for the two pathways is indicated by the abilities of agonists to use the one or two pathways to induce ERK phosphorylation. For example, isoproterenol (a β-adrenergic receptor agonist) induces ERK phosphorylation via both pathways, while ICI118551 (a β_2-adrenergic receptor agonist) induces ERK phosphorylation in a β-arrestin-dependent manner completely and CCL19 uses only the PKC/PKA pathway in cells expressing the chemokine receptor CCR7 (11, 92, 94).

ERK phosphorylated by different pathways has different subcellular locations. Phosphorylated ERK under the PKC/PKA pathway is retained in the cytosol, while the phosphorylated ERK under β-arrestin pathway translocates into the nucleus. However, there are controversial observations on the influence of β-arrestin on the nucleus translocation of phosphorylated ERK. Overexpression of β-arrestin has been reported both to enhance and to suppress the nucleus translocation of phosphorylated ERK (95-98). The difference has been attributed to the different GPCRs used in the experiments. However, the ability of β-arrestin to serve as a scaffold protein to hold the mitogen-activated protein kinase (MEK) and ERK and its ability to translocate into the nucleus

and regulate gene expression support the positive effect of β-arrestin on the nucleus translocation of phosphorylated ERK (5, 13, 99).

2.1.4 Additional agonist-selective signaling events

GPCRs exhibit other agonist-selective phenomena. 5-HT_2 serotonin receptor mediates the formation of inositol phosphates via phospholipase C and the release of arachidonic acid through phospholipase A_2 (100, 101). Four signaling events (phospholipase C activation, phospholipase C desensitization, phospholipase A_2 activation and phospholipase A_2 desensitization) have been analyzed with a series of agonists of 5-HT_2 serotonin receptor (102, 103). No correlation among their abilities to initiate these four signaling events has been identified. Inositol phosphates influences the intracellular calcium level and thereby the activities of calmodulin and Ca^{2+}/calmodulin-depedent protein kinases (CaMKs). The accumulation of arachidonic acid has critical effects on the functions of ion channels (104, 105). Therefore, different agonists of 5-HT_2 serotonin receptor have different effects on these cellular responses. Similar observations are obtained with D_2–dopamine receptor. Quinpirole and propyldihydrexidine are full agonists when used to activate adenylyl cyclase. However they have different abilities to inhibit the D_2–dopamine receptor-mediated release of dopamine (106, 107). There are other observations on the agonist-selective signaling, but my studies are focused on MOR and ERK phosphorylation because of the long-term goal of my research.

2.1.5 Pathway selectivity of agonist-selective signaling

The signaling pathways mentioned above can be activated by agonists differentially. If the differences among agonists are large enough for one signaling pathway, a special phenomenon will be observed: only a selective group of agonists can activate this signaling pathway. Furthermore, if the differences are large enough on two signaling pathways, a group of agonists will activate only one signaling pathway, while another

group of agonists will activate only the other, which is similar to what abstracted in Fig. 2-1. Agonist I is a full agonist on pathway A, while a neutral antagonist on pathway B. Agonist II is just opposite: full agonist on pathway B, while neutral antagonist on pathway A.

Moreover, if the two signaling pathways are highly related to each other, selectivity of agonists for the two related pathways will be observed. Although the pathway selection is an extremely condition of the agonist-selective signaling, it has larger implications, because the selectivity between signaling pathways enables agonists to perform totally different tasks. In addition, by understanding the pathway selectivity of agonists, new drugs can be developed which selectively induce the curing effects but not the side effects.

Selection between signaling pathways has been observed with a number of GPCRs, especially manifested by ERK phosphorylation mediated by GPCRs. Many agonists of GPCRs induce ERK phosphorylation via only one of the two pathways, PKC and β-arrestin pathways (11, 92, 94). Although the two pathways lead to the ERK phosphorylation with similar efficacies, the cellular location of phosphorylated ERK and the activation of the downstream factors are different between the two signaling pathways (92, 93).

2.2 Agonist-selective signaling with MOR

2.2.1 Different abilities of agonists to initial signaling events

The agonists-selective signaling has been reported with MOR. Several signaling pathways can be activated by nearly all agonists of MOR, but to different extents. For instance, morphine has much lower abilities than other agonists, including etorphine, fentanyl and [D-Ala^2,N-Me-Phe^4,Gly^5-ol]-enkephalin (DAMGO) to induce receptor phosphorylation, β-arrestin recruitment and receptor internalization (108-110). MOR

undergoes both basal phosphorylation in the absence of agonist and agonist-induced phosphorylation. Although morphine induces receptor phosphorylation, the induction is small. The β-arrestin recruitment to the cell membrane is indicated by the punctated spots on the cell membrane after the transfection with EGFP tagged β-arrestin and agonist treatment. In HEK cells stably expressed MOR (HEKHM), etorphine decreases the membrane receptor by 40% after thirty-minute treatment, while morphine does not. Although the morphine-induced receptor internalization has been observed in the primary cultures from the striatum (111), the ability of morphine to induce receptor internalization is low. These differences had been explained by considering morphine as a partial agonist, while the others as full agonists.

MOR couples to the Gi/o and inhibits the activity of adenylyl cyclase. Thus the intracellular level of cAMP decreases after acute agonist treatment. However, the level of intracellular cAMP increases gradually and returns to the basal level during the chronic treatment of agonist. If antagonist is used to terminate the chronic treatment with agonist, the level of intracellular cAMP increases to a level much higher than the basal level within a short time, which is considered as adenylyl cyclase superactivation. Morphine induces higher superactivation than etorphine (112). Morphine also has higher ability to induce analgesia tolerance than etorphine and fentanyl, when the agonists are used at equivalent doses to treat the animal (113, 114). Thus morphine is a full agonist, while etorphine seems to be a partial agonist in these cases.

In addition, the similar abilities of morphine and other agonists, especially etorphine and fentanyl, to induce ERK phosphorylation and to inhibit adenylyl cyclase activity suggest that these agonists are all full agonists (112, 115).

The inconsistent results obtained after analyzing different signaling pathways suggest that the agonist-selective signaling theory is more suitable than “intrinsic efficacy” concept in interpreting the signaling of MOR. Hence, the classification of these opioid agonists indicates the strength of stimulus-response coupling (or the

interaction between agonist efficacy and system sensitivity) could not be used to address all the observations on these agonists' activities. Moreover, the cellular content could be used in address the divergent observations because some of these studies were carried out with the same cell model (112). Hence, agonist-selective signaling theory is more suitable in interpreting the observations on OPRM1 signaling.

2.2.2 Agonist-selective desensitization

Desensitization (decrease in the activation of signaling pathway during the agonist treatment) represents an important physiological feedback mechanism that prevents the over-stimulation of GPCR. Although receptor desensitization helps the cells to adapt to outside challenges rapidly, it also decreases the therapeutic effects of many GPCR agonists.

GPCR desensitization involves G protein-coupled receptor kinase (GRK) and β-arrestin (116-118). The GRK family includes seven GRK subtypes. Four of them are expressed throughout the body and are suggested to account for most of the GPCRs regulation (119). GRK is normally recruited to receptor by the activated and free Gβγ subunits and mediates the phosphorylation on receptor after agonist binding (120-122). GRK-mediated phosphorylation on MOR, DOR and KOR has been identified in both endogenous and exogenous gene expression systems (109, 123-127). Usually, the GRK phosphorylation sites locate in the third intracellular loop and the C-terminus of GPCR. A series Ser/Thr residues in MOR have been suggested to contribute to the receptor phosphorylation (128, 129). Among them, Ser^{375} has been shown to be consistently phosphorylated and to account for over 90% of morphine-induced MOR phosphorylation in HEK293 cells (130).

Using the β2-adrenergic receptor as the model, Lefkowitz's lab has proposed once phosphorylated by GRK, the activated receptor recruits β-arrestin (10, 11). Because of the Gα subunit (131) and β-arrestin (132-136) share similar binding sites on

MOR, the association between receptor complex and β-arrestin leads to the uncoupling of G protein from the receptor complex, which eventually dampens the signal transduction. This desensitization mechanism of GPCR has been demonstrated with various receptors such as β_2-adrenergic receptor, m_2-muscarinic receptors, dopamine D_{1A} receptor (137-139). Likewise, agonist-mediated phosphorylation of DOR has also been shown to lead to the β-arrestin recruitment and eventually the receptor desensitization (123, 140, 141).

MOR also undergoes intensively desensitization in its signaling pathways (112, 142). However, the involvement of β-arrestin and GRK in MOR desensitization is equivocal, especially in morphine-induced receptor desensitization. On the one hand, the critical roles played by β-arrestin2 in morphine-induced *in vivo* analgesia tolerance have been indicated by using β-arrestin2 null mice (143, 144). Also, the ability of morphine to induce tolerance *in vivo* is impeded in the GRK3 null mice (145). On the other hand, GFP-fused β-arrestin1 and β-arrestin2 are recruited to etorphine-activated MOR, but not morphine-activated MOR (146, 147). In addition, etorphine induces β-arrestin-mediated receptor internalization intensively, while nearly no receptor internalization is observed when morphine is used (108, 109). Therefore, morphine-induced receptor desensitization has complex mechanisms.

2.2.3 Agonist-selective desensitization on calcium release

Our lab has studied the agonist-induced desensitization on intracellular calcium release. MOR agonists, morphine and DAMGO do not evoke intracellular calcium release when used alone, whereas 200nM ADP, an agonist of the universally expressed Gq-coupled purinergic P2Y receptor, induces transient but robust intracellular calcium release. In addition, ADP-induced intracellular calcium release is significantly potentiated by morphine, while MOR antagonist, Naloxone, blocks this potentiation when it was used to pre-treat the HEKHM (148). Thus the potentiation on ADP-induced

Intracellular calcium release can be used an indicator of MOR activity. Decrease in the potentiation is considered as the desensitization.

Research into the desensitization on intracellular calcium release induced by morphine and DAMGO identified different pathways that mediate receptor desensitization. DAMGO-induced, but not morphine-induced, receptor desensitization is attenuated when phosphorylation deficient mutant of MOR or mouse embryonic fibroblast (MEF) cells from β-arrestin$^{-/-}$ mice are used. In contrast, morphine-induced, but not DAMGO-induced, receptor desensitization is attenuated when PKC inhibitor is used to treat the cells. Thus desensitization on intracellular calcium release mediated by MOR is also agonist-selective.

2.2.4 Agonist-selective desensitization on potassium channel

Similar observations were obtained when desensitization on G protein-coupled inwardly rectifying potassium channel (GIRK) current is studied. Both DAMGO and morphine activate GIRK currents, and the responses desensitize rapidly. Expression of a dominant negative mutant of GRK2, GRK2-K220R, attenuates the DAMGO-induced desensitization, but has no effect on the morphine-induced desensitization (142). In contrast, PKC inhibitor reduces MOR desensitization induced by morphine, but not that induced by DAMGO. Thus DAMGO-induced desensitization is GRK2-dependent, whereas morphine-induced desensitization is PKC-dependent.

2.3 MOR agonist-selective ERK phosphorylation

2.3.1 Agonists induce ERK phosphorylation similarly

To determine the characteristics of agonist-induced ERK phosphorylation, we examined the time courses of morphine- and etorphine-induced ERK phosphorylation in HEKHM cells. The phosphorylation of ERK peaked 10 min after the initiation of

morphine treatment. Then, the stimulatory effect gradually declined, and returned to the basal level after one-hour (Fig. 2-3). We obtained similar results when etorphine was used to activate MOR. The maximum phosphorylation level of ERK appeared 10 min after the initiation of etorphine incubation and returned to the basal level within 1 hr (Fig. 2-3). Because the maximal ERK phosphorylation after either morphine or etorphine treatment was observed at 10 min, the concentration-dependent studies were performed 10 min after the initiation of agonist treatment. Immunoblotting data showed that the EC50 values of the two agonists were significantly different from each other: 30±22 nM for morphine and 0.32±0.17 nM for etorphine, but the maximum levels of ERK phosphorylation induced by the two agonists were not significantly different from each other (Fig. 2-4).

2.3.2 Etorphine induces ERK phosphorylation via β-arrestin

The differential effects of β-arrestin on morphine- and etorphine-induced ERK phosphorylation were confirmed in three types of MEF cells: MEF cells from wildtype mice, β-arrestin2 null mice, and β-arrestin1/2 null mice. These MEF cells were infected with adenovirus containing the MOR encoding sequence so as to transiently express MOR. The amount of adenovirus used to infect the MEF cells was titrated to express similar levels of MOR in the three cell types. [^{3}H]-Diprenorphine binding assays revealed that the amount of MOR expressed in the three types of MEF cells was 0.5±0.1 pmol/mg of protein, without any significant difference among the three cell lines. In the wildtype MEF cells, 10 min incubation with either morphine or etorphine led to significant ERK phosphorylation (Fig. 2-5). In MEF cells from β-arrestin2 null mice, morphine induced significant ERK phosphorylation, but etorphine did not. However, because β-arrestin1 was present in these MEF cells, we could not eliminate the possibility that the morphine-induced ERK phosphorylation was β-arrestin1-dependent. Therefore, we used MEF cells from β-arrestin1/2 null mice. Similar to the observations with MEF cells from β-arrestin2 null mice, morphine induced ERK phosphorylation with MEF cells from β-arrestin1/2 null mice, whereas etorphine did not (Fig. 2-5). Therefore,

Fig. 2-3 Time-dependent curves of agonists to induce ERK phosphorylation

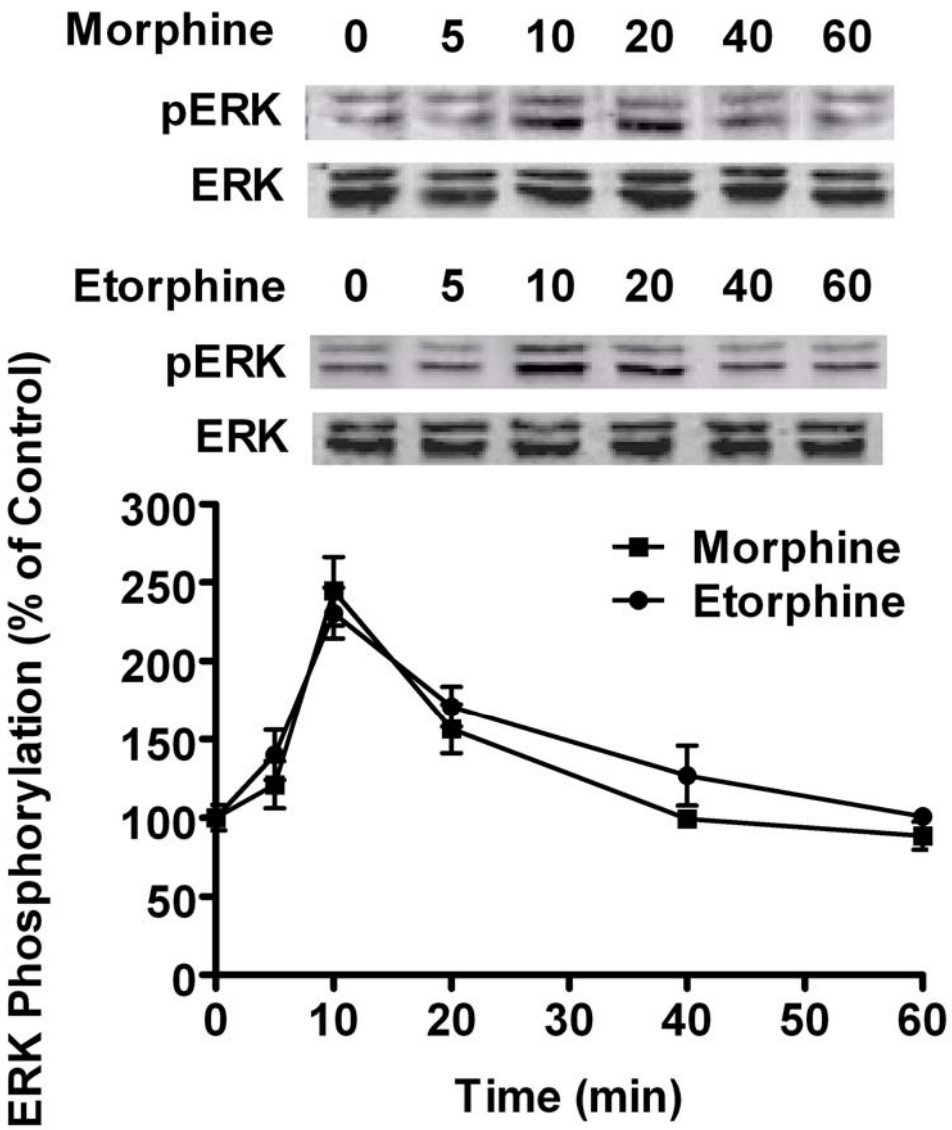

Fig. 2-3 Time-dependent curves of agonists to induce ERK phosphorylation

HEKHM cells were treated with 1 μM morphine or 1 μM etorphine for indicated times. The immunoreactivities of phosphorylated ERK were normalized against those of total ERK. The results were presented as the percentages of those in untreated samples in each group. The experiment was repeated for at least four times and the error bars stood for the standard deviations.

Fig. 2-4 Dose-dependent curves of agonists to induce ERK phosphorylation

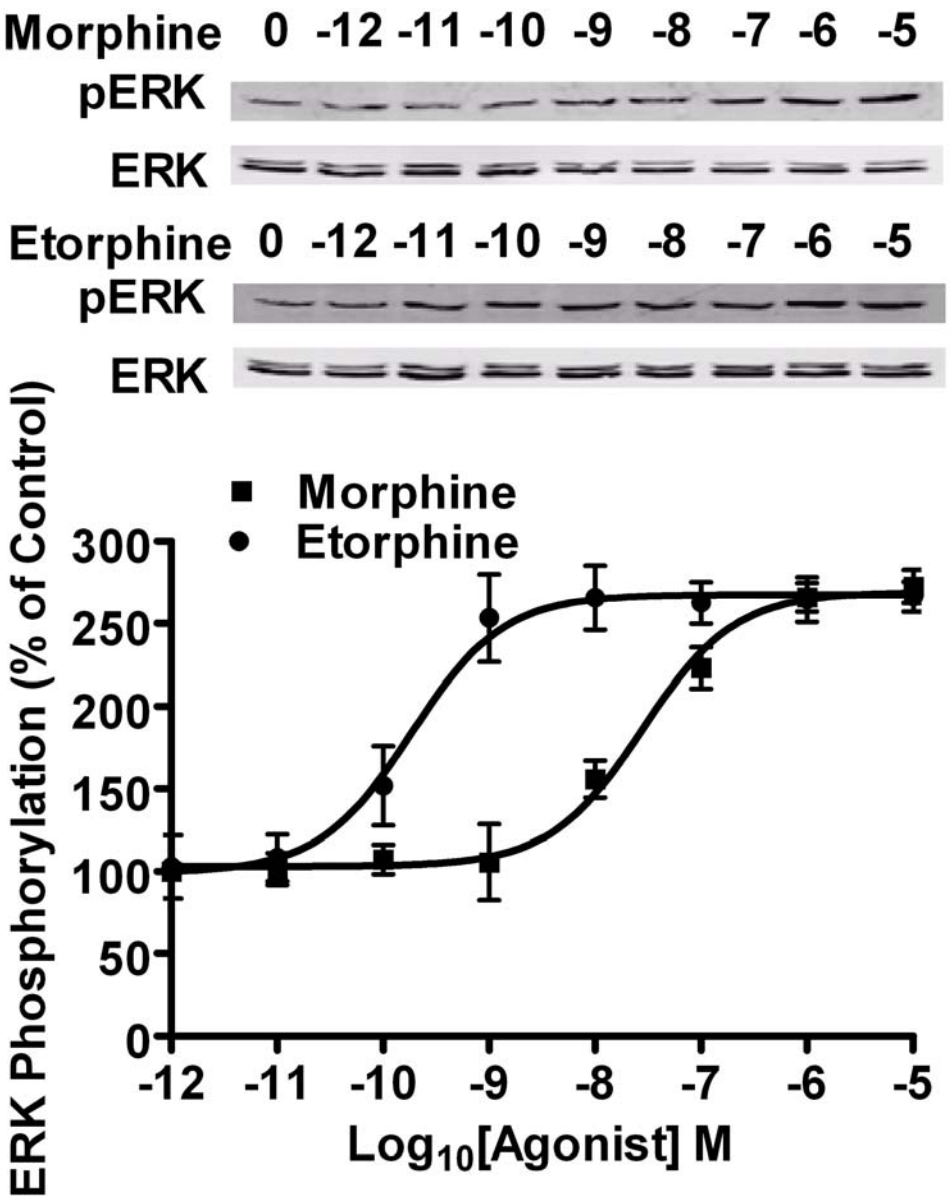

Fig. 2-4 Dose-dependent curves of agonists to induce ERK phosphorylation

HEKHM cells were treated with morphine or etorphine for 10 minutes at indicated concentrations. The immunoreactivities of phosphorylated ERK were normalized against those of total ERK. The results were presented as the percentages of those in untreated samples in each group. The experiment was repeated for at least four times and the error bars stood for the standard deviations.

Fig. 2-5 Etorphine induces ERK phosphorylation via β-arrestin2

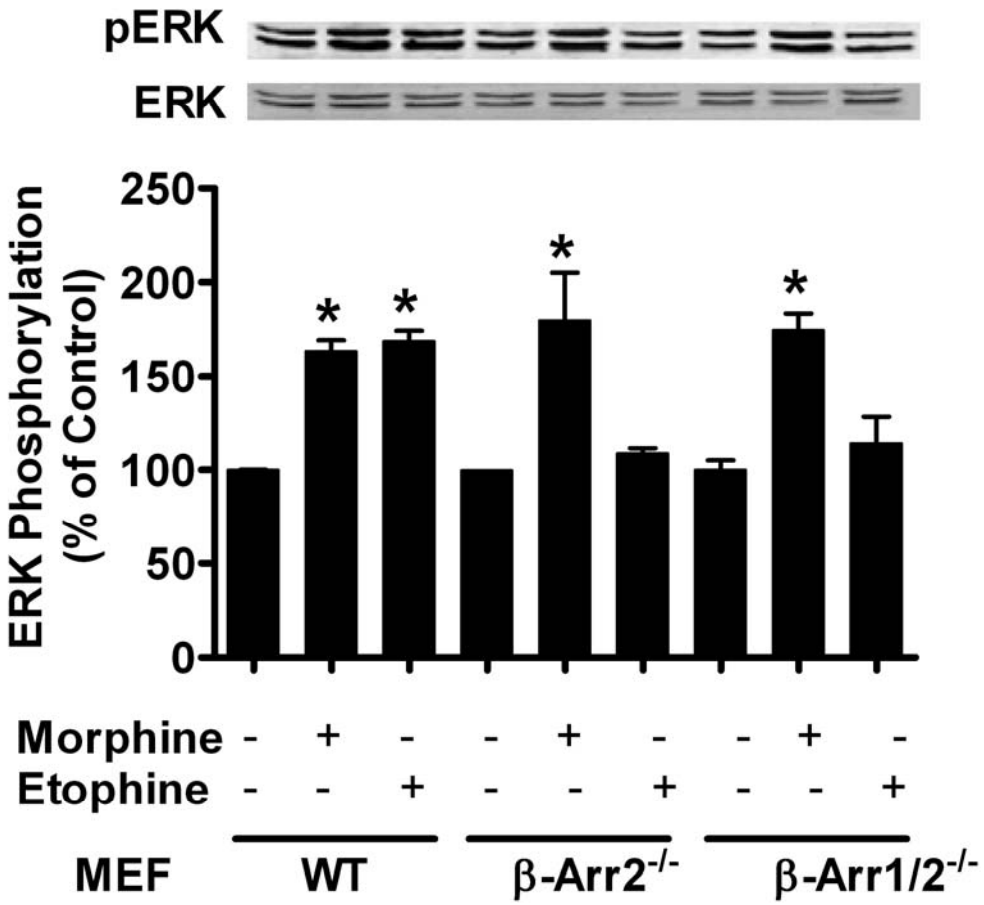

Fig. 2-5 Etorphine induces ERK phosphorylation via β-arrestin2

MEF cells from wildtype mice, β-arrestin2$^{-/-}$ mice and β-arrestin1/2$^{-/-}$ mice were treated with PBS (control), 1 μM morphine or 1 μM etorphine for 10 minutes. The immunoreactivities of phosphorylated ERK were normalized against those of total ERK. The results were presented as the percentages of those in control samples in each group. The experiment was repeated for at least four times and the error bars stood for the standard deviations.

etorphine-induced ERK phosphorylation was β-arrestin2-dependent, whereas morphine-mediated ERK phosphorylation was not β-arrestin-independent.

2.3.3 Morphine induces ERK phosphorylation via PKCε

As one of the two major pathways used by GPCRs to induce ERK phosphorylation, PKC/PKA pathway is the likely candidate pathway in mediating morphine-induced ERK phosphorylation.

PKC family is a large Ser/Thr kinases family and participates in numerous signaling events, such as receptor phosphorylation and desensitization, membrane structure modulation, transcription regulation, neuron-transmitter release, cell proliferation, synaptic remodeling and learning and memory (149). PKC family consists of 11 subtypes, which could be divided into three groups, conventional, novel, atypical depending on the sequence homology and activation mechanisms (150). Conventional PKCs include PKCα, βI, βII, and γ. They are sensitive to intracellular Ca^{2+}. Novel PKCs group includes PKCδ, ε, η, θ and μ. The activation of these subtypes does not require intracellular Ca^{2+} but the binding with diacylglycerol. Atypical PKCs include ξ and λ/ι (151). PKCs are cytosolic proteins; and after activation, they translocate onto the cell membrane and phosphorylate target proteins, which is used as the indicator of PKC activation (152).

The involvement of PKC activity in DOR desensitization has been demonstrated by using PKC inhibitors staurosporine and bisindolylmaleimide (GF109203X) (153, 154). PKC also contributes to the functions of morphine. PKC not only influences the desensitization induced by morphine *in vitro* (142, 155), but also is critical for the *in vivo* effects of morphine, like withdrawal syndrome (156-158), reinforcement effect (159, 160), tolerance development (161) and analgesia (157, 162-164).

Because MOR-mediated ERK phosphorylation has been reported to be inhibited by a PKC inhibitor (71), we used a selective PKC inhibitor, Ro-31-8425, to treat the HEKHM cells. Morphine-induced ERK phosphorylation decreased significantly when Ro-31-8425 was used before agonist treatment (Fig. 2-6A). In contrast, this PKC inhibitor did not affect either the kinetics or the magnitude of etorphine-induced ERK phosphorylation (Fig. 2-6B). Thus morphine-induced, but not etorphine-induced, ERK phosphorylation is mediated by PKC.

Three subtypes of PKC have been suggested to be important for morphine tolerance, PKCα, PKCγ and PKCε (165). Subtype specific peptide inhibitors have been used widely to study the involvement of PKC subtypes in different biological processes (150, 157). Thus to identify the PKC subtype that mediates the morphine-induced ERK phosphorylation, PKC inhibitor (Ro-31-8425), PKCα pseudosubstrate inhibitor (FARKGALRQ), antagonists of PKCγ (CRLVLASC) and PKCε (EAVSLKPT) were used to treated the HEKHM cells. To enable these inhibitors to penetrate the cell membrane, myristoylation was made on the N-termini of the peptides (166, 167). Ro-31-8425 and PKCε-specific inhibitor attenuated morphine-induced ERK phosphorylation in HEKHM cells from 228±22% to 136±15% ($n=4$, $t=11.08$, $p<0.001$) and to 142±9% ($n=4$, $t=10.33$, $p<0.001$), respectively (Fig. 2-7). However, PKCα- and PKCγ-specific inhibitor did not affect morphine-induced ERK phosphorylation (Fig. 2-7). Because there is no significant difference between the abilities of Ro-31-8425 and PKCε-specific inhibitor to attenuate morphine-induced ERK phosphorylation ($t=0.791$, $p>0.05$), PKCε is the major PKC subtype that contributes to the morphine-induced ERK phosphorylation.

Fig. 2-6 Morphine induces ERK phosphorylation via PKC

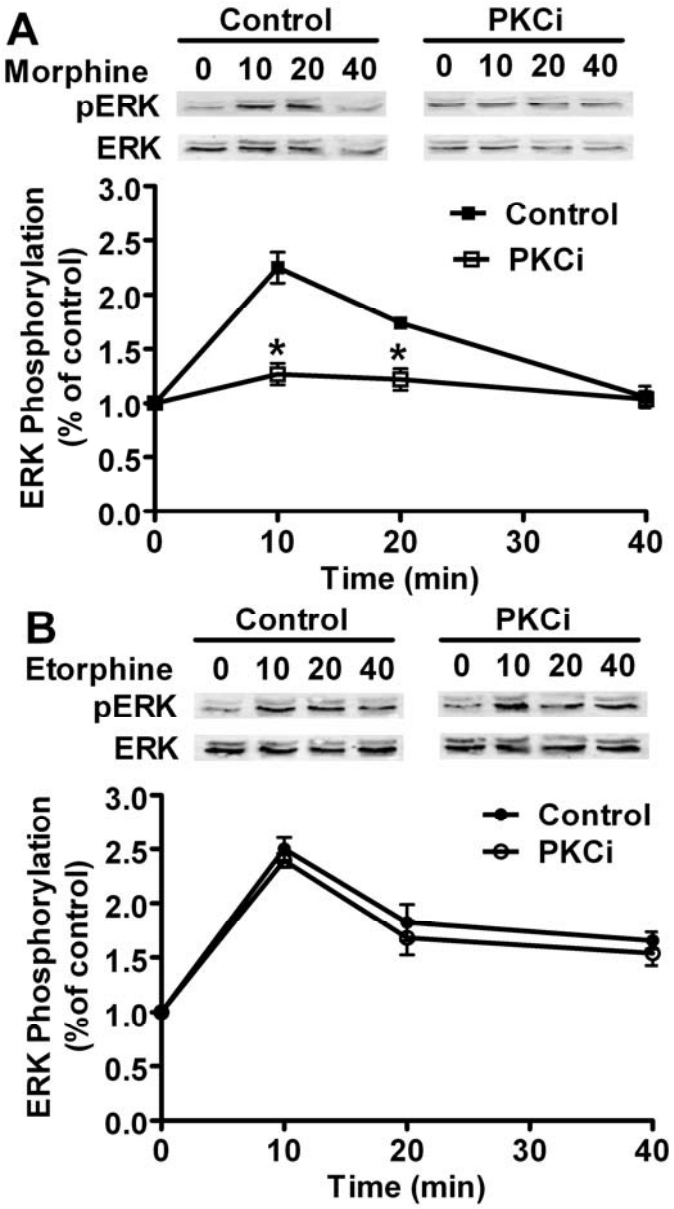

Fig. 2-6 Morphine induces ERK phosphorylation via PKC

HEKHM cells were treated with 1 μM morphine or 1 μM etorphine for indicated times in the presence or in the absence of three-hour pre-treatment with 2 μM Ro-31-8425. The immunoreactivities of phosphorylated ERK were normalized against those of total ERK. The results were presented as the percentages of those in control samples in each group. The experiment was repeated for at least four times and the error bars stood for the standard deviations.

Fig. 2-7 Morphine induces ERK phosphorylation via PKCε

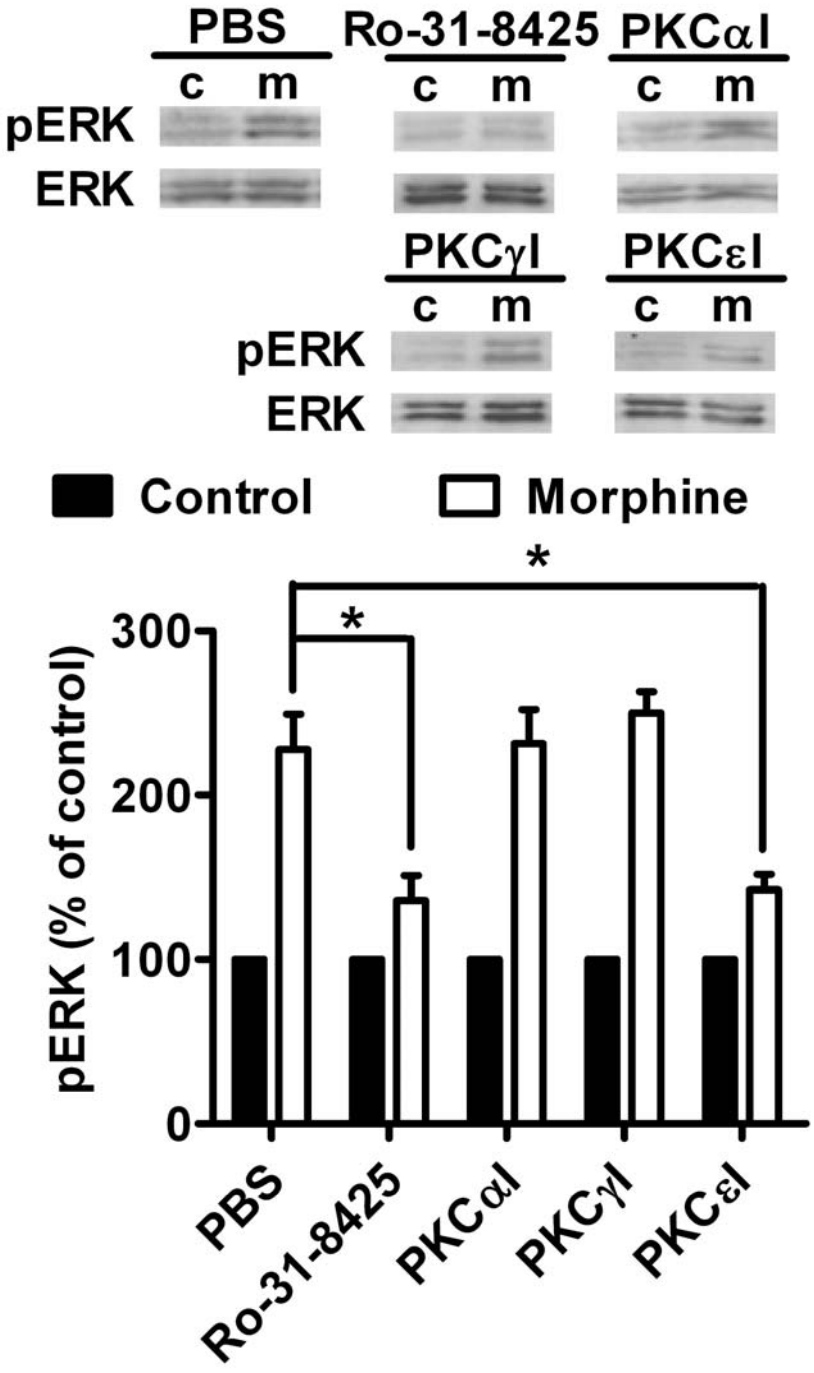

Fig. 2-7 Morphine induces ERK phosphorylation via PKCε

HEKHM cells were treated for three hours with 2 μM the PKC inhibitor Ro-31-8425, or 50 μM peptide inhibitors specific for PKCα (PKCαi: Myristoylated-FARKGALRQ), PKCγ (PKCγi: Myristoylated-WAVSLKPT) or PKCε (PKCεi: Myristoylated-CRLVLASC). Cells were then challenged for 5 minutes with 1 μM morphine. The immunoreactivities of phosphorylated ERK were normalized against those of total ERK. The results were presented as the percentages of those in untreated samples in each group. The experiment was repeated for at least four times and the error bars stood for the standard deviations.

3. Mechanism of agonist-selective signaling

Mechanism of agonist-selective signaling has been studied for a long time. The accepted notion is that the conformational changes of receptor induced by agonists are different from each other. Because different conformational changes of receptor favor the activation of different signaling pathways, agonists activate signaling pathways differentially. Although the crystal structures of G proteins, β-arrestin and serveral GPCRs like rodposine and β2-adregneric receptor have been solved (134, 168, 169), the structural information of the receptor-agonist complex is not available so as to predict the conformational changes induced by different agonists.

3.1 Categorization of signaling pathways

Although the agonist-selective theory suggests that agonist can induce signaling pathways differentially, it is not true that there is difference between every two signaling pathways. Thus various groups have attempted to categorize the signaling pathways and to use the activation of one signaling pathway within the category to predict the activation of the activation of others. Actually, there are two categories have been well studied.

One category of signaling pathways is the G protein-, to be more specific Gα subunit, related signaling pathways. Previous studies indicated that Gα subunit is more efficient in transducing receptor signals than Gβγ-subunits (170). This is probably the reason why opioid receptor desensitized in hours when Gα-mediated inhibition of adenylyl cyclase activity was measured, while desensitized in minutes when Gβγ-mediated activation of potassium channel was monitored (171). Take advantage of the high efficient of Gα subunit in transducing signals, the signaling pathways downstream of Gα subunit have high possibility to be activated similarly by agonists. For example, there is a strong correlation between morphine-induced ERK phosphorylation and morphine-induced adenylyl cyclase inhibition (172).

Another category of signaling pathways is the β-arrestin-related signaling pathways. The abilities of morphine, etorphine, DAMGO and fentanyl to induce receptor phosphorylation have strong correlations with their abilities to recruit β-arrestin onto cell membrane, to induce β-arrestin-mediated receptor internalization and to induce ERK phosphorylation via β-arrestin pathways (95, 108-110).

3.2 β-arrestin related signaling pathways

β-arrestin belongs to the arrestin family which is a small family of cytosolic scaffold proteins. Arrestin1 and arrestin4 (x-arrestin) are found exclusively in retinal rods and

cones, while arrestin2 (β-arrestin1) and arrestin3 (β-arrestin2) are expressed ubiquitously. Arrestins are discovered originally in the desensitization of rhodopsin and β_2-adrenergic receptor (173-175). Recently, β-arrestin has been suggested to function as a scaffold protein which bridges GPCRs and intracellular effectors (176). In addition, abilities of β-arrestin to translocate into nucleus and to regulate the gene expression have also been suggested (13).

Understanding on β-arrestin-related signaling pathways is based on the β-arrestin-mediated receptor desensitization. In the classical desensitization paradigm, binding of agonist to GPCR leads to receptor phosphorylation, which increases the affinity of agonist-receptor complex for the cytosolic protein β-arrestin. Translocation of β-arrestin to receptor complex disrupts receptor-G protein interaction and ceases the activation of G protein-related signaling pathways (177). Then several β-arrestin-mediated signaling pathways will be activated. Receptor phosphorylation is normally mediated by GRK and free Gβγ subunits (178, 179). Because Gβγ subunits dissociate from Gα after G protein activation, the activation of β-arrestin-related signaling pathways requires the activation of G protein under this paradigm.

By using G protein interaction deficient mutants of GPCRs, G protein-independent β-arrestin-related signaling is identified (92, 172, 180). β_2-adrenergic receptor mutants lacking G protein coupling mediates the ERK phosphorylation through a GRK5/6-β-arrestin pathway. The I35 mutant of MOR (lacking the last five amino acids in the third intracellular loop to interact with G protein) still mediates etorphine-induced ERK phosphorylation in a β-arrestin dependent manner.

In addition, overexpression of β-arrestin enables morphine which normally does not induce receptor internalization to induce intensively receptor internalization (181), suggesting a basal affinity of receptor for β-arrestin in the absence of receptor phosphorylation. Moreover, the activation of GRK5/6 is not dependent on the free Gβγ subunits (182). G protein-independent receptor phosphorylation has been observed on

the Ser^{363} of rat DOR (183). Therefore, β-arrestin-related signaling pathways can be activated without G protein activation.

3.3 Pre-coupling of G protein

3.3.1 Pre-coupling model

Two models have been used to explain how G proteins couple to the GPCRs. In the "collision coupling" model, G proteins couple to GPCRs after receptor activation (or agonist binding) by free lateral diffusion on the cell membrane (184). The "pre-coupling" model suggests that G proteins interact with receptors before agonist binding. Much data that supports the pre-coupling hypothesis comes from FRET studies using fluorescence labeled receptors and G proteins (185). However, the controversial still exist, because of the inconsistent reports on the pre-coupling, the overexpression of exogenous receptors and G proteins, and the large fluorescent proteins tagged to the molecules (186). The existence of pre-coupled receptor-G-protein complex has also been suggested by the apparent dissociation constants between G proteins and GPCRs (187-189). The pre-coupling model is more attractive because it not only accounts for the specificities between receptors and G proteins in part, but also explains the rapid intracellular responses.

3.3.2 The pre-coupling between Gαi2 and MOR

3.3.2.1 Gαi2

In order to determine whether pre-coupling exists between G protein and MOR, we tried to measure the interaction between G protein and MOR in the absence of agonist. However, because of the existence of multiple G proteins, it is required to identify the major G protein that mediates the signal transduction of MOR. Because Gβγ subunits have been suggested to bind with GPCR via Gα subunit, the experiments were focused

on the identification of Gα subunit that participates in MOR signaling (4, 186). In addition, the “G protein” is referred to “G protein α subunit” if not specified.

MOR is a typical Gi/o coupled receptor. Therefore, the Gαi2, Gαi3 and Gαo were the subjects of the current experiments. Three adenovirus constructs were used to deliver the pertussis toxin (PTX)-resistant Gαo, Gαi2, and Gαi3 to murine neuroblastoma neuro2A (N2A) cells (56, 190). The mutations at the C-termini of these G proteins (Gαi2, C352L; Gαi3, C351L; Gαo, C352L) made them functional under the treatment with PTX (190). Overnight treatment with 0.1 μg/ml PTX attenuated ERK phosphorylation induced by either morphine or etorphine in the control cells (Fig. 3-1A). The similar attenuation on ERK phosphorylation was observed when the adenovirus containing PTX-resistant Gαo or Gαi3 was used (Fig. 3-1B and D). However, when adenovirus delivering the PTX-resistant Gαi2 was used to infect the cells, the inhibitory effects of PTX on agonist-induced ERK phosphorylation were blocked (Fig. 3-1C), indicating Gαi2 mediated the signal transduction of MOR, at least MOR-mediated ERK phosphorylation. But we still could not rule out the involvement of other Gα in the activation of other signaling pathways, even Gαi2 has also been suggested to function during receptor desensitization on intracellular calcium release (148).

Because morphine-induced ERK phosphorylation is dependent on the PKC which is a downstream signaling molecule of G protein, and etorphine-induced ERK phosphorylation is mediated by β-arrestin2, thus ERK phosphorylation should be related to both two categories of signaling pathways (G protein- and β-arrestin-related signaling pathways).

3.3.2.2 Gαi2 binds to MOR in the absence of agonist

The interaction between Gαi2 and MOR was determined in HEKHM cells. By using the immunoprecipitation, MOR was precipitated from cell lysis by using the antibody against HA (which is tagged at the N-terminus of MOR). After immunoprecipitation, the

Fig. 3-1 Gαi2 mediates morphine-induced ERK phosphorylation

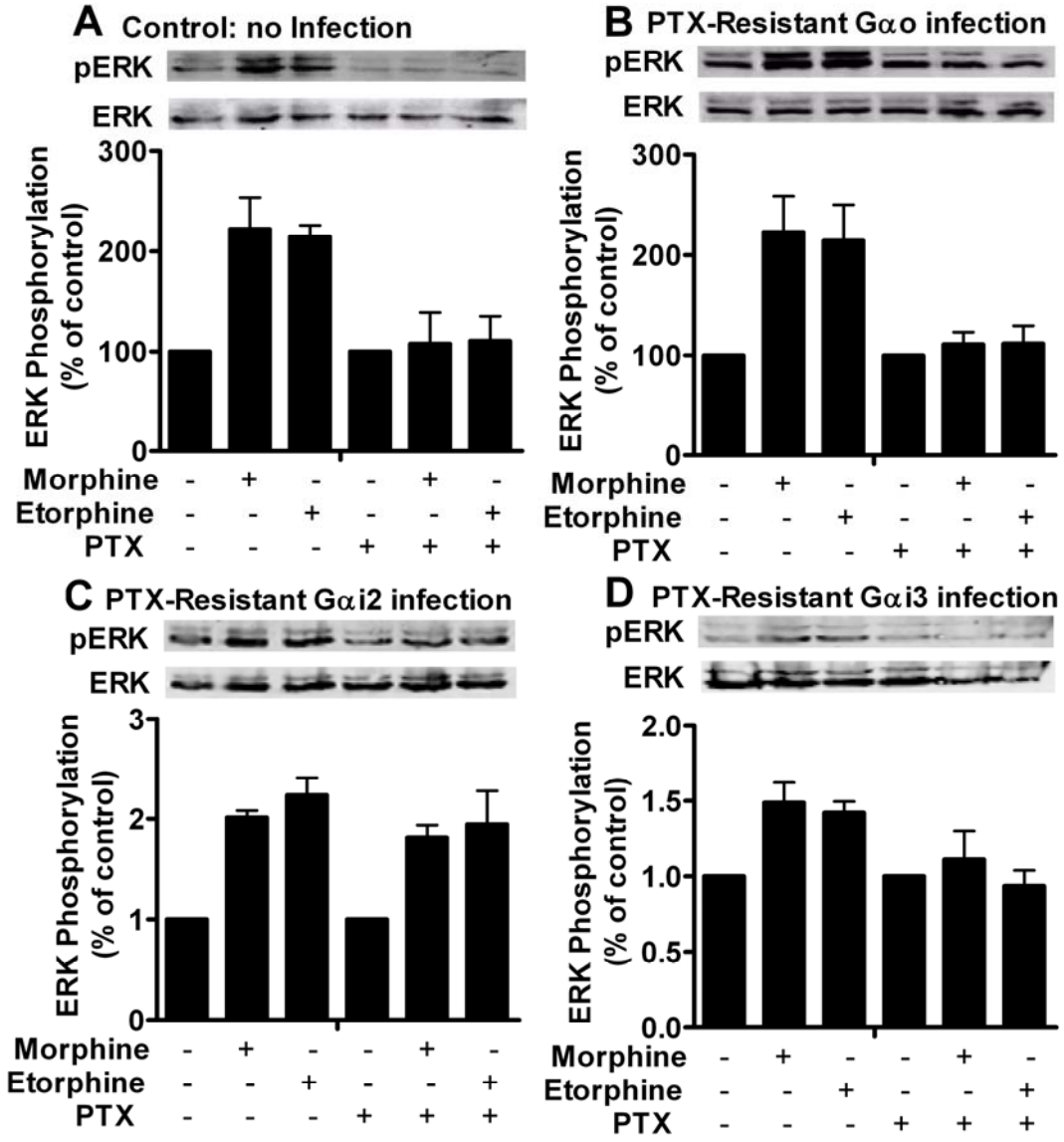

Fig. 3-1 Gαi2 mediates morphine-induced ERK phosphorylation

N2A cells with MOR-HA stably expressed were infected with different PTX-insensitive Gα, control (A), Gαo (B), Gαi2 (C) and Gαi3 (D). Before experiments, 100ng/ml PTX was used to treat the cells overnight. Then the cells were exposed to 1μM morphine or 10nM etorphine for 10 minutes. The immunoreactivities of phosphorylated ERK were normalized against those of total ERK. The results were presented as the percentages of those in untreated samples in each group. The experiment was repeated for at least four times and the error bars stood for the standard deviations.

amount of Gαi2 associated with MOR was determined. As indicated in Fig. 3-2, MOR precipitated large amount of Gαi2 in the absence of agonists, which was similar to the amount of Gαi2 precipitated with MOR when the cells were treated with 1 μM morphine, suggesting the pre-coupling between Gαi2 and MOR.

However, when etorphine was used to treat the cells, a significant decrease in the amount of Gαi2 precipitated with MOR was observed compared with that in control cells. This decrease is not due to the high level of receptor internalization induced by etorphine, because this decrease was not inhibited when 0.4 M sucrose was used to block receptor internalization (Fig. 3-2). Then antibody against Gαi2 was used to perform immunoprecipitation, and similar observations were obtained. Gαi2 precipitated large amount of MOR in the absence of agonist, while this amount decreased after etorphine treatment. Treatment with morphine did not affect the interaction between Gαi2 and MOR.

3.3.3 Gαi2 anchors MOR to lipid raft

3.3.3.1 Lipid raft

Lipid rafts are enriched with cholesterol, sphingomyelin, gangliosides and various signaling proteins, including heterotrimeric G proteins, adenylyl cyclase and Src kinases (191, 192). They provide an environment in which GPCRs interact freely with a selective set of signaling molecules to execute their functions (172, 191). Lipid rafts regulate the signaling of several GPCRs, such as gonadotropin-releasing hormone receptor, type-1 cannabinoid receptor, α1-adrenergic receptor, NK1 receptor, and opioid receptors (191). This regulatory function normally is demonstrated by the decreased signaling during lipid raft disruption. For example, methyl-β-cyclodextran (MβCD) and simvastatin disrupt lipid raft by extracting cholesterol from cell membrane and blocking the synthesis of cholesterol, respectively.

Fig. 3-2 The pre-coupling between Gαi2 and MOR

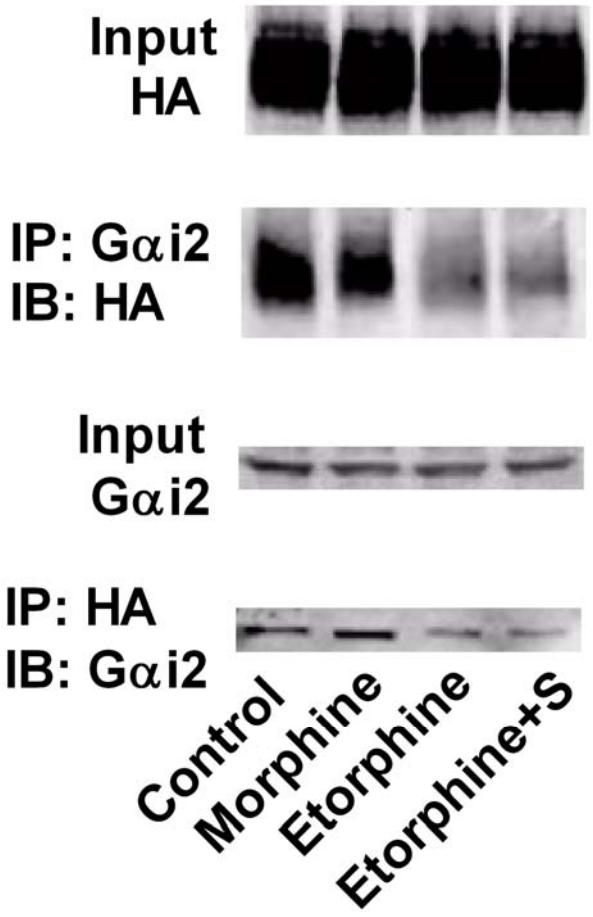

Fig. 3-2 The pre-coupling between Gαi2 and MOR

HEKHM cells were treated with PBS (control), 1 μM morphine, 10 nM etorphine or 10 nM etorphine plus 0.4 M sucrose (5 min before agonist, Etorphine+S) for 10 minutes. Antibodies against HA and Gαi2 were used to immunoprecipitation. The amounts of MOR/Gαi2 precipitated with Gαi2/MOR were presented.

Although the existence of lipid raft has not been accepted by all the scientists, a low-density high-cholesterol microdomain can be separated from the cell membrane by using a 5%-30% continuous sucrose gradient. Microdomains on the cell membrane were separated depending on their density, after being centrifuged at the bottom of a 5%-30% continuous sucrose gradient. The gradient was fractionized into 12 fractions from lowest density to the highest density. As indicated in Fig. 3-3, majority of the protein was located in the last two fractions, where should be the fractions of cell debris and large cellular components

When cholesterol concentration was measured in each fraction, high cholesterol levels were detected in the 4^{th} and the 5^{th} fractions (Fig. 3-4), which were about 150% of those in other fractions, suggesting a high-cholesterol microdomain distributes between the 4^{th} and the 5^{th} fractions. However, because of the lower density of cholesterol, it should float on the top of sucrose gradient, if it was not associated with other molecules (e.g. protein). Therefore, the high-cholesterol microdomain between the 4^{th} and the 5^{th} fractions suggests the existence of lipid raft microdomain on cell membrane and a successful separation of lipid raft microdomain.

The distribution of different proteins across sucrose gradient was determined by immunoblotting. Four proteins were analyzed, Gαq, Gαi2, MOR and transferring receptor (TR). High amounts of Gαq and Gαi2 were detected in the 4^{th} and the 5^{th} fractions (Fig. 3-5), which are consistent with the distribution of cholesterol. Thus Gαq and Gαi2 located in the lipid raft microdomain (192-194). TR is normally used as a marker for the non-raft microdomain on cell membrane (195). The highest amount of TR was detected in the 6^{th} fraction. In addition, the immunoreactivities of MOR suggested the localization of MOR in lipid raft microdomain.

Fig. 3-3 Protein distribution across the sucrose gradient

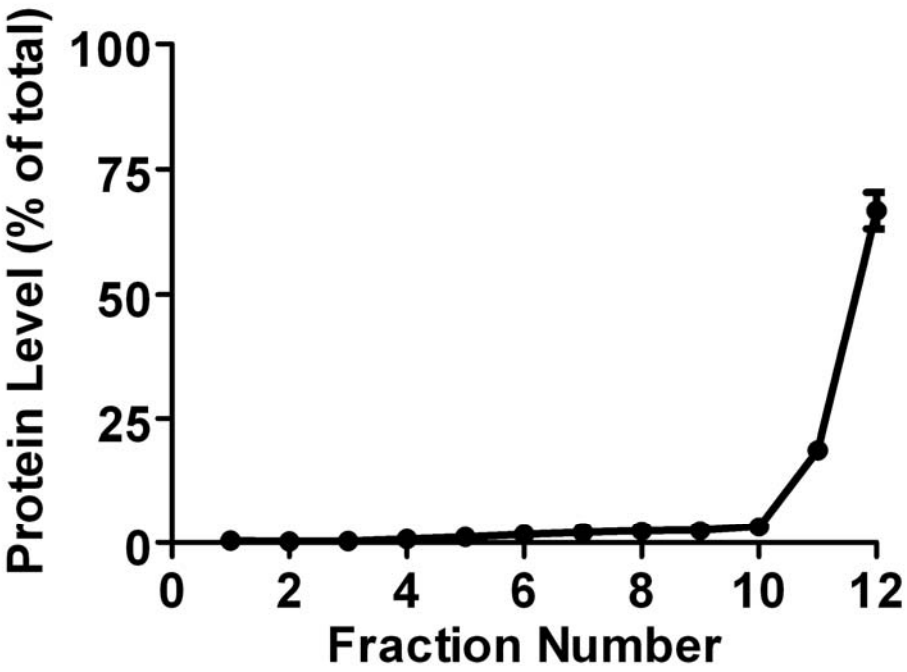

Fig. 3-3 Protein distribution across the sucrose gradient

The HEKHM cells were subject for the 5%-30% continuous sucrose gradient. 12 fractions were collected after the centrifugation. The protein concentration was measured in each fraction and normalized against the total protein amount.

Fig. 3-4 Cholesterol distribution across the sucrose gradient

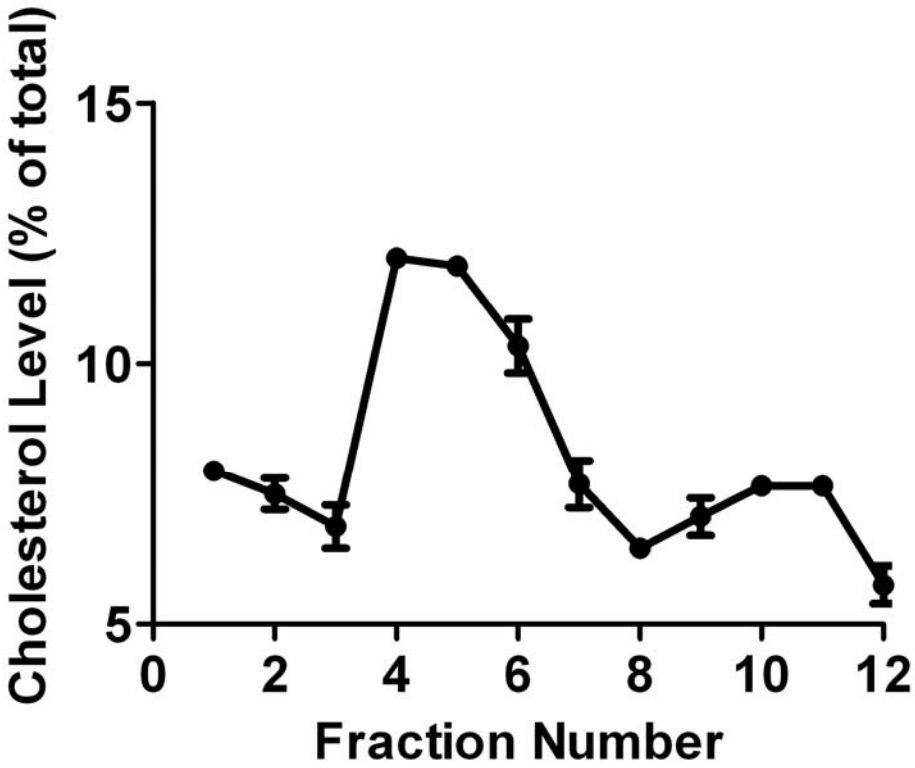

Fig. 3-4 Cholesterol distribution across the sucrose gradient

The HEKHM cells were subject for the 5%-30% continuous sucrose gradient. 12 fractions were collected after the centrifugation. The cholesterol concentration was measured in each fraction and normalized against the total cholesterol amount.

Fig. 3-5 MOR distribution across the sucrose gradient

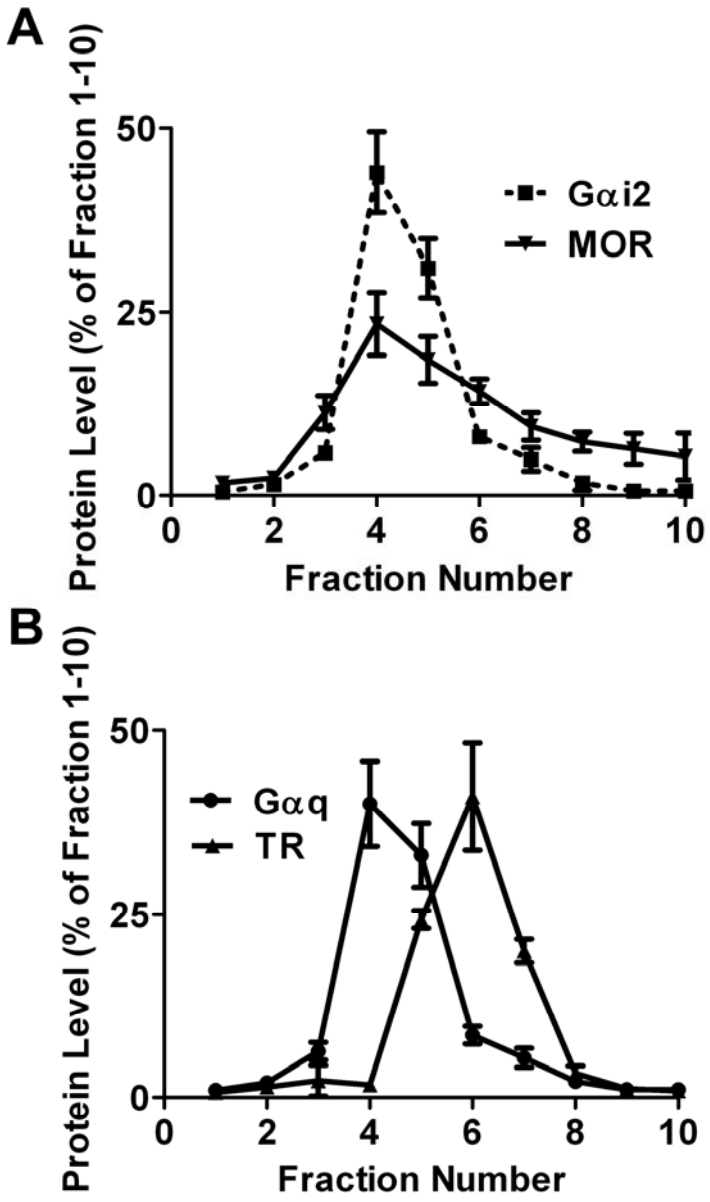

Fig. 3-5 MOR distribution across the sucrose gradient

The HEKHM cells were subject for the 5%-30% continuous sucrose gradient. 12 fractions were collected after the centrifugation. The amounts of Gαi2 and TR were measured in each fraction and normalized against the total amount in the first 10 fractions (A). The amounts of Gαq and MOR were measured in each fraction and normalized against the total amount in the first 10 fractions (B).

3.3.3.2 MOR locates in lipid raft

Lipid raft and non-raft microdomains were separated by using continuous sucrose gradient. Successful separation was confirmed by using antibodies against Gαq (a lipid raft marker) and TR (a non-raft marker). Because the immunoreactivities of Gαq and TR peaked at the fourth and sixth fraction of continuous sucrose gradient, respectively, the ratio of MOR amounts in these two fractions was calculated and used to represent the relative distribution of MOR between lipid raft and non-raft microdomains. In addition, MOR amount in each fraction was calculated as the percentage of the total MOR amount in the first 10 fractions to indicate the overall distribution of MOR on cell membrane.

Consistent with a previous report (112), MOR was shown to locate within the lipid raft in the absence of agonists (Fig. 3-6). The ratio of MOR amount in the sixth to that in the fourth fraction was 0.95±0.29. However, when the cells were treated with etorphine for 10 min, MOR translocated from lipid raft to the non-raft microdomains (Fig. 3-6). The ratio of MOR amount in the sixth to that in the fourth fraction increased to 3.02±0.36. This translocation was not observed after morphine treatment. The ratio of MOR amount in the sixth to that in the fourth fraction was 0.94±0.26 in morphine-treated cells. This translocation was not a result of receptor internalization because etorphine-induced MOR translocation was not attenuated when 0.4 M sucrose was used to block the receptor internalization. The ratio of MOR amount in the sixth to that in the fourth fraction was 2.88±0.39 in sucrose+etorphine-treated HEKHM cells.

Moreover, confocal microscope imaging also indicated the colocalization of MOR with the cholera toxin subunit B (CT-B), a lipid raft marker (196). CT-B binds to the pentasaccharide chain of plasma membrane ganglioside G_{M1}, which selectively partititions into lipid raft microdomain. In the absence of agonist, 75±15% (n=8) of MOR colocalized with CT-B (Fig. 3-7A). Ten-minute exposure to 1 μM morphine did not alter this percentage (73±17%, n=5). However, 10 minutes after 10 nM etorphine treatment, the colocalization between MOR and CT-B decreased significantly to

Fig. 3-6 Agonists affect MOR distribution on cell membrane

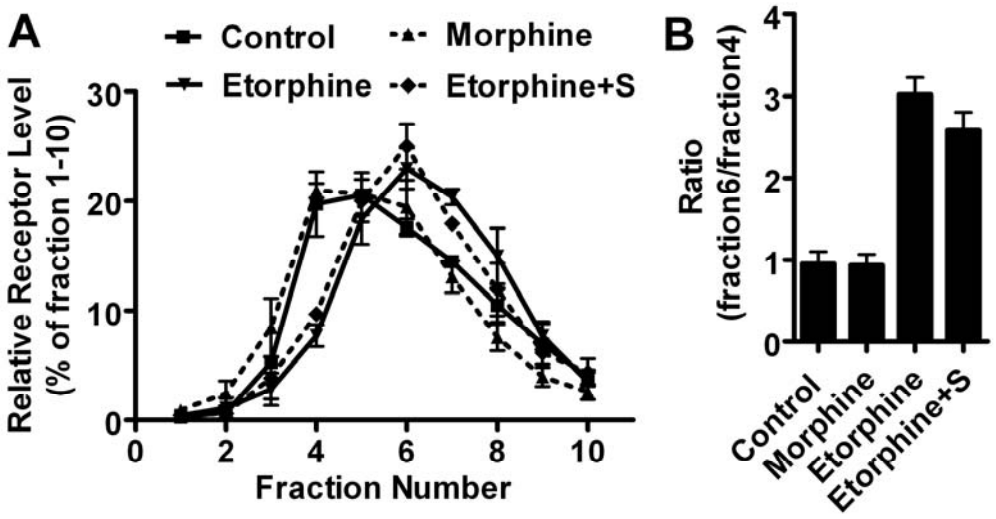

Fig. 3-6 Agonists affect MOR distribution on cell membrane

HEKHM cells were treated with PBS (control), 1 μM morphine, 10 nM etorphine or 10 nM etorphine plus 0.4 M sucrose (5 min before agonist, Etorphine+S) for 10 minutes. The cells were subject for the 5%-30% continuous sucrose gradient. 12 fractions were collected after the centrifugation. The amounts of MOR were measured in each fraction and normalized against the total amount in the first 10 fractions (A). The amounts of MOR in fraction 6 and fraction 4 were compared and listed in (B).

Fig. 3-7 Agonists affect the colocalization between MOR and CT-B

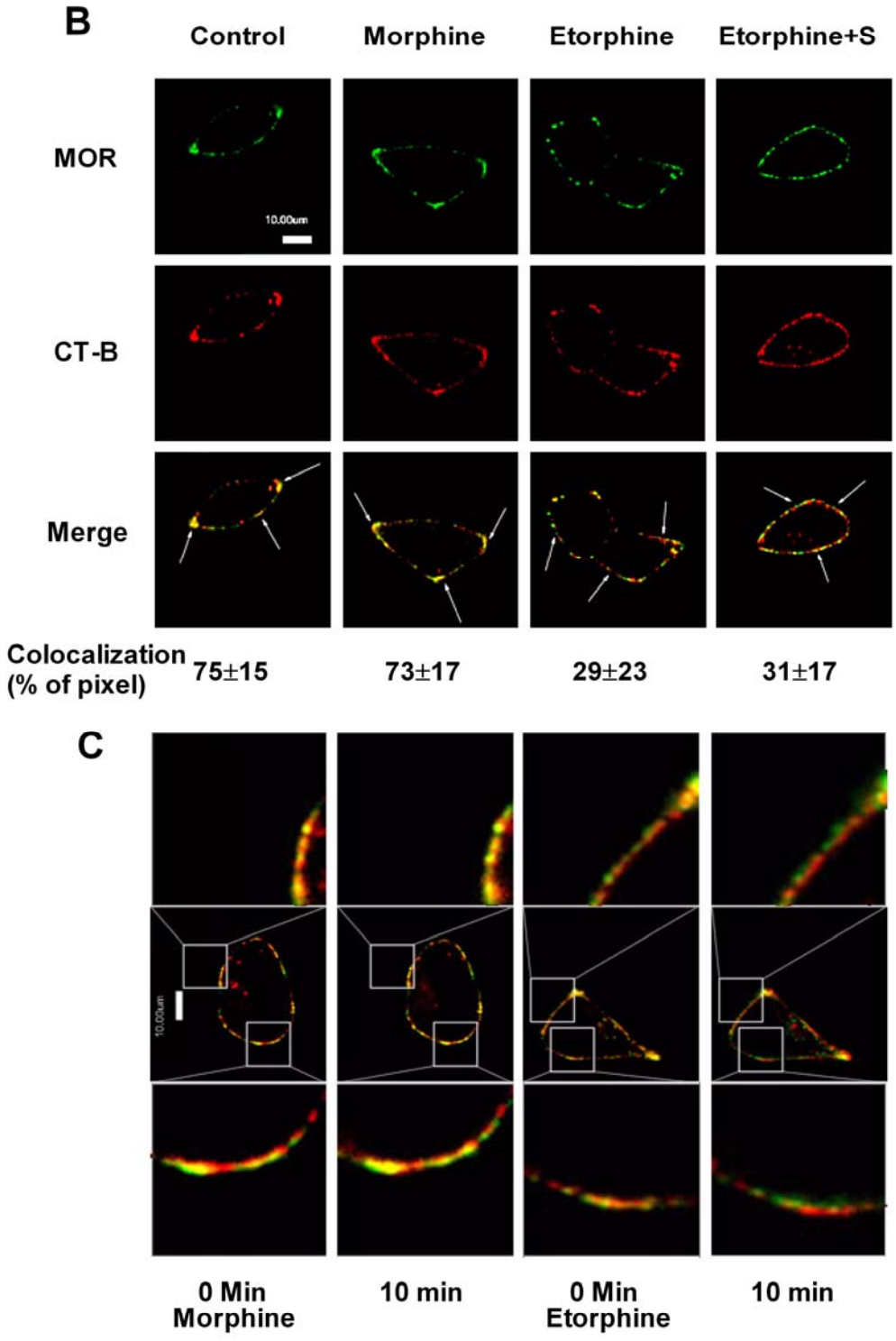

Fig. 3-7 Agonists affect the colocalization between MOR and CT-B

HEKHM cells were treated as in Fig. 3-6. MOR was stained by HA-antibody and Alexa 488. CT-B was stained by CT-B antibody and Alexa 596.

29±23% (n=6) in the absence of 0.4M sucrose and to 31±17% (n=4) in the presence of 0.4 M sucrose. Colocalization of MOR with CT-B was demonstrated also with live images. HEKHM cells were treated with morphine and fentanyl for 10 minutes. The same cells were captured before and 10 minutes after agonist challenge. The changes of colocalization were illustrated by comparing the same cells at two different time points. The areas which displayed significant changes were enlarged (Fig. 3-7B). Again, only etorphine-treated cells showed a decrease in the colocalization between MOR and CT-B.

3.3.3.3 Gαi2 determines the location of MOR

Accumulating data suggests that G protein α-subunits are located within the lipid raft microdomains (193). The myristoylation and palmitoylation on N-termini target Gα subunits to cell membrane and enable the interaction between lipids molecules and Gα subunits (4, 197, 198). Because the pre-coupling has been identified between Gαi2 and MOR, it is reasonable to suggest that Gαi2 anchors MOR to lipid raft. In addition, the distribution of MOR on cell membrane was affected by the expression level of Gαi2.

The expression level of Gαi2 was manipulated by transfecting HEKHM cells with constructs encoding sense and anti-sense Gαi2 (Fig. 3-8A). The expression level of Gαi2 was decreased by introducing the anti-sense Gαi2 construct, while increased when the sense Gαi2 construct was used.

The transfection with sense Gαi2 construct did not affect the distribution of MOR on cell membrane. The ratio of MOR amounts in the sixth and fourth fraction was 1.00±0.12 in control HEKHM cells. When Gαi2 level was increased by the sense construct, the ratio of MOR amount in the sixth to that in the fourth fraction was constant (0.95±0.29). However, etorphine-induced translocation of MOR was attenuated significantly in HEKHM cells transfected with the sense Gαi2 construct. The ratio was 1.43±0.26, which was much lower than that in etorphine-treated control cells (3.02±0.36, Fig. 3-6).

Fig. 3-8 Gαi2 regulates MOR distribution

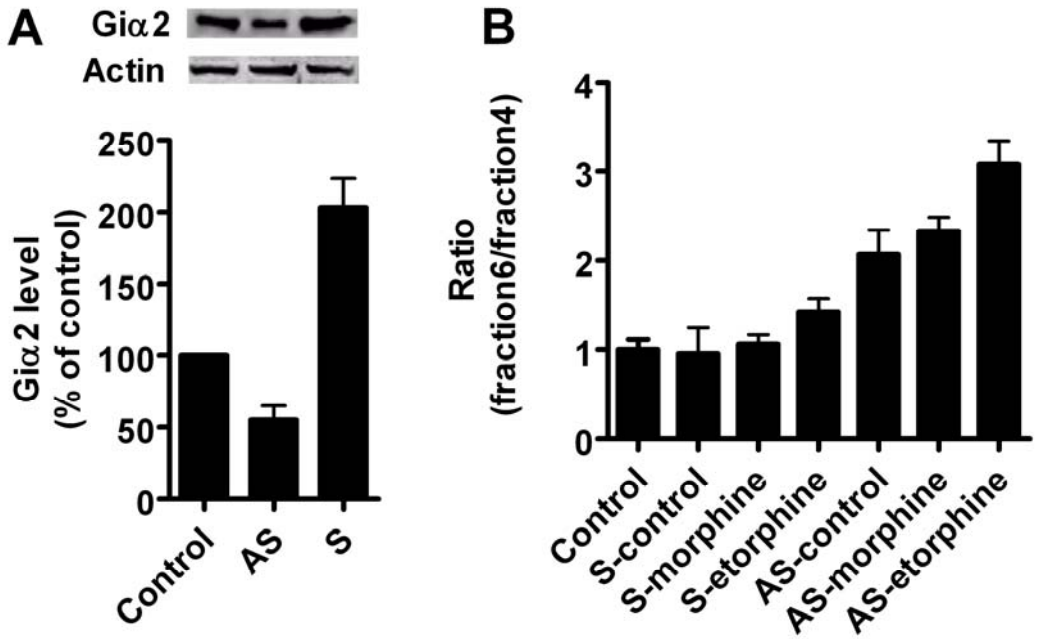

Fig. 3-8 Gαi2 regulates MOR distribution

HEKHM cells were transfected with sense and anti-sense Gαi2 constructs for 24 hours. The expression of Gαi2 was presented in (A) with actin as internal control. The cells were treated with PBS (control), 1 μM morphine or 10 nM etorphine for 10 minutes and subjected for the sucrose gradient experiments. The ratio of MOR amounts in fraction 6 and fraction 4 was indicated in (B).

When Gαi2 was down-regulated by the anti-sense construct, MOR translocated to non-raft microdomains in the absence of etorphine (Fig. 3-8B). The ratio of MOR amount in the sixth to that in the fourth fraction was 2.06±0.28. Such translocation of MOR was not affect by the treatment with morphine, but was enhanced by the treatment with etorphine. Thus Gαi2 is essential for the localization of MOR on cell membrane. Modulating the expression level of Gαi2 controls the distribution of MOR between lipid raft and non-raft microdomains.

Roles played by the interaction between MOR and Gαi2 in determining the lipid raft location of MOR were investigated further with a MOR mutant that lacks the BBXXB motif required for G protein interaction. The deletion of the ^{276}RRITR^{280} sequence (the last five amino acids in the third intracellular loop) from rat MOR (I35) resulted in the decreased interaction between MOR and Gαi2 and the inability of receptor to mediate AC inhibition (199). The weaker interaction between I35 and Gαi2 was confirmed by the less amount of MOR precipitated with Gαi2 and the less amount of Gαi2 precipitated with MOR (Fig. 3-9A), even though I35 was expression at a similar level to that of wildtype MOR (Fig. 3-9A). The decrease in MOR-Gαi2 interaction resulted in the non-raft location of I35 in the absence of agonist (Fig. 3-9B), but did not influence the locations of Gαq and Gαi2. The ratio of the amount of I35 in the sixth to that in the fourth fraction was 2.91±0.80.

3.4 Competition between G protein and β-arrestin

Activation of G protein-dependent β-arrestin-related pathway requires the activation of G proteins and the uncoupling of G proteins from receptor complexes. In addition, because of the pre-coupling between G proteins and GPCRs, activation of G protein-independent β-arrestin-related pathway also requires the uncoupling of G proteins from receptor complexes. If β-arrestin uncouples G protein from receptor complex before G protein activation, G protein-independent β-arrestin-related pathways will be activated. Otherwise, G protein will be activated. If β-arrestin uncouples G protein from receptor

Fig. 3-9 Gαi2 anchors MOR in lipid raft

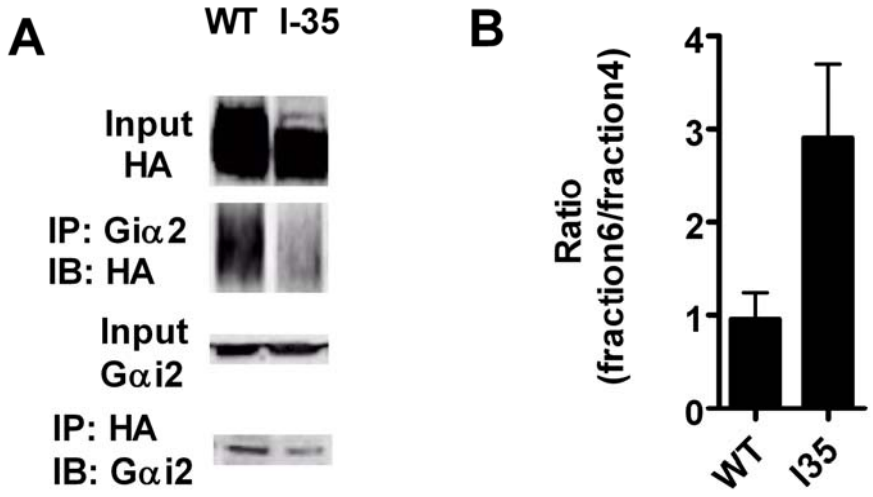

Fig. 3-9 Gαi2 anchors MOR in lipid raft

The HEKHM and HEKI35 cells were used. The antibodies against Gαi2 and HA were used for immunoprecipitation, the amounts of Gαi2/MOR precipitated with MOR/ Gαi2 were presented in (A). Then the cells were used for continuous sucrose gradient, the ration of the amounts of MOR in fraction 6 and fraction 4 were listed in (B). The experiment was repeated for at least four times and the error bars stood for the standard deviations.

complex after G protein activation, G protein-dependent β-arrestin-related pathways will be activated. Otherwise, G protein-related pathways, e.g. PKC/PKA pathway, will be activated. Thus competition between G protein and β-arrestin determines the selectivity of agonist between downstream signaling pathways.

3.4.1 Binding site of G protein on GPCRs

After the binding of appropriate agonists, GPCRs activate G proteins selectively. Although GPCRs can couple to multiple G proteins, especially when the GPCRs or G proteins are over-expressed, the affinities of the receptor to non-specific G proteins are relative low (200). By doing deletion and mutation studies on a variety of GPCRs, The most critical regions on GPCRs for G protein coupling are demonstrated to be the second intracellular loop, the N-terminus and the C-terminus of the third intracellular loop (131). The Asp/Glu-Arg-Tyr triplet is conserved in N-terminus of the second intracellular loop in most class 1 GPCRs (rhodoposin family). Replacing the arginine residue with other amino acids abolishes or dramatically reduces the coupling between receptor and G protein (201). In addition, although the size of the third intracellular loop varies from 240 to 15 amino acids in different GPCRs, 8-15 amino acids in N-terminus and C-terminus of the third intracellular loop are critical for G protein coupling (201). Moreover, the first intracellular loop whose length is highly conserved and membrane-proximal 8-16 amino acids of the forth intracellular loop also contribute to the coupling of G proteins (186).

3.4.2 Binding site of β-arrestin on GPCRs

Receptor phosphorylation can increase the affinity of receptor for β-arrestin, therefore phosphorylation site contributes to the binding of β-arrestin to receptor complex. Because most GPCRs have their phosphorylation sites on their C-termini, C-termini have been considered as the critical part for the binding of β-arrestin (202). The C-terminus phosphorylation not only functions in recruiting β-arrestin, but also regulates

the accessibility of β-arrestin to several non-phosphorylated residues (203). These non-phosphorylated residues are in the second intracellular loop, the N-terminus and the C-terminus of the third intracellular loop, as demonstrated with dopamine receptors, adrenergic receptors and opioid receptors (132-136). Deletion or mutation on these regions decreases the binding affinity between β-arrestin and receptor.

3.4.3 A competition model

G protein and β-arrestin share similar binding sites on the GPCRs (the second intracellular loop, N-terminus and C-terminus of the third intracellular loop), indicating that the G protein uncoupling by β-arrestin may be due to the competition of binding site. However, it is also proposed that G protein can uncouple β-arrestin from receptor complex when the affinity between G protein and the receptor is enhanced. However, because of the receptor internalization mediated by β-arrestin and the membrane location of G protein (4, 204), it is impossible for G protein to uncouple β-arrestin after receptor internalization. Thus, increasing the binding affinity of G protein for receptor complex can only prevent β-arrestin-mediated uncoupling of G protein. For instance, modulating the expression level of G protein successfully decreases G protein uncoupling mediated by β-arrestin (172).

Basing on the discussion above, a new model has been proposed (Fig. 3-10). β-arrestin has a basal affinity for receptor complex and G protein-independent receptor phosphorylation exists in GPCR system (183). These two factors favor the activation of G protein-independent β-arrestin-related pathways rather than G protein-related pathways. After G protein activation, both G protein-independent receptor phosphorylation and G protein-dependent receptor phosphorylation favor the activation of G protein-dependent β-arrestin-related pathways by increasing the affinity of β-arrestin for receptor complex. In addition, receptor phosphorylation also decreases the interaction between G protein and receptor (205, 206). The possible dissociation of G

Fig. 3-10 Schematic of the competition between Gαi2 and β-arrestin

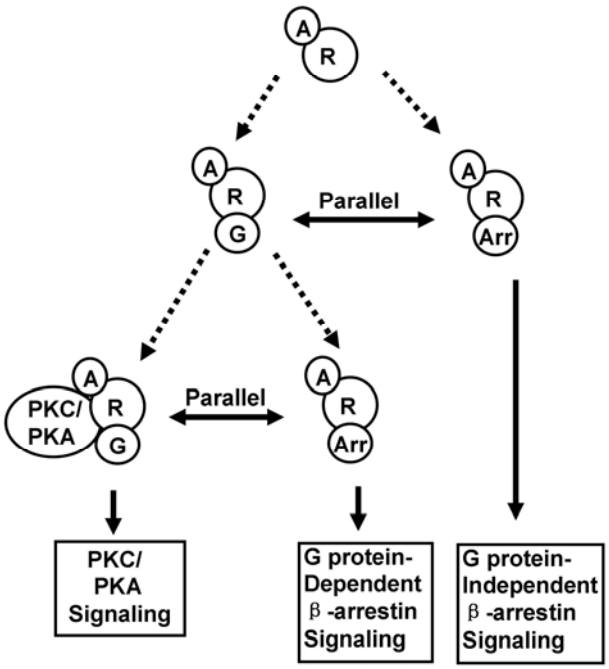

protein from receptor complex after G protein activation also moves the selection towards G protein-dependent β-arrestin-related pathways (207).

Alternatively, G protein-mediated signaling (from G protein to PKC/PKA or adenylyl cyclase) can be considered as the major signaling cascade. Although the competition between G protein and β-arrestin exists at any time point, it is only observed when the affinity of β-arrestin for receptor complex is increased to a level which is sufficient to uncouple G protein. Thus competitions at several time points are suggested during the signal transduction. As indicated in Fig. 3-11, the basal affinity of β-arrestin for receptor complex enables it to compete with G protein even before agonist binding. However, because the affinity is relative low, nearly no β-arrestin binds to receptor complex at that time. After agonist binding, G protein-independent receptor phosphorylation increases the affinity of β-arrestin for receptor complex and subsequently initiates the G protein-independent β-arrestin-related signaling. After G protein activation, the G protein-dependent receptor phosphorylation and G protein dissociation may initiate the G protein-dependent β-arrestin-related signaling. If both G protein-independent and G protein–dependent β-arrestin-related signaling are not initiated, the signaling pathways downstream of G protein will be activated. In addition, the uncoupling of G protein from receptor complex by β-arrestin requires time, thus the signaling pathways downstream of G protein that are under quick activation still could be activated, even though the β-arrestin-related signaling will be activated finally.

3.5 The factors that affect the competition

Competition between G protein and β-arrestin determines the activation of downstream signaling pathways. Thus by monitoring the activations of downstream signaling pathways, competition between G protein and β-arrestin will be reviewed. In order to fulfill the purpose, suitable signaling pathways should be monitored. The inhibition of adenylyl cyclase activity is induced by agonists via G α subunit and has been used as an indicator for the activation of G protein-related signaling pathways. In

Fig. 3-11 Schematic of GPCR signaling

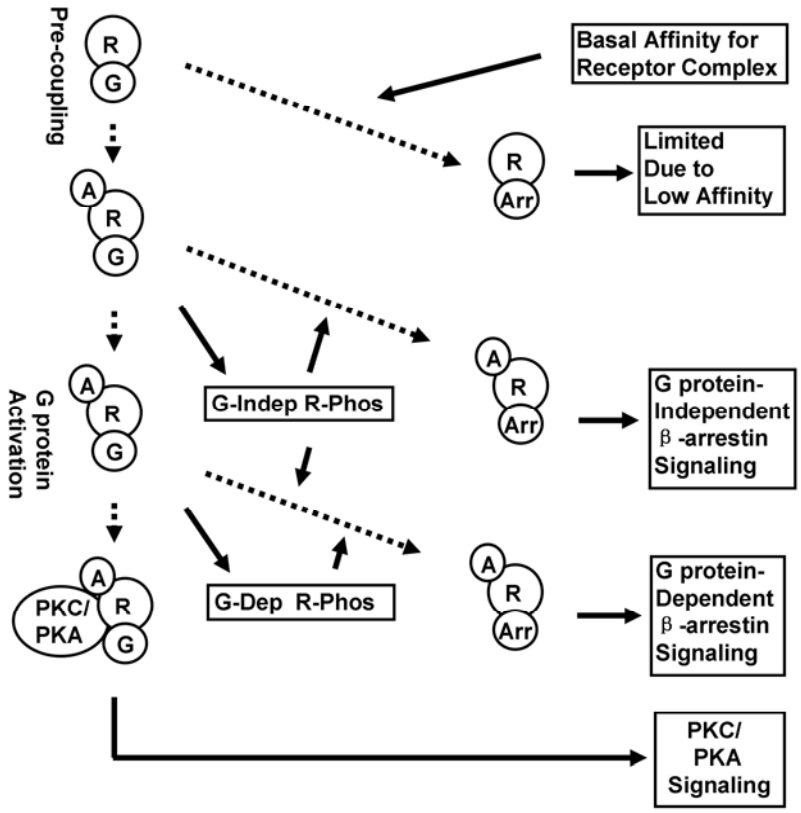

addition, morphine induces ERK phosphorylation through G protein-PKC pathway, while β-arrestin mediates ERK phosphorylation induced by etorphine, DAMGO and fentanyl. Thus adenylyl cyclase inhibition and ERK phosphorylation were measured to evaluate the competition between G protein and β-arrestin.

3.5.1 Receptor Phosphorylation

As mentioned above, both G protein-dependent and G protein-independent receptor phosphorylation have been observed. In addition, receptor phosphorylation increases the affinity between receptor complex and β-arrestin. Thus receptor phosphorylation increases the ability of β-arrestin to uncouple G protein from MOR complex. Receptor phosphorylation may also affects the ability of G protein to couple receptor complex, because etorphine did not used PKC pathway for ERK phosphorylation even when the MEF cells for β-arrestin1/2$^{-/-}$ mice.

3.5.1.1 Agonist-selective receptor phosphorylation

Because the phosphorylation sites of MOR have been demonstrated to be Ser^{363}, Thr^{370} and Ser^{375} (the last two residues are phosphorylated after etorphine or DAMGo treatment) on C-terminus (208), we generated a mutant of MOR (3A) which have three point mutations: S363A, T370A and S375A. To determine the role played by the receptor phosphorylation in activating G protein-related signaling pathways (e.g. PKC pathway), two cell lines (HEKHM and HEK3A cells) and four agonists (morphine, etorphine, fentanyl and DAMGO) were used. HEKHM and HEK3A cells have similar receptor expression levels: 6.3±0.4 and 5.8±0.2 pmol/mg protein, respectively. The four agonists were used at equivalent concentrations, morphine and DAMGO at 1μM, while etorphine and fentanyl at 10nM (148). Because the phosphorylation sites of MOR have been demonstrated to be the Ser^{363}, Thr^{370} and Ser^{375} on the C-terminus domain (208), the antibody against phosphorylated Ser^{375} of MOR (pS^{375}) and the antibody against

phosphorylated amino acids (pAAs) were used to monitor the phosphorylation status of MOR.

In HEKHM cells, agonists except morphine induced significant increase in MOR phosphorylation (Fig. 3-12A). Although the fentanyl-induced phosphorylation on Ser^{375} (29±7.3 folds of basal level, n=4) was lower than those induced by etorphine (43±4.2 folds, n=4) and DAMGO (45±5.6 folds, n=4), it is much higher than that induced by morphine (5.3±1.1 folds, n=4). When HEK3A cells were activated by these four agonists, increase in the receptor phosphorylation was not observed, confirming MOR3A is a phosphorylation deficient mutant of MOR (Fig. 3-12B).

3.5.1.2 Agonist-selective regulation on PKC substrates

As the important protein kinase in a variety of biological processes, PKC exerts its functions by phosphorylating its downstream substrates (150). An antibody against the phosphorylated PKC substrates was used to detect the activation of PKC. As indicated in Fig. 3-12A, morphine (165±13%, n=4) but not etorphine (103±7%, n=4) or DAMGO (98±8%, n=4) increased the amount of phosphorylated PKC substrates. Consistent with its lower ability to induce receptor phosphorylation, fentanyl also increased the amount of phosphorylated PKC substrates, although the increase (123±11%, n=4) was smaller than that induced by morphine. However, in the HEK3A cells where agonist-induced MOR phosphorylation was not observed, all four agonists increased the amount of phosphorylated PKC substrates: morphine (161±4%, n=4), etorphine (135±7%, n=4), fentanyl (158±4%, n=4) and DAMGO (136±6%, n=4) (Fig. 3-12B).

3.5.1.3 Agonist-selective PKC activation

PKC is a protein kinase family and is divided into three subfamilies, conventional, atypical and novel depending on their activation mechanisms (150). PKCε is the subtype mediating MOR functions including: tolerance, ERK phosphorylation and

Fig. 3-12 Receptor phosphorylation

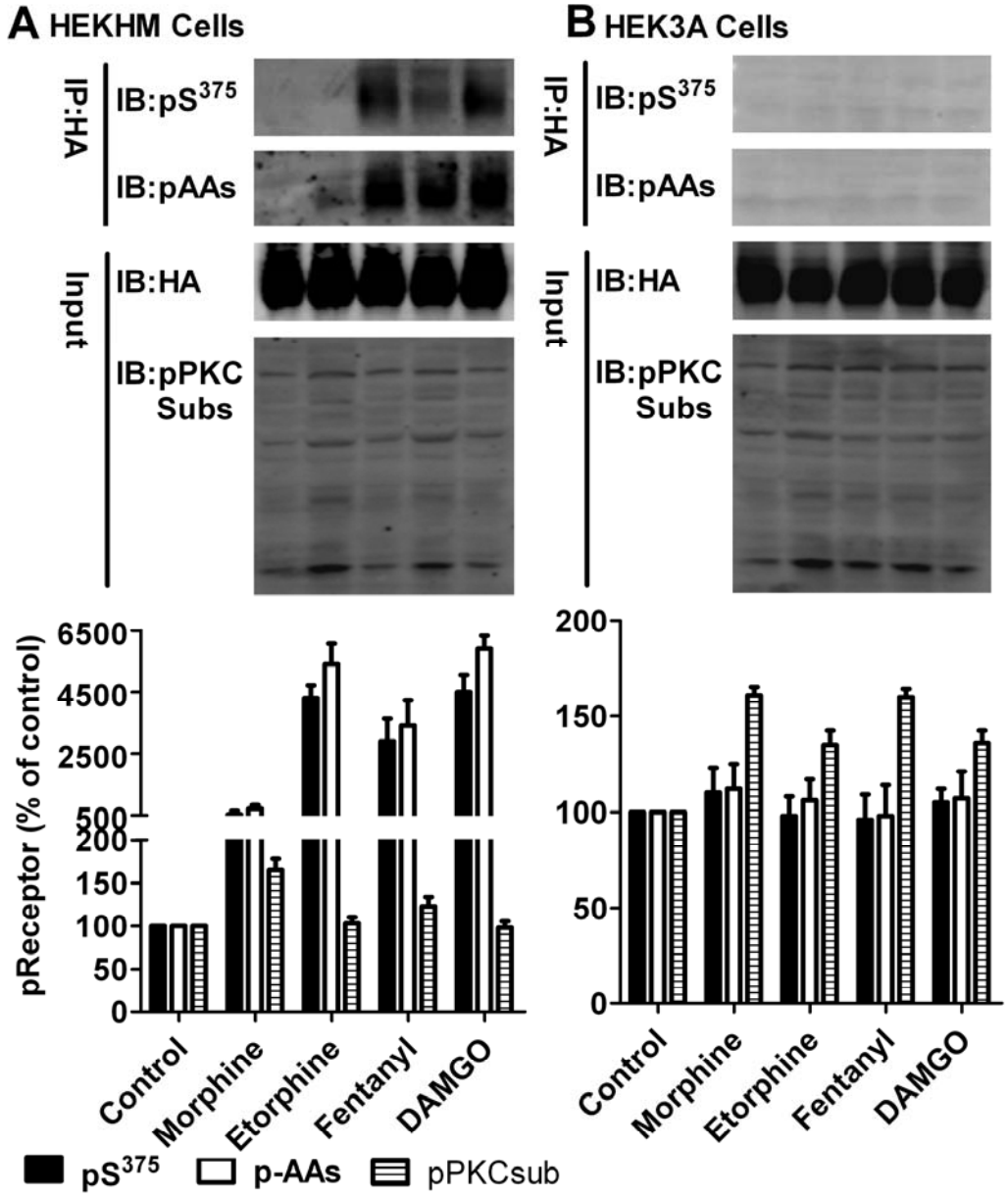

Fig. 3-12 Receptor phosphorylation

HEKHM and HEK3A cells were treated with PBS (control), 1 μM morphine, 10 nM etorphine, 10 nM fentanyl or 1 μM DAMGO for 10 minutes. The receptor were immunoprecipitated with the HA antibody. The phosphorylated Ser^{375} on MOR (pS^{375}) and the phosphorylated amino acids (pAAs) were measured in the immunoprecipitated MOR to indicate the receptor phosphorylation. The amounts of phosphorylated PKC substrates were determined in the inputs. The experiment was repeated for at least four times and the error bars stood for the standard deviations.

desensitization on intracellular calcium release (148, 165). To further confirm this observation, the activities of PKCα, PKCγ and PKCε were determined with a PKC activity assay kit from Cell Signaling. Briefly, PKC subtypes were immunoprecipitated by subtype-specific antibodies, and the kinase activities of these subtypes were determined by incubating with a general PKC substrate. The amount of the PKC substrate being phosphorylated after incubation represented the activities of PKC subtypes. Substrate concentration and incubation time were titrated in order to make sure that the results locate in the linear region of the stand curve.

As predicted, morphine induced the activation of PKCε, but not PKCα or PKCγ in HEKHM cells. Fentanyl was the only agonist among other three that activated PKCε, although to a much less extent (178±21%, n=4) than did morphine (314±34%, n=4) (Fig. 3-13A). These results correlated with the amounts of phosphorylated PKC substrates (Fig. 3-13A). When the activities of PKC subtypes were determined in the HEK3A cells with the same kit, all four agonists activated PKCε significantly (Fig. 3-13B). Etorphine and DAMGO induced lower activation of PKCε (248±22% and 267±35%, n=4) than did morphine and fentanyl (335±37% and 317±18%, n=4).

In summary, PKCε activation was induced in a rank order of morphine>fentanyl>etorphine and DAMGO, while receptor phosphorylation was induced in a rank order of etorphine and DAMGO>fentanyl>morphine. Thus there is a strong inverse correlation between PKCε activation and receptor phosphorylation. In HEK3A cells, all four agonists activated PKCε while receptor phosphorylation was not observed. Therefore the abilities of agonists to activate PKCε inversely correlate with their abilities to induce receptor phosphorylation. That is receptor phosphorylation attenuates PKCε activation.

Fig. 3-13 PKC activation induced by agonists

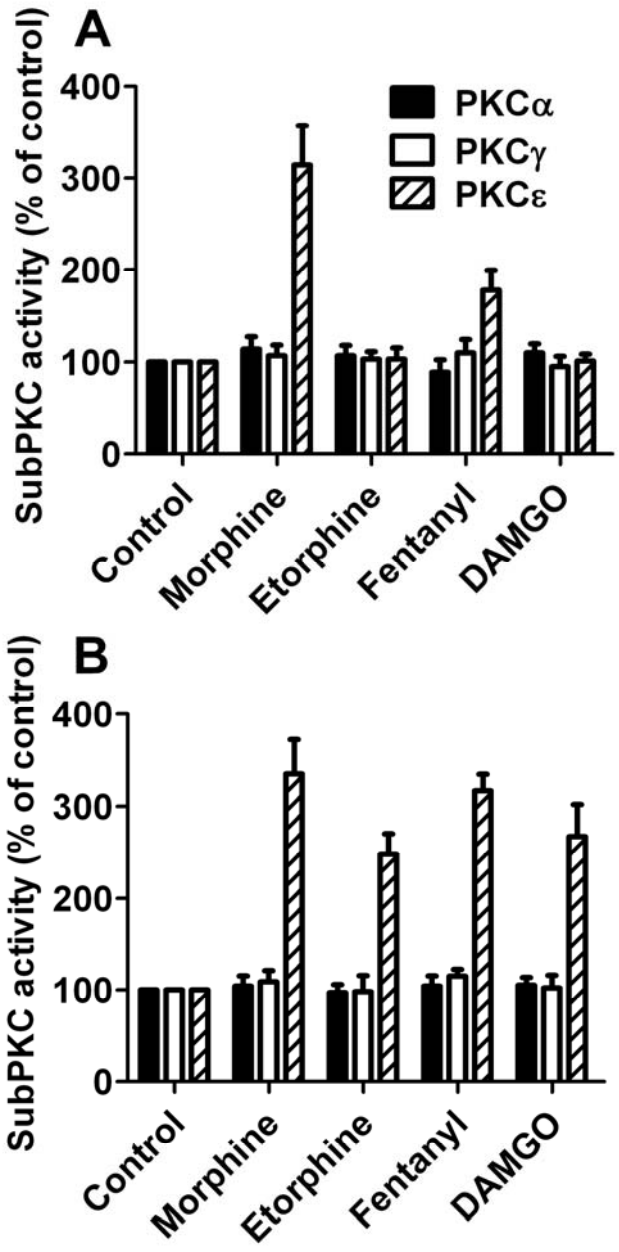

Fig. 3-13 PKC activation induced by agonists

HEKHM and HEK3A cells were treated with PBS (control), 1 μM morphine, 10 nM etorphine, 10 nM fentanyl or 1 μM DAMGO for 10 minutes. The activities of PKC subtypes were measured. The experiment was repeated for at least four times and the error bars stood for the standard deviations.

3.5.2 Cholesterol

3.5.2.1 Cholesterol functions

Cholesterol, the major sterol in animal tissues, is amphipathic, with a polar head group (the hydroxyl group at C-3) and a non-polar hydrocarbon body (the steroid nucleus and the hydrocarbon side chain at C-17) about as long as 16-carbon fatty acid in its extended form. Cholesterol is an essential component of mammalian cell membranes where it is required to establish proper membrane permeability and fluidity (209). In addition, cholesterol is an important precursor molecule for the biosynthesis of bile acids, steroid hormones, and several fat soluble vitamins. Synthesis of cholesterol within the body starts with one molecule of acetyl CoA and one molecule of acetoacetyl-CoA, which are dehydrated to form 3-hydroxy-3-methylglutaryl CoA (HMG-CoA). This molecule is then reduced to mevalonate by the enzyme HMG-CoA reductase. This step is an irreversible step in cholesterol synthesis (210, 211) .

Cholesterol contributes to GPCR signaling by supporting the entirety of lipid raft microdomain. Currently, the influence of lipid raft microdomain on GPCR signaling is illustrated by using the cholesterol lowering chemicals. Methyl-β-cyclodextrin (MβCD) removes cholesterol from cultured cells by forming soluble inclusion complexes with cholesterol, thereby enhancing its solubility in aqueous solution (212). The statins (or HMG-CoA reductase inhibitors) are a class of drugs that lower cholesterol levels in people with or at risk of cardiovascular disease. They lower cholesterol by inhibiting the enzyme, HMG-CoA reductase, which is the rate-limiting enzyme of cholesterol synthesis.

3.5.2.2 Cholesterol in the central nervous system

Cholesterol is enriched in the central nervous system. Higher cholesterol content (2% body weight accounts for 25% cholesterol) has been identified in the central

nervous system. A tighter regulation of cholesterol metabolism was also detected in the central nervous system, suggesting the involvement of cholesterol in a variety of processes in the central nervous system (213-216). Moreover, many GPCRs are expressed in the central nervous system and function as recipients of various signals (217). Thus the interaction between cholesterol and GPCRs should affect many aspects of neuronal circuit, presumably via the cholesterol-rich microdomain.

3.5.2.3 Cholesterol affects MOR distribution

To study the effects of cholesterol on MOR, simvastatin and AY9944 were used to reduce the cholesterol level within the cells. Simvastatin, as an inhibitor of HMG-CoA reductase, blocks cellular synthesis of cholesterol at the initial step (218). AY9944, blocks the last step of cholesterol synthesis, from lanosterol to cholesterol (219). After treating cells with these two inhibitors together with serum-free incubation, the cellular cholesterol levels were measured. Both inhibitors decreased cholesterol concentration in the whole cells and on cell membrane (Fig. 3-14). These decreases in cholesterol could be reversed by providing high concentration of cholesterol in the medium.

The effects of simvastatin and AY9944 on lipid raft were further demonstrated by determining the cholesterol concentration in each fraction of a continuous sucrose gradient (5%-30%), which separates the microdomains on cell membrane depending on their densities. Normally cholesterol concentration peaked in the 4^{th} and the 5^{th} fractions, indicating the existence of lipid raft in these fractions (Fig. 3-15). Simvastatin and AY9944 destructed such cholesterol enrichment or lipid raft as indicated by the larger decrease in cholesterol levels in the 4^{th} and the 5^{th} fractions than in the other fractions. However, using 20 ng/ml cholesterol restored the cholesterol enrichment.

Fig. 3-14 Simvastatin decreases cellular cholesterol

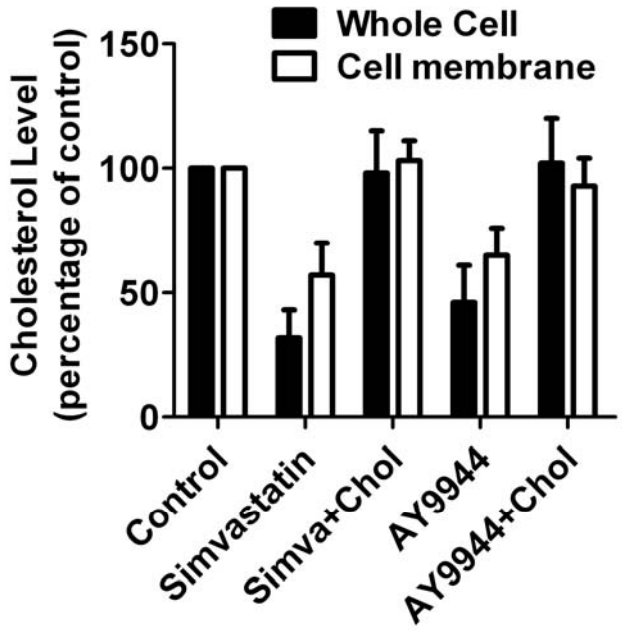

Fig. 3-14 Simvastatin decreases cellular cholesterol

HEKHM celles with serum free medium was treated with PBS (control), 0.5 μM simvastatin, 0.5 μM simvastatin with 20 ng/ml cholesterol, 1 μM AY9944 or 1 μM AY9944 with 20 ng/ml cholesterol overnight. The cholesterol levels were determined both in whole cell but also on the cell membrane. he results were presented as the percentages of those in control samples in each group. The experiment was repeated for at least four times and the error bars stood for the standard deviations.

Fig. 3-15 Simvastatin disrupts the lipid raft

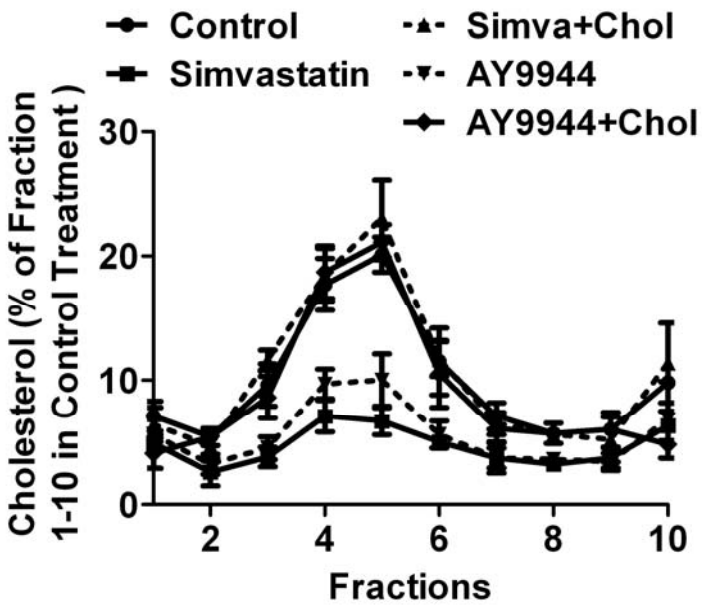

Fig. 3-15 Simvastatin disrupts the lipid raft

HEKHM celles with serum free medium was treated with PBS (control), 0.5 μM simvastatin, 0.5 μM simvastatin with 20 ng/ml cholesterol, 1 μM AY9944 or 1 μM AY9944 with 20 ng/ml cholesterol overnight. The cholesterol levels were determined in each fraction and normalized against the total cholesterol levels in the first 10 fraction in control cells. The experiment was repeated for at least four times and the error bars stood for the standard deviations.

At the same time, the location of MOR on cell membrane was determined by measuring the immunoreactivities of MOR in each fraction. In control cell, MOR and Gαi2 were enriched in lipid raft. However, in simvastatin- or AY9944-treated cells, translocations of MOR and Gαi2 were observed. Translocations were summarized as the distribution of MOR in sucrose gradient as indicated by the ratio of MOR amount in lipid raft (fraction 4) to that in non-raft (fraction 6) microdomains (Fig. 3-16). The ratio of MOR amount in the sixth to that in the fourth fraction was 3.48±0.23 and 3.01±0.32 in the simvastatin- and AY9944-treated cells respectively. In addition, the ability of high cholesterol medium to reverse the translocation suggested the two chemicals functions by lowering cholesterol. Thus decreasing cholesterol content disrupts the lipid raft and leads to the translocation of MOR from lipid raft to non-raft microdomain.

3.5.2.4 Cholesterol affects MOR- Gαi2 interaction

MOR is anchored to lipid raft through its interaction with Gαi2. In addition, Gαi2 mediates many signals transduced by MOR, including adenylyl cyclase inhibition and morphine-induced ERK phosphorylation. Two assays were used to determine the interaction between Gαi2 and MOR under the usages of simvastatin. Firstly, the co-localization of receptor and Gαi2 was measured by using immunofluorescence techniques (Fig. 3-17). Then, the association of Gαi2 with receptor was further determined by co-immunoprecipitation (Fig. 3-18). Simvastatin resulted in a dissociation of Gαi2 from receptor complex. Confocal immunofluorescence microscopy indicated that simvastatin reduced the colocalization of MOR with Gαi2 from 71±12% to 45±13% in HEKHM cells. Similarly, simvastatin decreased the coimmunoprecipitation of Gαi2 and MOR to 68±12% of control level.

Fig. 3-16 Simvastatin translocates MOR

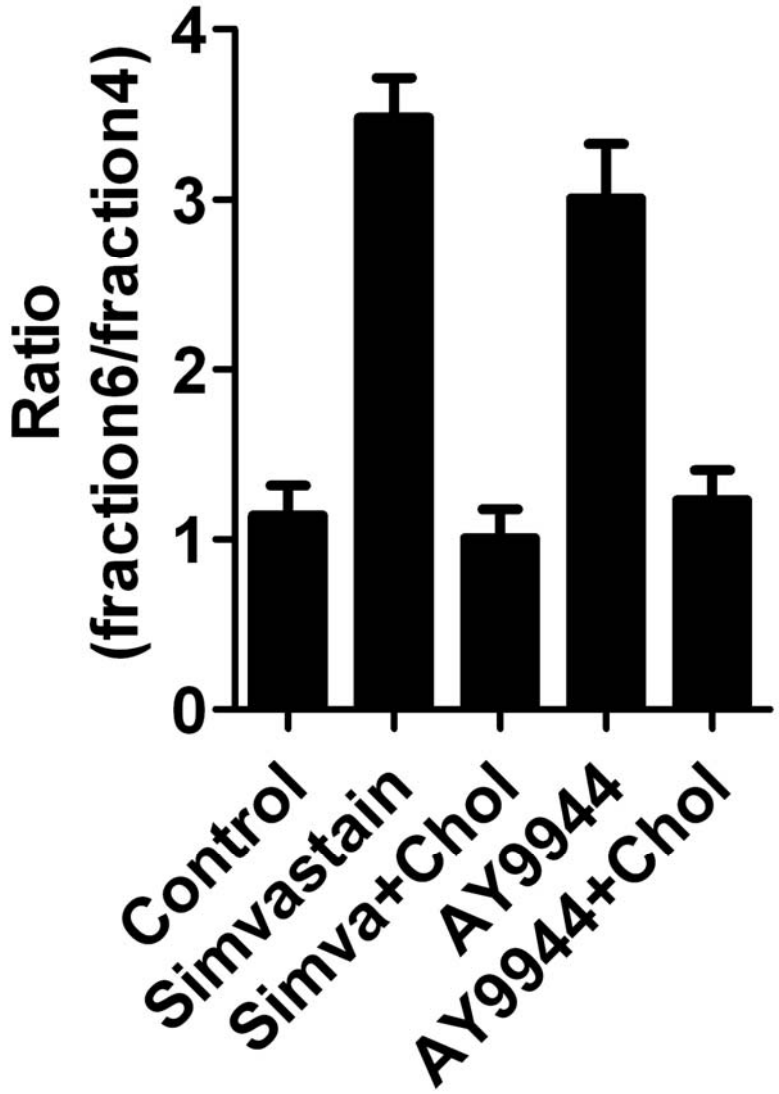

Fig. 3-16 Simvastatin translocates MOR

HEKHM celles with serum free medium was treated with PBS (control), 0.5 μM simvastatin, 0.5 μM simvastatin with 20 ng/ml cholesterol, 1 μM AY9944 or 1 μM AY9944 with 20 ng/ml cholesterol overnight. The ratio of the MOR amounts in the fraction 6 and fraction 4 was listed. The experiment was repeated for at least four times and the error bars stood for the standard deviations.

Fig. 3-17 Receptor-Gαi2 interaction by immunofluorescence

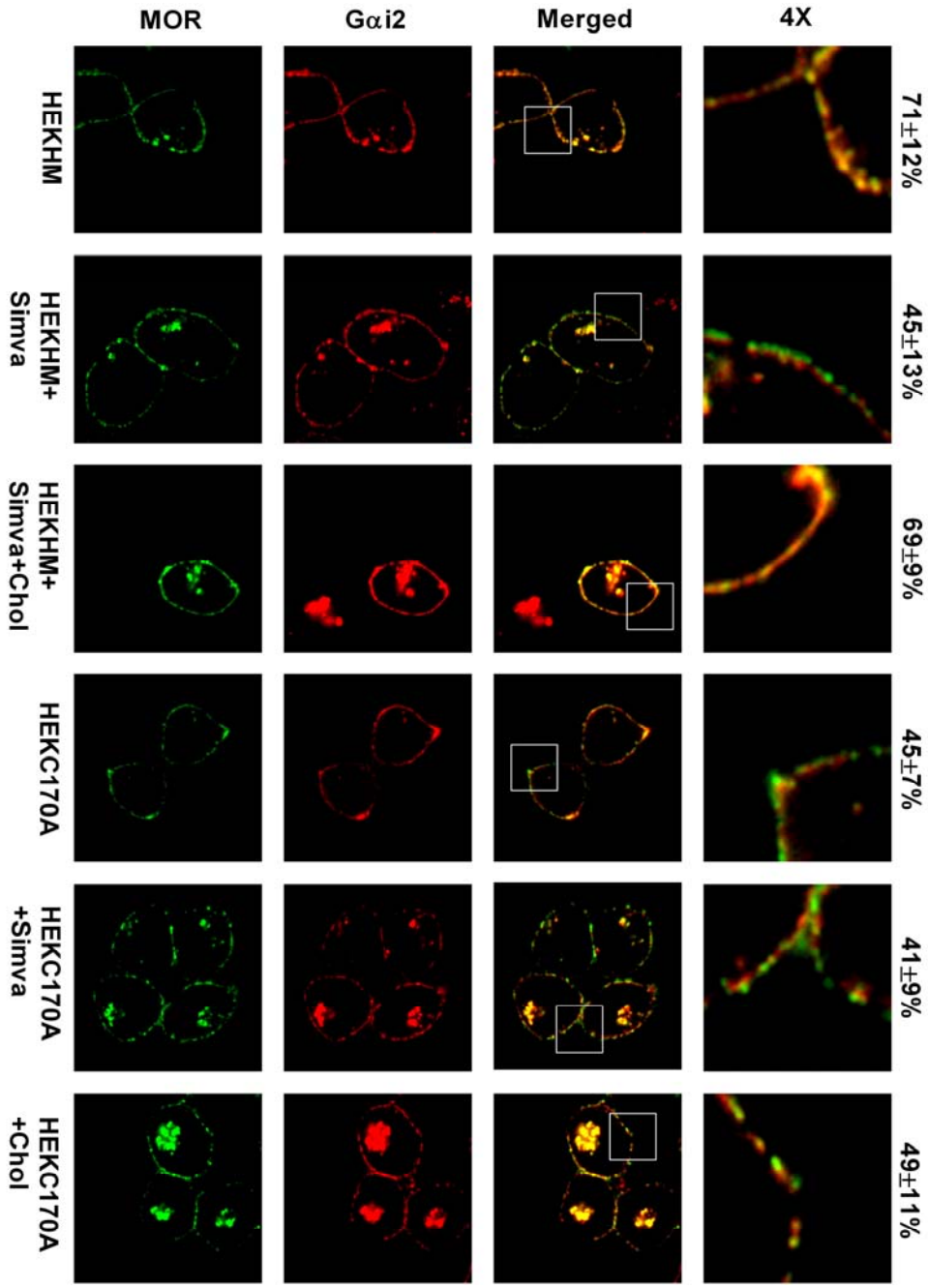

Fig. 3-17 Receptor-Gαi2 interaction by immunofluorescence

Six groups of cells were used: HEKHM, HEKHM treated with 0.5 μM simvastatin overnight (HEKHM+Simva), HEKHM treated with 0.5 μM simvastatin and 20 ng/ml cholesterol (HEKHM+Simva+Chol), HEKC170A, HEKC170A treated with 0.5 μM simvastatin overnight (HEKC170A+Simva) and HEKC170A treated with 20 ng/ml cholesterol (HEKC170A+Chol). Receptor was labeled with HA antibody and Alexa 488. Gαi2 was labeled with Gαi2 antibody and Alexa 594. Colocalization of Gαi2 with MOR was calculated after merging the two color channels. The percentage of colocalization was indicated beside. 8-12 independent images were analyzed per group.

Fig. 3-18 Receptor-Gαi2 interaction by immunoprecipitation

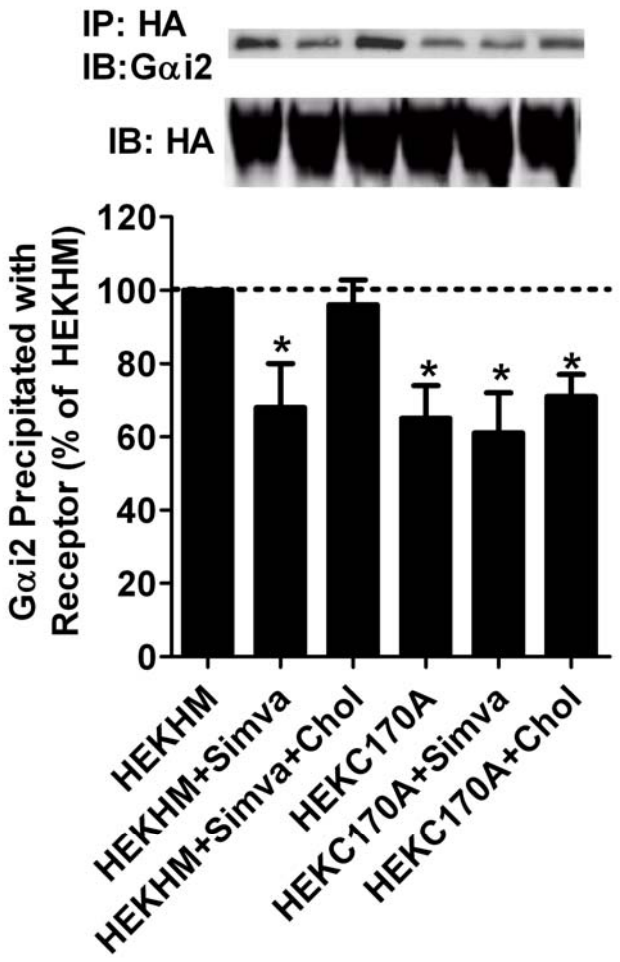

Fig. 3-18 Receptor-Gαi2 interaction by immunoprecipitation

Cells were treated as in Fig. 3-17. HA-antibody was used to precipitate MOR. The amounts of Gαi2 co-immunoprecipitated with receptor were normalized against that observed in HEKHM. Experiments were repeated for four times. The experiment was repeated for at least four times and the error bars stood for the standard deviations.

3.5.2.5 Cholesterol affects Gαi2-related signaling

Two signal events, adenylyl cyclase inhibition and morphine-induced ERK phosphorylation (both of them are Gαi2-related) were tested, and two MOR agonists, morphine and etorphine, were used after simvastatin treatment. Simvastatin blocked adenylyl cyclase inhibition induced by either morphine or etorphine (Table 3-1). Similar observations were obtained with morphine-induced ERK phosphorylation. Simvastatin attenuated ERK phosphorylation induced by morphine from 238.6±10.1% to 132.6±16.2%. In contrast, etorphine-induced ERK phosphorylation was not influenced by simvastatin (Table 3-1). Thus cholesterol is required to support the Gαi2-related signaling but not the β-arrestin-related signaling.

3.5.3 Palmitoylation

3.5.3.1 Palmitoylation on GPCRs

Palmitoylation is a covalent attachment of fatty acids (usually the 16-carbon palmitic acid) to cysteine residues of membrane proteins via a thioester bond. Palmitoylation enhances protein hydrophobicity and contributes to their membrane associations. Palmitoylation of GPCRs has been reported extensively (220). Sequence alignment has identified the cysteine residues in C-termini as potential palmitoylation sites in about 78% of 74 GPCRs examined (221). However, these cysteines are not the only palmitoylation sites. Although rat MOR has two cysteines (Cys^{346} and Cys^{351}) in C-terminus, mutation of these cysteines did not eliminate the palmitoylation (222), suggesting that Cys^{170} (the only other intracellular cysteine of rat MOR) may be the palmitoylation site of MOR (222). Similarly, V_{1A} vasopressin receptor also has a palmitoylation site outside C-terminus (223).

Table 3-1 Cholesterol and palmitoylation affect MOR signaling

	Morphine			Etorphine		
	AC inhibition		Phos-ERK	AC inhibition		Phos-ERK
	K_I nM	Max. Inh. %	% of Control	K_I nM	Max. Inh. %	% of Control
HEKHM	9.3±2.4	87.6±3.4	238±10	0.09±0.01	87.9±3.7	235±11
HEKHM+Simva	**25.8±6.1**	**42.1±2.1**	**133±16**	**0.31±0.06**	**40.5±4.5**	232±19
HEKHM+Simva+Chol	11.3±2.1	85.4±6.1	221±14	0.10±0.02	82.3±4.2	237±21
HEKC170A	**15.9±3.8**	**62.9±3.7**	**179±18**	**0.16±0.03**	**60.6±2.3**	221±13
HEKC170A+Simva	**26.7±5.4**	**40.7±3.1**	**125±11**	**0.29±0.05**	**42.3±3.1**	227±12
HEKC170A+Chol	**14.7±2.5**	**55.6±2.7**	**184±17**	**0.16±0.02**	**57.2±3.1**	236±34

Table 3-1 Cholesterol and palmitoylation affect MOR signaling

0.5 μM simvastatin and 20 ng/ml cholesterol were used to treat HEKHM and HEKC170A overnight. 1μM morphine and 10nM etorphine were used to treat the cells for 5 minutes before measuring ERK phosphorylation. A series does of morphine or etorphine was used to determine the dose response of the two agonists to induce AC inhibition. In each treatment, the ERK phosphorylation and AC inhibition induced by agonists were normalized to the basal levels.

3.5.3.2 Functions of palmitoylation

Palmitoylation of GPCRs is a dynamic process. Palmitic acid linked to GPCR is chemically labile and turns over rapidly. Palmitoylation targets proteins to the correct membrane location and also contributes to GPCR signaling (224). Both of the two functions are related to receptor-G protein interaction. On the one hand, take MOR as an example, lipid raft marker Gαi2 (195) couples with MOR in the absence of agonist, anchoring it to the lipid raft microdomain (172). On the other hand, G proteins mediate almost all GPCR signaling, although β-arrestin-dependent G protein-independent signaling has also been reported (225). Decreased receptor-G protein interaction attenuates receptor signaling significantly (4). In addition, palmitoylation-dependent receptor-G protein interaction is observed with both β2-adrenergic receptor and M2 muscarinic acetylcholine receptor, even though negative responses have also been observed with the α2A-adrenergic receptor and dopamine D1 receptor (226-229).

3.5.3.3 Palmitoylation assay

Palmitoylation site on MOR was identified by using a recently reported palmitoylation assay (230). Briefly, target protein is concentrated initially by immunoprecipitation. After blocking the free sulfhydryl groups with N-ethylmaleimide (NEM) and hydrolyzing the palmitoylation with hydroxylamine, the assay links biotin to the depalmitoylated cysteines with 1-biotinamido-4- [4′-(maleimidomethyl) cyclohexane carboxamido] butane (btn-BMCC). The immunoreactivity of biotin indicates the palmitoylation of target protein. The technique reportedly has a higher sensitivity than labeling with [^{3}H]-palmitate (230). In the current study, HEKWT and HEKHM cells were used to validate the assay. Receptor was immunoprecipitated with purified MOR antibody and then subjected to the palmitoylation assay.

High level of palmitoylated MOR was detected in HEKHM, as indicated by the high level of biotin immunoreactivity (Fig. 3-19, lane 2). However, immunoreactivity of

Fig. 3-19 Palmitoylation assay.

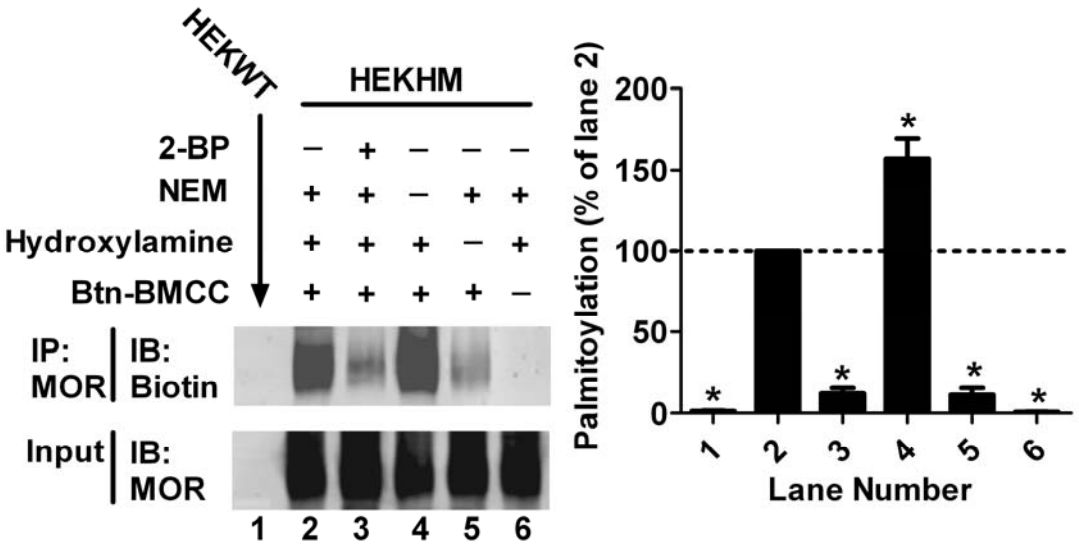

Fig. 3-19 Palmitoylation assay

Palmitoylation assays were performed in HEKWT and in HEKHM after OPRM1 immunoprecipitation. The amounts of palmitoylated receptor were determined by measuring biotin immunoreactivities as described in *Materials and Methods*. The amounts of palmitoylated receptor were normalized against that in HEKHM (lane 2). 50 μ M 2-BP was used to treated HEKHM for 12 hours (Lane 3). Individual steps (treatment with NEM, hydroxylamine or btn-BMCC) were omitted to validate the assay (lane 4-6). Experiments were repeated for four times. Data were analyzed by one-way ANOVA with Dunnett-test as post-hoc test to do comparisons. The error bars and "*" presented the standard deviations and significant difference from lane 2, respectively.

biotin in HEKWT (Fig. 3-19, lane 1) was only 1.2±0.4% (n=4, q=25.46, p<0.001) of that in HEKHM, suggesting the palmitoylation detected is specific to MOR. The immunoreactivity of biotin increased when the free sulfhydryl groups were not blocked (Fig. 3-19, lane 4, 157±12%, n=4, q=14.69, p<0.001), whereas decreased when hydroxylamine-mediated depalmitoylation (Fig. 3-19, lane 5, 11.5±4.2%, n=4, q=22.89, p<0.001) or btn-BMCC-mediated biotinylation was omitted (Fig. 3-19, lane 6, 0.7±0.2%, n=4, q=25.59, p<0.001) (Fig. 3-19). Low level of receptor palmitoylation (12.3±3.4% of that in HEKHM, n=4, q=22.60, p<0.001) was also observed when HEKHM were treated for 12 hours with the palmitoylation inhibitor, 2-BP (Fig. 3-19, lane 3). Therefore this palmitoylation assay is suitable to detect the palmitoylation of MOR.

3.5.3.4 Palmitoylation site on MOR

Mutating two conserved cysteine residues (Cys^{346} and Cys^{351}) in C-terminus of MOR does not affect MOR palmitoylation (222). Thus the only other intracellular cysteine of MOR, Cys^{170}, is the putative palmitoylation site. Cys^{170}, Cys^{346} and Cys^{351} were mutated individually to Ala to generate C170AMOR, C346AMOR and C351AMOR, respectively. These mutated receptors were expressed stably in HEK293 cells to obtain three stable cell lines: HEKC170A, HEKC346A and HEKC351A. The levels of receptor expressed in these cell lines were determined using a [^{3}H]-diprenorphine binding assay to ensure that similar amounts of receptor were used in subsequent studies (Fig. 3-20A).

Receptor palmitoylation was then determined in these cell lines, as well as in HEKWT and HEKHM. Consistent with previous report (222), similar amounts of palmitoylated receptor were detected in HEKHM, HEKC346A (113±17% of that in HEKHM, n=4, q=2.028, p>0.05) and HEKC351A (109±13% of that in HEKHM, n=4, q=1.404, p>0.05) (Fig. 3-20B). However, mutation of Cys^{170} to Ala blocked receptor palmitoylation significantly, the amount of palmitoylated receptor in HEKC170A was

Fig. 3-20 Cys^{170} is the palmitoylation site on OPRM1.

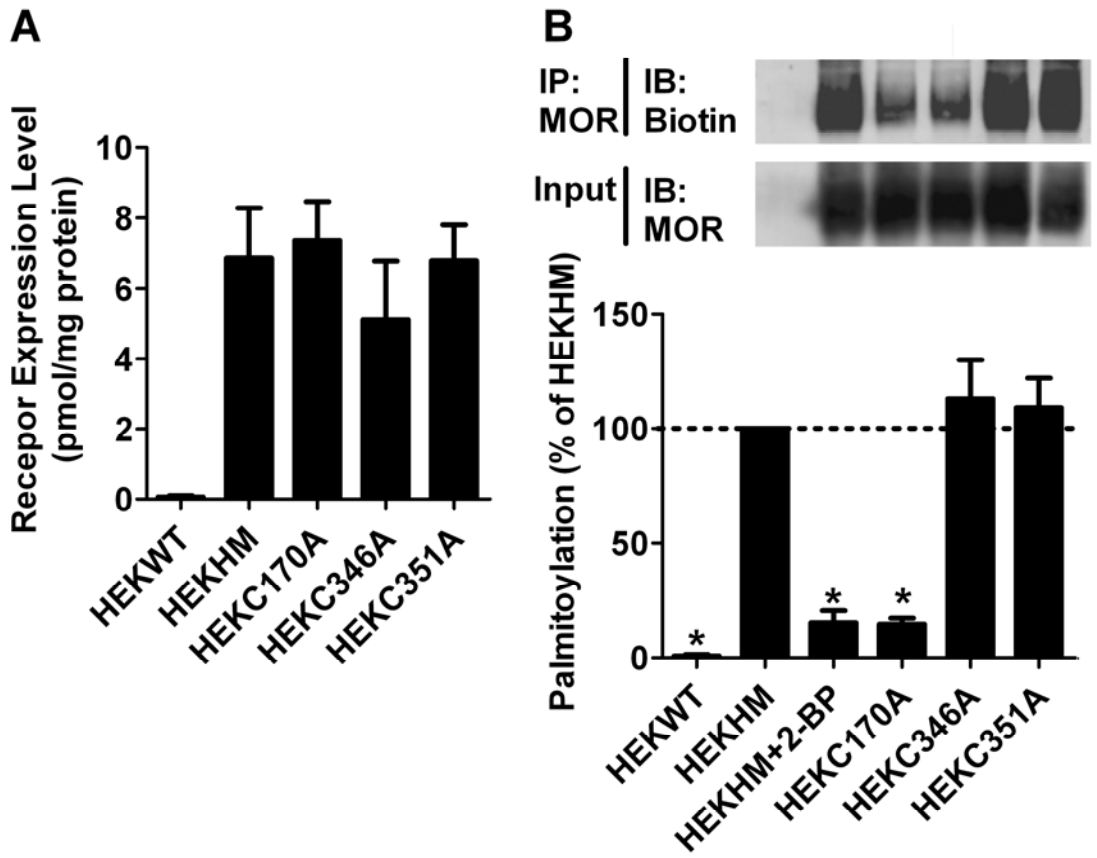

Fig. 3-20 Cys^{170} is the palmitoylation site on OPRM1.

(A) Expression levels of OPRM1 in HEKWT, HEKHM, HEKC170A, HEKC346A and HEKC351A were determined by ^{3}H-diprenorphine binding.

(B) Palmitoylation assays performed in HEKWT, HEKHM, HEKC170A, HEKC346A and HEKC351A. The amounts of palmitoylated receptor were normalized against that in HEKHM (lane 2). 50 μM 2-BP was used to treated HEKHM for 12 hours (Lane 3). The influences of cysteine mutations on receptor palmitoylation were determined in lane 4-6. Experiments were repeated for four times. Data were analyzed by one-way ANOVA with Dunnett-test as post-hoc test to do comparisons. The error bars and "*" presented the standard deviations and significant difference from lane 2, respectively.

only 14.7±2.6% (n=4, q=12.31, p<0.001) of that in HEKHM, similar to the amount observed when 2-BP was used to treat HEKHM (Fig. 3-20B).

3.5.3.5 Palmitoylation affects MOR-Gαi2 interaction

Two assays were used to determine the interaction between Gαi2 and MOR. Firstly, the co-localization between receptor and Gαi2 was measured by using immunofluorescence techniques (Fig. 3-17). Then, the association of Gαi2 with receptor was further determined by co-immunoprecipitation (Fig. 3-18). Blocking receptor palmitoylation resulted in a dissociation of Gαi2 from receptor. Confocal immunofluorescence microscopy indicated that blocking receptor palmitoylation reduced the colocalization of MOR with Gαi2 from 71±12% to 45±7%. Similarly, blocking receptor palmitoylation decreased the co-immunoprecipitation of Gαi2 with MOR to 65±9% of control level.

3.5.3.6 Palmitoylation affects MOR signaling

To determine the influence of palmitoylation on receptor signaling, morphine-induced adenylyl cyclase inhibition and ERK phosphorylation were monitored. Morphine maximally inhibited adenylyl cyclase activity by 87.6±3.4% (n=4, t=6.980, p<0.001) in HEKHM, while only by 62.9±3.7% (n=4, t=20.88, p<0.001) in HEKC170A (Table 3-1). Hence, the abilities of morphine to inhibit adenylyl cyclase activity in these two cell lines were different significantly. In addition, morphine increased the amount of phosphorylated ERK to 238±10% of basal levels (n=4, t=36.61, p<0.001) in HEKHM, but to 179±18% in HEKC170A (n=4, t=20.96, p<0.001) (Table 3-1). Hence the abilities of morphine to induce ERK phosphorylation in these two cell lines were different significantly (t=15.65, p<0.001). Therefore MOR signaling is attenuated when receptor palmitoylation is blocked.

Both signaling events monitored above require Gαi2 (172). However, MOR also transduces G protein-independent signaling. For example, etorphine-induced adenylyl cyclase inhibition requires Gαi2, but etorphine-induced ERK phosphorylation depends on β-arrestin2 (95, 172). Thus etorphine was used to examine the effects of receptor palmitoylation. Adenylyl cyclase inhibition induced by etorphine was attenuated when receptor palmitoylation was blocked, 87.9±3.7% in HEKHM and 60.6±2.3% in HEKC170A ($n=4$, $t=14.76$, $p<0.001$). However, etorphine-induced ERK phosphorylation was not affected: 235±11% of basal level in HEKHM and 221±13% in HEKC170A ($n=4$, $t=2.325$, $p>0.05$) (Table 3-1). Thus receptor palmitoylation contributes to the Gαi2-, but not β-arrestin2-, related signaling.

4. Downstream events

Although the observations of agonist-selective signaling and the mechanisms of agonist-selective signaling are important, the downstream events result from agonist-selective signaling is more critical for providing the implication of agonist-selective signaling on a variety of biological processes.

4.1 Agonist-selective gene expression

4.1.1 Agonist-selective location of phosphorylated ERK

G protein-dependent and β-arrestin-dependent activation of ERK results in the different cellular locations of the activated enzymes. Generally, β-arrestin-activated ERK retains in the cytosol, while the PKC-activated ERK translocates into the nucleus (231). Whether MOR-mediated ERK phosphorylation will follow this cellular translocation scenario remains to be demonstrated.

In order to investigate the cellular location of phosphorylated ERK, nucleus fractions were separated after agonist treatment. Phosphorylated ERK in nucleus fractions isolated from etorphine-treated cells was 220±30% of that in nucleus fractions isolated from control cells (Fig. 4-1A). In contrast, 1 μM morphine did not lead to a significant nuclear translocation of phosphorylated ERK at either 10 minutes or 20 minutes after treatment. Successful nucleus isolation from cytosol fractions could be demonstrated by the absence of β-actin and Rab4 immunoreactivities in the isolated nucleus fractions and the absence of histone 3 immunoreactivities in the isolated cytosol fractions (Fig.4-1A). Concentration-dependent studies with the two agonists illustrated the same phenomena. Morphine did not induce ERK translocation even at 10 μM, while etorphine-induced ERK translocation could be observed at 10nM (Fig.4-1B). Thus morphine-activated ERK is retained in cytocol, while etorphine-activated ERK translocates into the nucleus.

In order to obtain broader understanding of agonist-selective ERK phosphorylation, we tested additional clinical relevant agonists such as methadone and fentanyl. The four agonists equally activated ERK, but induced the nuclear translocation of phosphorylated ERK differentially (Fig. 4-2). Fentanyl increased the amount of phosphorylated ERK in the nucleus similarly to etorphine, while morphine and methadone could not (Fig. 4-2). Hence morphine and methadone use PKC pathway for ERK phosphorylation and retain

Fig. 4-1 Etorphine induces ERK translocation

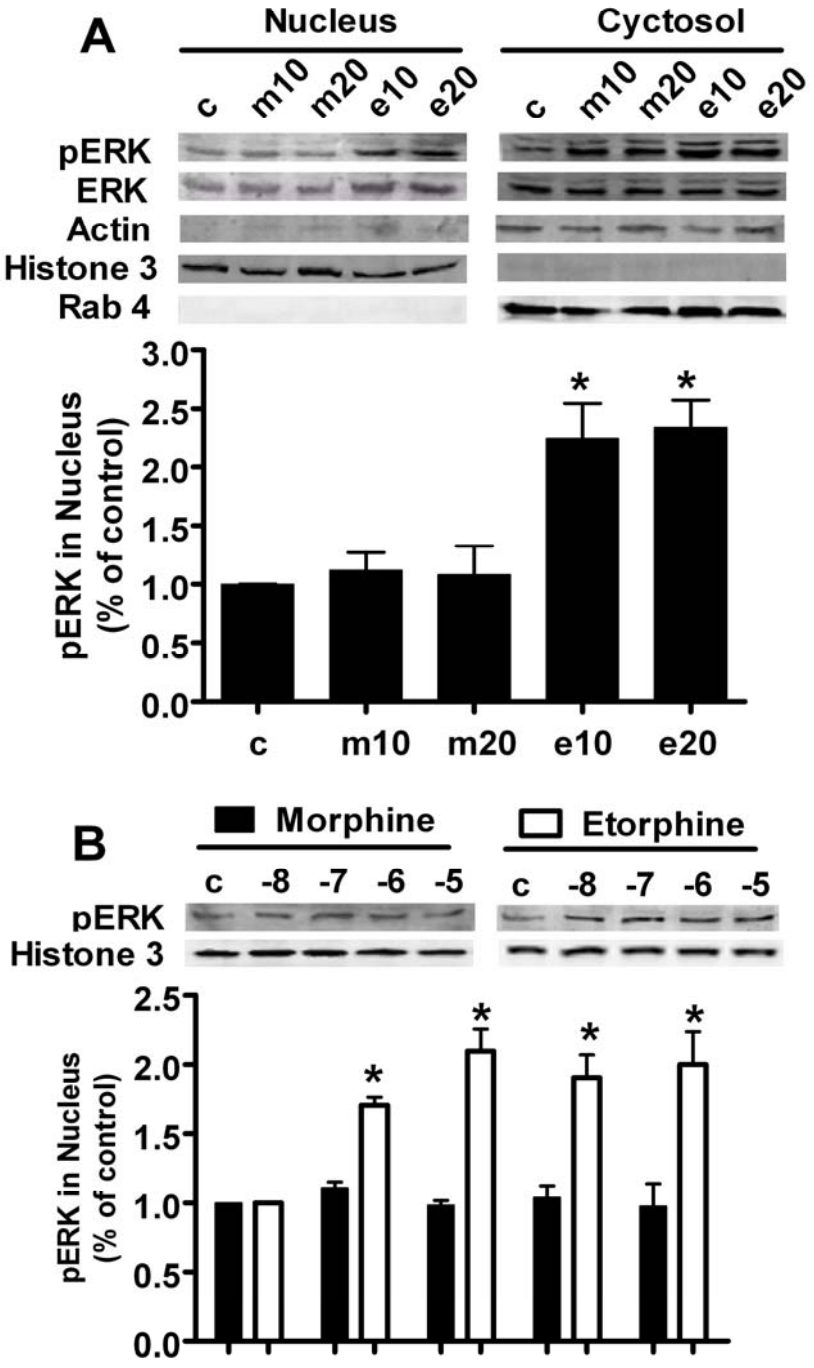

Fig. 4-1 Etorphine induces ERK translocation

HEKHM cells were treated with morphine and etorphine for indicated time and at indicated concentration. The amounts of phosphorylated ERK were used to indicate the ERK translocation. The experiment was repeated for at least four times and the error bars stood for the standard deviations.

Fig. 4-2 Agonists induce ERK translocation differentially

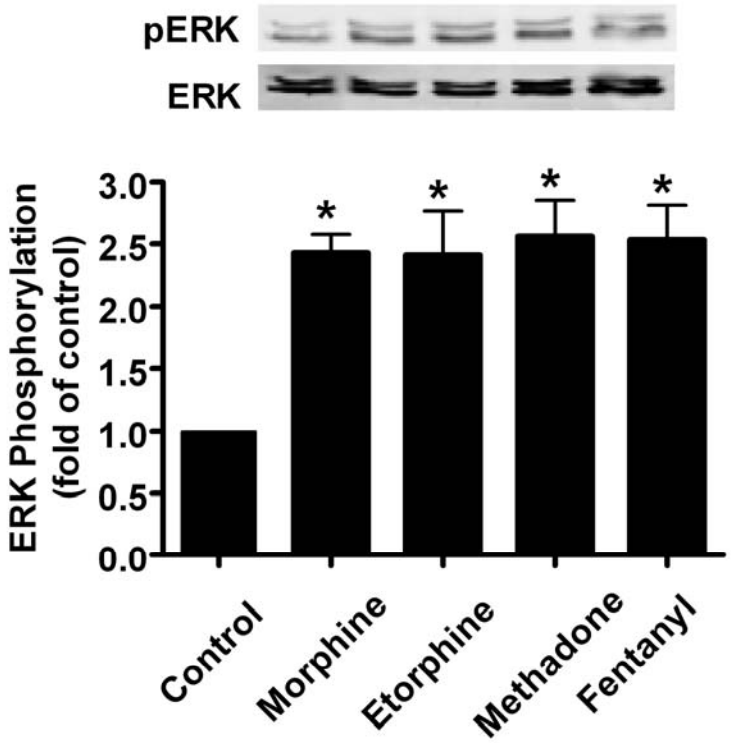

Fig. 4-2 Agonists induce ERK translocation differentially

HEKHM cells were treated with PBS (control), 1 μM morphine, 10 nM etorphine, 10 nM fentanyl or 1 μM methadone for 10 minutes. The amounts of phosphorylated ERK were used to indicate the ERK translocation. The experiment was repeated for at least four times and the error bars stood for the standard deviations.

the phosphorylated ERK in the cytosol, while etorphine and fentanyl use PKC pathway for ERK phosphorylation and translocate the phosphorylated ERK into the nucleus.

Normally the nucleus translocation of ERK is under the regulation of MEK which contains a nucleus export signal (232). MEK binds with ERK and holds ERK in the cytocol in inactivated status. When MEK is phosphorylated, it phosphorylates ERK and dissociates from ERK, which enables ERK to translocate into nucleus. Thus phosphorylated ERK under G protein pathway translocates into the nucleus, while phosphorylated ERK under β-arrestin pathway remains in the cytosol, because β-arrestin holds MEK and ERK together and stays in the cytosol (5, 8, 176). Basing on this hypothesis, it was proposed that overexpression of β-arrestin will attenuate the nucleus translocation of phosphorylated ERK, which is supported by several observations (96, 97, 231). However, there are opposite observations, overexpression of β-arrestin increased the nucleus translocation of phosphorylated ERK (98). Although the difference has been interpreted by the involvement of different GPCRs, the positive effects of β-arrestin on nucleus translocation of phosphorylated ERK has been supported by the ability of β-arrestin to translocates into the nucleus and to regulate the gene expression (13).

4.1.2 Agonist-selective activation of transcription factor

Treatment with agonists lead to the modulation of gene expression (233). Although the list of genes whose expression can be modulated by morphine is long and increasing, e.g. heat shock protein 70 and MOR itself (234), little comparison has been performed among agonists. We have hypothesized that the agonist-selective gene regulation is the key consequence of agonist-selective signaling. Thus the effects of agonists on the gene expression were investigated.

Transcription factor Elk-1 localizes predominantly in the nucleus (235) and is one of the important substrates of translocated ERK (236, 237). In order to demonstrate the

actual nuclear translocation of ERK, Elk-1-driven luciferase reporter system was used (238). A 10% FBS treatment was used as the positive control. Treating the HEK293 cells with FBS increased the activity of Elk-1. In addition, a 12-hour etorphine treatment increased Elk-1 activity (1.5±0.1 fold p=0.0004). Under similar conditions, morphine treatment did not result in a significant increase in Elk-1 activity (Fig. 4-3). Since 12 hours were required to allow the expression of luciferase proteins, the observed increase in Elk-1 activity could be resulted from the prolonged agonist treatment. This scenario was eliminated by adding MOR antagonist, naloxone, to the medium 10 minutes after the initiation of the agonist treatment. Under this paradigm, etorphine remained able to induce the increase of Elk-1 activity, while morphine could not (Fig. 4-3). In addition, the increase in Elk-1 activity was shown to be a direct result of the ERK activation. When the HEK293 cells were pre-treated with a selective MEK inhibitor PD98059 (239), etorphine-induced increase in Elk-1 activity was blocked completely (Fig. 4-3).

Since morphine-induced phosphorylation of ERK did not result in the nuclear translocation of the phosphorylated enzymes, we investigated whether such phosphorylated ERK could phosphorylate cytosolic substrates. 90 kD ribosomal S6 kinase (90RSK), a cytosolic protein kinase, is one of the substrates of activated ERK (240, 241). After a 10-minute morphine treatment, the phosphorylation level of 90RSK increased. However, when MOR was activated by etorphine, increase in the 90RSK phosphorylation level was not observed (Fig. 4-4). In order to demonstrate 90RSK is a substrate of morphine-activated ERK, PKC inhibitor, Ro-31-8425, and the MEK inhibitor, PD98059, were used to pre-treat the cells. As expected, the two inhibitors attenuated the phosphorylation of 90RSK induced by morphine (Fig. 4-4).

Several groups have reported that the transcriptional factor, cAMP response element binding protein (CREB), serves as a substrate of the activated and nucleus-translocated 90RSK (240, 241). If ERK phosphorylated via G protein-dependent pathway activated 90RSK, an increase in CREB activity should be observed after morphine treatment. Thus, we used a luciferase reporter system to determine CREB activity. As expected,

Fig. 4-3 Agonists activate Elk-1 differentially

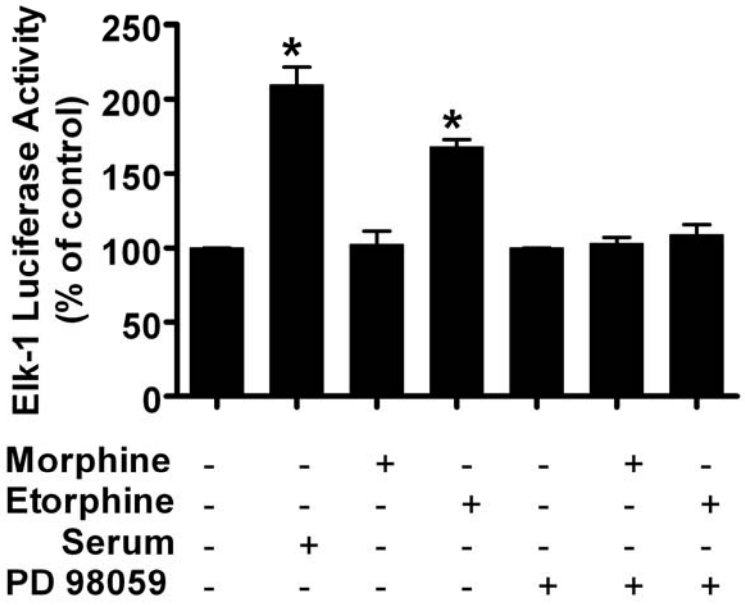

Fig. 4-3 Agonists activate Elk-1 differentially

HEKHM cells were transfected with the Elk-1 reporter system and incubated with serum free medium overnight. The cells were treated with the different combinations of 1 μM morphine, 10 nM etorphine, 40 μM PD 98059 and 10% serum. The activity of Elk-1 was determined by luciferase assay. The results were presented as the percentages of those in control samples. The experiment was repeated for at least four times and the error bars stood for the standard deviations.

Fig. 4-4 Agonists activate 90RSK differentially

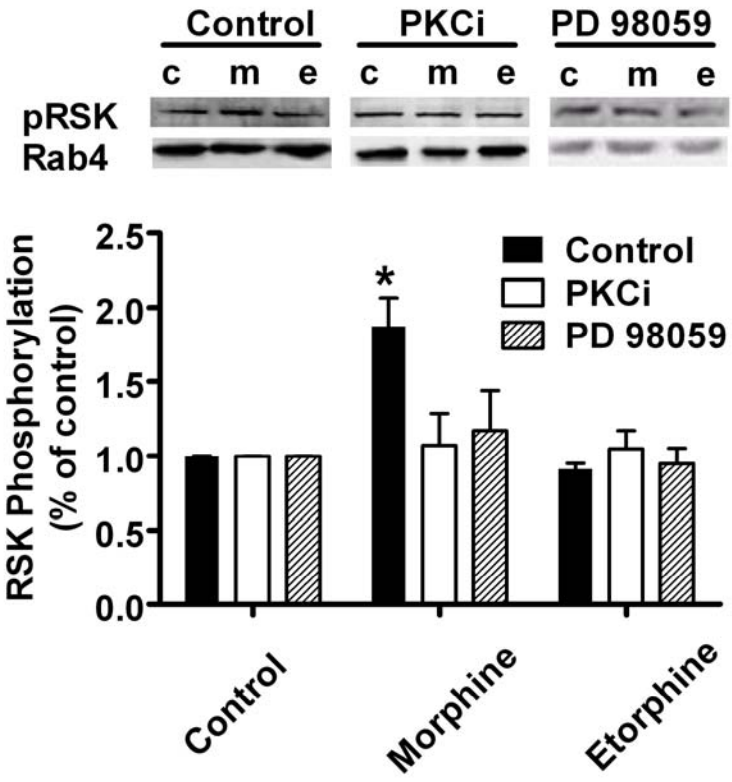

Fig. 4-4 Agonists activate 90RSK differentially

HEKHM cells were treated with the PBS (c) of 1 μM morphine (m) or 10 nM etorphine (e) after the pretreatment with 2 μM Ro-31-8425 or 40 μM PD 98059. The amount of phosphorylated 90RSK was determined. The results were presented as the percentages of those in control samples in each group. The experiment was repeated for at least four times and the error bars stood for the standard deviations.

morphine, but not etorphine, induced an increase in CREB reporter luciferase activities (Fig. 4-5). To confirm the results, several control experiments were carried out. In one group, 10 μM naloxone was added 10 minutes after the initiation of agonist incubation to eliminate any effects stemming from prolonged agonist treatment. In the two other groups, a PKC inhibitor or an MEK inhibitor was used to pre-treat the cells to determine if CREB activation was through a MOR-PKC-ERK pathway. The addition of naloxone 10 minutes after the initiation of morphine treatment could not block agonist-induced CREB activation, while PKC inhibitor and MEK inhibitor attenuated agonist-induced CREB activation significantly.

4.1.3 Agonist-selective expression of miRNAs

miRNAs are a class of approximately 22-nucleotide-long RNA molecules widely expressed in organisms ranging from worms to humans (242). They bind to their target mRNAs through sequence complementarities to inhibit mRNA translation and/or destabilize the mRNAs (243, 244). By regulating the expression of a vast number of genes, miRNAs play critical roles in a variety of biological processes, including those in the central nervous system (CNS) (245). For example, miR-196 and miR-10a influence the patterning of anterior-posterior axis of the CNS (64), whereas miR-134 regulates dendritic spine morphology by controlling actin filament dynamics (246).

To examine the effects of MOR agonists on miRNA expression, miRNA microarray experiments were performed in the primary cultures of rat hippocampal neurons and in the mouse hippocampi. In order to compare the effects of morphine and fentanyl, the potencies of these two agonists were determined initially. For the primary cultures of rat hippocampal neurons, ERK phosphorylation was measured after treating the primary cultures with different concentrations of agonists. The EC50 of morphine (100±17 nM, n=4) is about 100 fold of that of fentanyl (1.1±0.2 nM, n=4). Therefore the equivalent concentrations of 1 μM morphine and 10 nM fentanyl were used in treating the rat primary cultures. For the *in vivo* agonist treatment, the potencies of these two

Fig. 4-5 Agonists activate CREB differentially

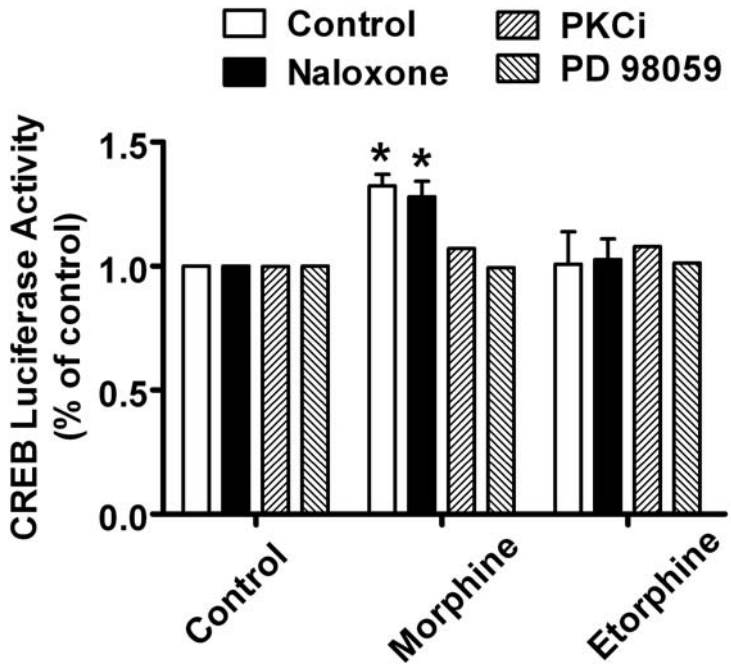

Fig. 4-5 Agonists activate CREB differentially

HEKHM cells were transfected with the CREB reporter system and incubated with serum free medium overnight. HEKHM cells were treated with the PBS of 1 μM morphine or 10 nM etorphine after the pretreatment with 2 μM Ro-31-8425 or 40 μM PD 98059. The activity of CREB was determined by luciferase assay. The results were presented as the percentages of those in control samples in each group. The experiment was repeated for at least four times and the error bars stood for the standard deviations.

agonists in the antinociceptive test were measured. The analgesia effect of morphine peaked at 30 min and the ED50 was 2.4 (1.9~3.0) mg/kg. The analgesia effect of fentanyl peaked at 15 min and the ED50 was 27 (20~35) μg/kg. Therefore mice were infused with saline (control), 12 μg/hr morphine (1 ED50 dose/per 5 hours), or 0.31 μg/hr fentanyl (1 ED50 dose/per 2 hours) for three days by using the micro-osmotic pump. The hippocampi and cerebella were dissected from the mouse brains after infusion and subjected to microarray analysis. Mouse cerebella served as negative control in the current study, because there is minimal expression of MOR in cerebellum (247).

4.1.3.1 miRNA microarray

Custom miRNA microarray experiments and data analyses were performed according to Kalscheuer et al. (248). Microarray data have been deposited into the National Center for Biotechnology Information's Gene Expression Omnibus database under the series GSE14268. Rat primary cultures and mouse hippocampi samples were prepared in triplicate; mouse cerebella samples were examined in duplicate. The data was normalized against internal control in each chip initially. Then the expression of miRNAs whose sequences are conserved in human, mouse and rat were examined. In the rat primary cultures, the expression of miRNAs in fentanyl-treated or morphine-treated samples were compared with those in control samples. The miRNAs with significant expressional change (>125% or <80%, and $p<0.225$ by two tailed t-test) were identified. The miRNAs whose changes were identified in both rat primary cultures and mouse hippocampi, but not in mouse cerebella were subjected for real-time PCR (Qiagen, CA). The miRNAs modulated by the agonists in the rat primary cultures and in mouse hippocampi, but not in mouse cerebella, were further monitored by using real-time PCR. As listed in Table 4-1, three miRNAs, miR-224, miR-331 and miR-365, were modulated by both morphine and fentanyl. One miRNA, miR-20a, was modulated only by morphine. Another three miRNAs, miR-184, miR-190 and miR-301, were modulated by fentanyl only.

4.1.3.2 Agonist-selective regulation on miR-190

The changes of miR-190 level in rat primary culture and in mouse hippocampi were not only highly consistent, but also larger than those of other miRNAs (Table 4-1). In addition, only fentanyl but not morphine could decrease the level of miR-190. Hence, the effects of agonists on miR-190 level were agonist-selective and subjected to further analysis. miR-190 level in rat primary cultures was monitored by real-time PCR at different time points after initiation of agonist treatment. Morphine did not reduce miR-190 level at any time point tested (Fig. 4-6A). In contrast, a significant decrease in miR-190 level was observed 24 hrs after initiation of fentanyl treatment (73±15%, n=4, $q=3.249$, $p<0.01$). The decrease reached the status state 48 hrs after initiation (60±11%, n=4, $q=4.728$, $p<0.001$), and persisted at least until 72 hrs after initiation of fentanyl treatment (63±17%, n=4, $q=4.356$, $p<0.01$) (Fig. 4-6A).

Although morphine did not decrease miR-190 level at any dose tested (Fig. 4-6B), fentanyl decreased miR-190 level at 100 nM (60±7%, n=4, $q=7.285$, $p<0.001$), 10 nM (65±11%, n=4, $q=6.375$, $p<0.001$) and 1 nM (81±7%, n=4, $q=3.461$, $p<0.05$) (Fig. 4-6B). The EC50 of fentanyl to regulate the miR-190 level was also calculated, 1.4±0.2nM (n=4), which is similar to the EC50 of fentanyl in inducing ERK phosphorylation.

4.1.3.3 ERK phosphorylation and miR-190 decrease

To understand the upstream signaling events controlling miR-190 level, rat primary cultures were treated with agonists after incubation with the general opioid receptor antagonist, naloxone, or the MOR-specific antagonist ,D-Pen-Cys-Tyr-D-Trp-Orn-Thr-Pen-Thr-NH_2 (CTOP). In the absence of antagonists, fentanyl decreased miR-190 expression to 60±11% (n=4, $t=5.695$, $p<0.001$) (Fig. 4-7A). In the presence of either antagonist, fentanyl did not decrease miR-190 expression: naloxone 95±11% (n=4, $t=0.712$ $p>0.05$) and CTOP 93±17% (n=4, $t=0.997$, $p>0.05$). The influence of naloxone ($t=6.315$, $p<0.001$) and CTOP ($t=4.643$, $p<0.001$) on fentanyl-induced miR-190 down-

Table 4-1 Agonists modulate miRNA expression differentially.

Chronic Morphine Treatment (% of Control)					
	Microarray for miRNAs			Real-Time PCR	
	Pri	Hippo	Cere	Pri	Hippo
miR-224	**137**	**162**	109	**131±12**	**127±7**
miR-331	**131**	**127**	95	**176±23**	**152±8**
miR-365	**129**	**126**	101	**125±13**	**120±9**
miR-20a	**132**	**132**	110	**143±21**	**128±9**

Chronic Fentanyl Treatment (% of Control)					
miR-224	**147**	**172**	101	**135±14**	**154±23**
miR-331	**128**	**131**	91	**120±11**	**131±11**
miR-365	**194**	**129**	98	**176±33**	**143±27**
miR-184	**76**	**56**	88	**84±8**	**63±23**
miR-190	**68**	**65**	103	**55±18**	**70±6**
miR-301	**79**	**49**	109	**70±8**	**53±17**

Table 4-1 Agonists modulate miRNA expression differentially.

Rat primary cultures were treated with PBS, 1 μM morphine or 10 nM fentanyl for three days. CD1 mice were infused with saline (control), 12 μg/hr morphine (1 ED50 dose/per 5 hours), or 0.31 μg/hr fentanyl (1 ED50 dose/per 2 hours) for three days by using the micro-osmotic pump. Microarray experiments were performed in rat primary cultures (Pri. three times), mouse hippocampi (Hippo. three times) and mouse cerebella (Cere. two times). The results were analyzed as described in the *Materials and Methods*. The identified the miRNAs have conserved sequences in human, mouse and rat. Their expression was modulated by agonists in rat primary cultures and mouse hippocampi, but not in mouse cerebella. The expression these miRNAs were also measured by using real-time PCR in rat primary cultures and mouse hippocampi. Real-time PCR results were repeated for four times and had p-value less than 0.05. Data were analyzed by one-way ANOVA with Dunnett-test as post-hoc test to do comparisons.

Fig. 4-6 Agonist-selective regulation on miR-190 expression.

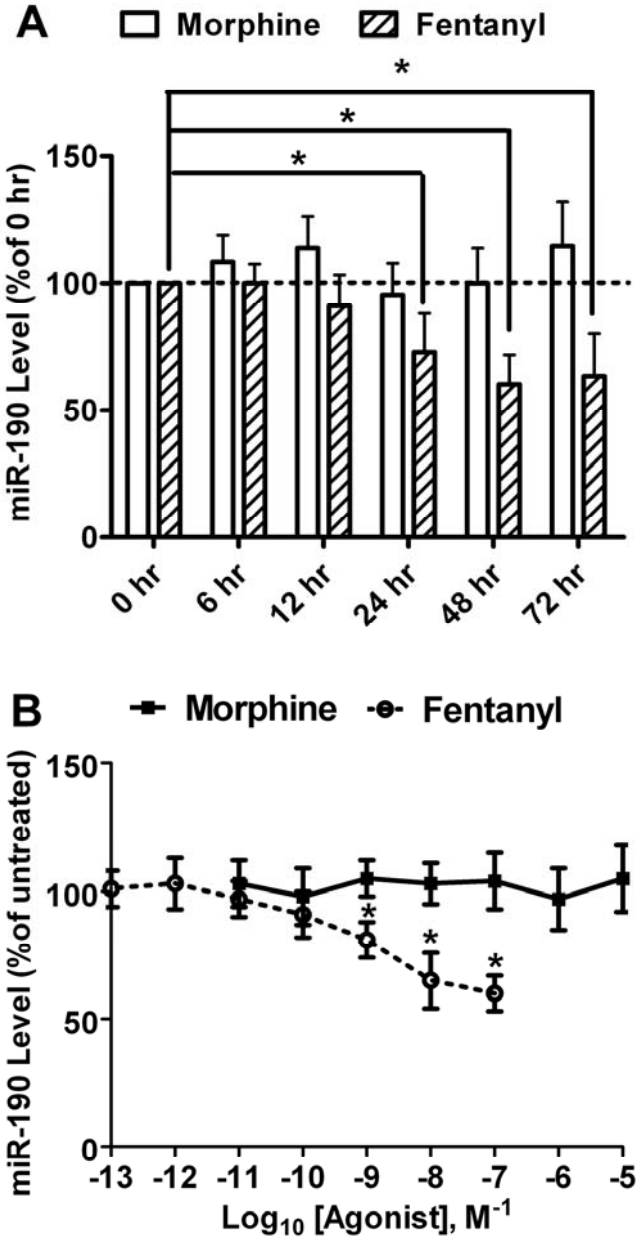

Fig. 4-6 Agonist-selective regulation on miR-190 expression.

(A) Time-dependent abilities of morphine and fentanyl to modulate the expression of miR-190 in rat primary cultures. Cultures were treated with 1μM morphine or 10nM fentanyl for indicated times. The expression of miR-190 was determined by real-time PCR and normalized against the mRNA level of β-actin as described in *Materials and Methods*. The normalized results were further normalized against the results in untreated cultures (0hr). (C) Dose-dependent curves of morphine and fentanyl to modulate the expression of miR-190 in rat primary cultures. Cultures were treated with indicated doses of agonists for three days. The expression of miR-190 was determined as in (A). Experiments were repeated for four times.

Fig. 4-7 ERK phosphorylation is required for miR-190 suppression

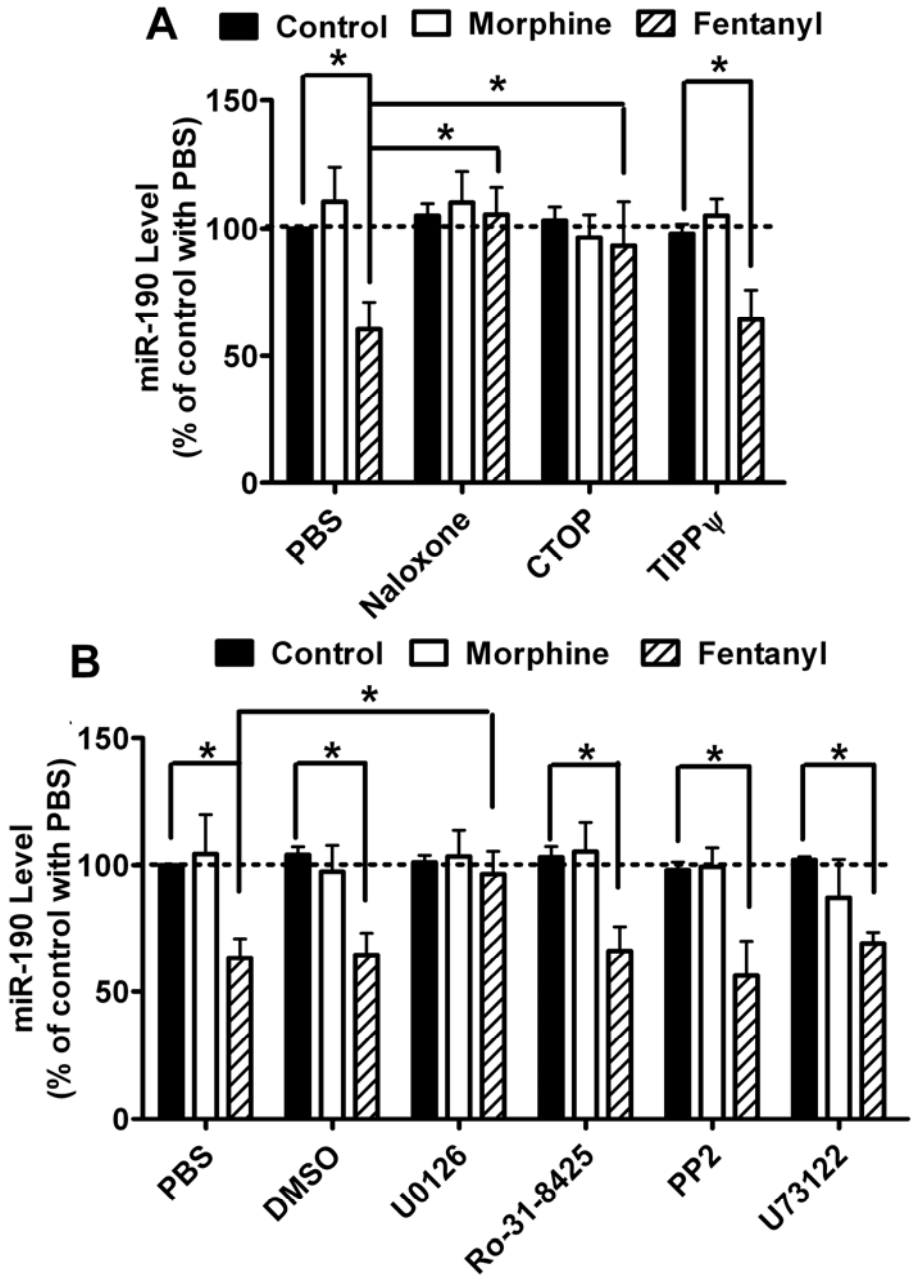

Fig. 4-7 ERK phosphorylation is required for miR-190 suppression

(A) Rat primary cultures were treated with PBS, 10 μM naloxone, 10 μM CTOP or 10 μM TIPPψ for three hours. Then the cultures were treated with 1μM morphine or 10nM fentanyl for additional three days. The expression of miR-190 was determined by real-time PCR. The results of miR-190 were normalized against those of β-actin, and further normalized against the result obtained from untreated cultures (control) in PBS group. (B) Rat primary cultures were treated with PBS, 0.2% DMSO, 2 μM U0126, 4μM Ro-31-8425, 10μM PP2 or 10μM U73122 for three hours. Then the cultures were treated with 1μM morphine or 10nM fentanyl for additional three days. The expression of miR-190 was determined as in (A). Experiments were repeated for four times.

regulation was significantly. However, when DOR-specific inhibitor H-Tyr-Ticψ[CH2NH]-Phe-Phe -OH (TIPPψ) was used, fentanyl-induced decrease in miR-190 expression (64±11%, n=4, t=7.837, p<0.001). Therefore, although DOR is detected in the hippocampus, fentanyl decreases the cellular content of miR-190 in primary cultures of rat hippocampal neurons via the activation of MOR.

To explore the mechanism of fentanyl to control the cellular content of miR-190, inhibitors of MEK (U0126), PKC (Ro-31-8425), Src kinase (PP2) and phospholipase C (U73122) were used. The inhibitor were used at effective doses depending on the previous reports (249-252). Because these inhibitors were dissolved in the DMSO to form concentrations which are 500 fold of working concentrations, the ability of fentanyl to decrease miR-190 level was determined in the rat primary cultures pretreated with 0.2% DMSO in medium. As indicated in Fig. 4-7B, fentanyl decreased the level of miR-190 to 64±9% (n=4, t=5.854, p<0.001) of basal level in DMSO-treated cultures, which was not significantly different from that in PBS-treated cultures (t=0.167, p>0.05).

Fentanyl did not affect the level of miR-190 (96±9%, n=4, t=0.588, p>0.05) in U0126-treated rat primary cultures. U0126 blocks the phosphorylation of ERK by inhibiting the activities of MEK1 and MEK2 (249). Hence blocking ERK activation attenuated fentanyl-induced miR-190 down-regulation (t=5.513, p<0.001) (Fig. 4-7B). In rat primary cultures pretreated with other inhibitors, fentanyl decreased miR-190 level similarly to what it did in PBS-pretreated cultures (Fig. 4-7B). Therefore, fentanyl decreases miR-190 level via ERK phosphorylation.

Morphine induces ERK phosphorylation via PKC-pathway, while fentanyl functions in a β-arrestin2-dependent manner (95). Primary cultures of hippocampal neurons from wildtype and β-arrestin2-/- mice were used to determine the role played by β-arrestin2. In addition, PKC inhibitor, Ro-31-8425, was used to determine the contribution of PKC. When primary cultures from β-arrestin2$^{-/-}$ mice were used, the down-regulation of miR-190 induced by fentanyl was not observed (98±17%, n=4,

t=0.985, p>0.05). When the ability of fentanyl to decrease miR-190 expression in the primary cultures from β-arrestin2$^{-/-}$ mice was compared with that in primary cultures from wild type mice, a significant difference were identified (t=0.538, p<0.001). Therefore, the decrease in miR-190 level requires fentanyl-induced β-arrestin2-mediated ERK phosphorylation.

4.2 miR-190 and Talin2

4.2.1. miR-190 in talin2 gene locus

A miRNA is initially transcribed as part of a much longer primary transcript, which can be longer than 1 kb (253). This primary miRNA transcript then undergoes extensive processing to generate an approximately 22nt mature miRNA. Although the processing of primary transcript is under tight regulation, the initial transcription is a potential checkpoint in the miRNA expression (254). Over 50% of mammalian miRNAs are located within the intronic regions of annotated protein-coding or non-protein-coding genes (255), suggesting that the expression of these miRNAs might be controlled by the promoters of their host genes.

miR-190 is conserved in human mouse and rat, and locates in the intronic regions of the *talin2* gene in the mouse, rat, and human genomes (256). The transcript of *talin2* is detected with higher levels in the heart and brain than in other tissues (257). The transcription of *talin2* in the brain further suggests the involvement of its promoter in miR-190 production. It is, therefore, hypothesized that fentanyl regulated miR-190 expression at transcriptional level.

4.2.2 Fentanyl suppresses the expression of Talin2

4.2.2.1 Talin2 mRNA and agonists

If miR-190 is transcribed from the Talin2 promoter, a correlation between the Talin2 mRNA and miR-190 expression should be expected. Talin2 mRNA level was monitored by real-time PCR in primary hippocampal cultures from rats after treatment with fentanyl or morphine (Fig. 4-8A). A significant decrease in Talin2 mRNA was first observed 24 hrs after the initiation of fentanyl treatment and persisted at least till 72 hrs. In contrast, morphine did not reduce Talin2 mRNA level at any time point. In addition the dose-dependent effects of morphine and fentanyl were also determined. Fentanyl decreased the mRNA level of Talin2 at 1 nM, 10nM and 100nM, while morphine did not influence the mRNA level of Talin2 at any concentration (Fig. 4-8B). Because fentanyl and morphine influence the expression of miR-190 in a similar manner (Fig. 4-6), there exists a strong, positive correlation between Talin2 mRNA and miR-190 level under these conditions.

4.2.2.2 Talin2 mRNA and ERK phosphorylation

Inhibitor of protein kinase C (Ro-31-8425) and TIPPψ did not block the inhibitory effects of fentanyl on Talin2 mRNA (Fig. 4-9A). However, naloxone, CTOP and U0126 prevented the fentanyl-induced decrease in Talin2 mRNA (Fig. 4-9A). Probably, miR-190 level is strongly influenced by the transcription of *talin2*. Fentanyl-induced decrease in miR-190 level results from β-arrestin-mediated ERK phosphorylation (Fig. 4-7). Thus a correlation between the decrease in Talin2 mRNA and β-arrestin-mediated ERK phosphorylation was determined. Morphine induces ERK phosphorylation through PKC pathway, while fentanyl functions in a β-arrestin2-dependent manner (95). Thus Ro-31-8425 was used to block morphine-PKC pathway, while primary hippocampal culture from β-arrestin2$^{-/-}$ mice for fentanyl-β-arrestin2 pathway. In primary hippocampal cultures from wildtype mice, fentanyl reduced Talin2 mRNA by 35±4% (n=4, Fig. 4-9B), which is similar to that induced by fentanyl in rat primary cultures (32±7%, n=4, Fig. 4-8A). This reduction could be blocked by U0126, but not by Ro-31-8425 (Fig. 4-9A). In primary hippocampal cultures from β-arrestin2$^{-/-}$ mice, the decrease in Talin2 mRNA was not observed after fentanyl treatment (Fig. 4-9B).

Fig. 4-8 Fentanyl regulates the Talin2 mRNA level.

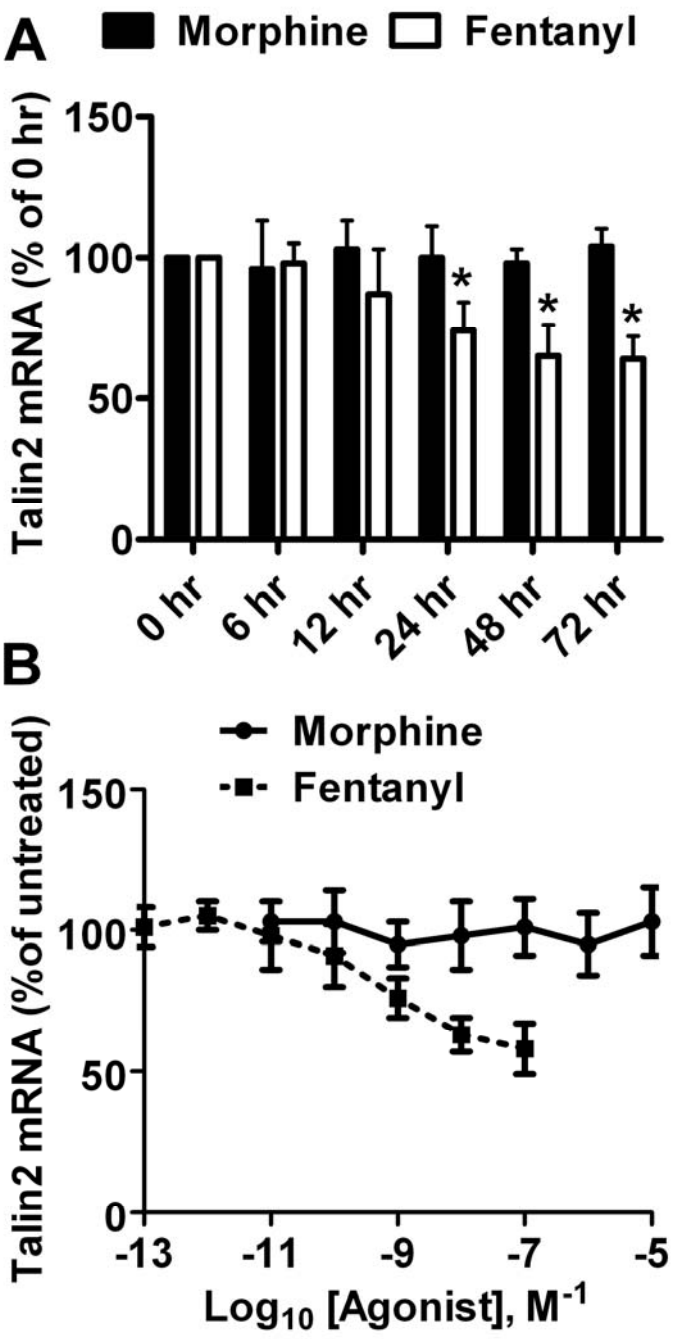

Fig. 4-8 Fentanyl regulates the Talin2 mRNA level.

Primary hippocampal cultures from rat were treated with morphine or fentanyl for indicated times (A) or at indicated concentrations (B). The levels of Talin2 mRNA were assayed by real-time PCR. The results were normalized against those obtained at 0 hr in each group. The results were presented as the percentages of those in untreated samples in each group. The experiment was repeated for at least four times and the error bars stood for the standard deviations.

Fig. 4-9 ERK phosphorylation is required for Talin2 suppression

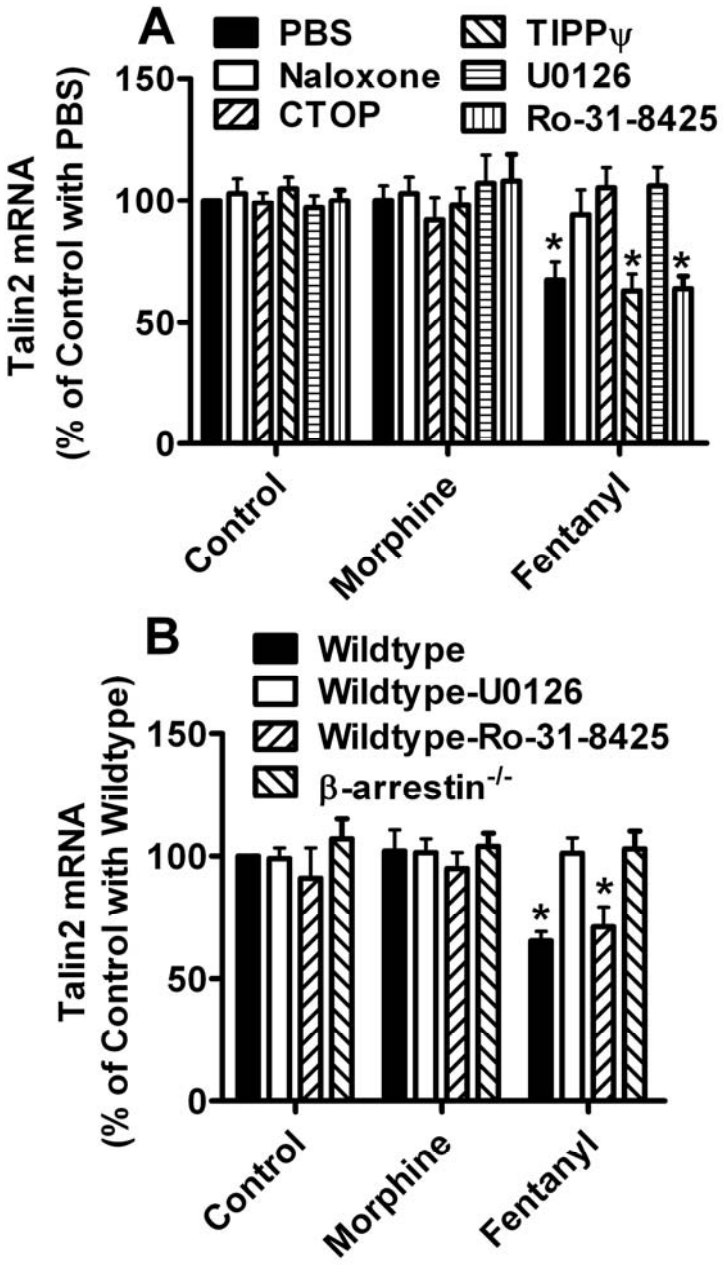

Fig. 4-9 ERK phosphorylation is required for Talin2 suppression

(A) Primary hippocampal cultures from rat were pretreated with PBS, 10 μM naloxone, 10 μM CTOP, 10 μM TIPPψ, 2 μM U0126 or 4 μM Ro-31-8425 for three hours followed by three-day treatment with 1 μM morphine or 10nM fentanyl. The levels of Talin2 mRNA were normalized agonist that in control sample of "PBS" group. (B) Primary hippocampal cultures from wildtype mice were pretreated with PBS, 2 μM U0126 or 4 μM Ro-31-8425 for three hours followed by three-day treatment with 1 μM morphine or 10 nM fentanyl. Primary hippocampal cultures from β-arrestin$^{-/-}$ mice were treated with PBS for three hours before agonist treatment.

4.2.3. Yin Yang 1 (YY1) affects miR-190 expression

If fentanyl decreased the expression of miR-190 by affecting the transcription of *talin2* gene locus, there should be a transcription factor to mediate the effects of fentanyl. By analyzing the promoter region of *talin2* gene locus, we identified a highly conserved region which contains a binding site of YY1. YY1 can function as both the transcription activator and the suppressor in different contexts. It not only regulates cell proliferation, differentiation and survival, but also plays critical roles in the central nervous system. Knockout of *yy1* in mice leads to the embryonic lethality, while a small number of *yy1* heterozygotes display neuronal defects (258).

To determine the effects of YY1 on miR-190 level, lentiviruses (YYup-vir and YYdn-vir) were generated to increase and to decrease the level of YY1. As indicated in Fig. 4-10, YYup-vir increased the levels of YY1 mRNA (412±87%, n=4) and YY1 protein (187±12%, n=4), while YYdn-vir decreased them (mRNA: 43±13%, n=4; protein: 56±11%, n=4).

Consistent changes on Talin2 mRNA and miR-190 were observed after modulating YY1 expression. YYup-vir increased Talin2 mRNA to 215±13% (n=4) of basal level, and miR-190 to 276±44% (n=4). YYdn-vir decreased Talin2 mRNA and miR-190 to 67±12% (n=4) and 63±9% (n=4), respectively.

4.2.4. YY1 phosphorylation

YY1 undergoes extensive post-translational modifications, including phosphorylation, acetylation, and caspase-dependent cleavage (259). Because YY1 phosphorylation has been suggested to modulate its ability to bind DNA (260), the phosphorylated YY1 was quantified after agonist treatment. The primary cultures were treated with the two agonists for 1 hour in the presence or in the absence of a three-hour pretreatment with U0126. Fentanyl induced a significant increase in YY1

Fig. 4-10 YY1 regulates miR-190 expression

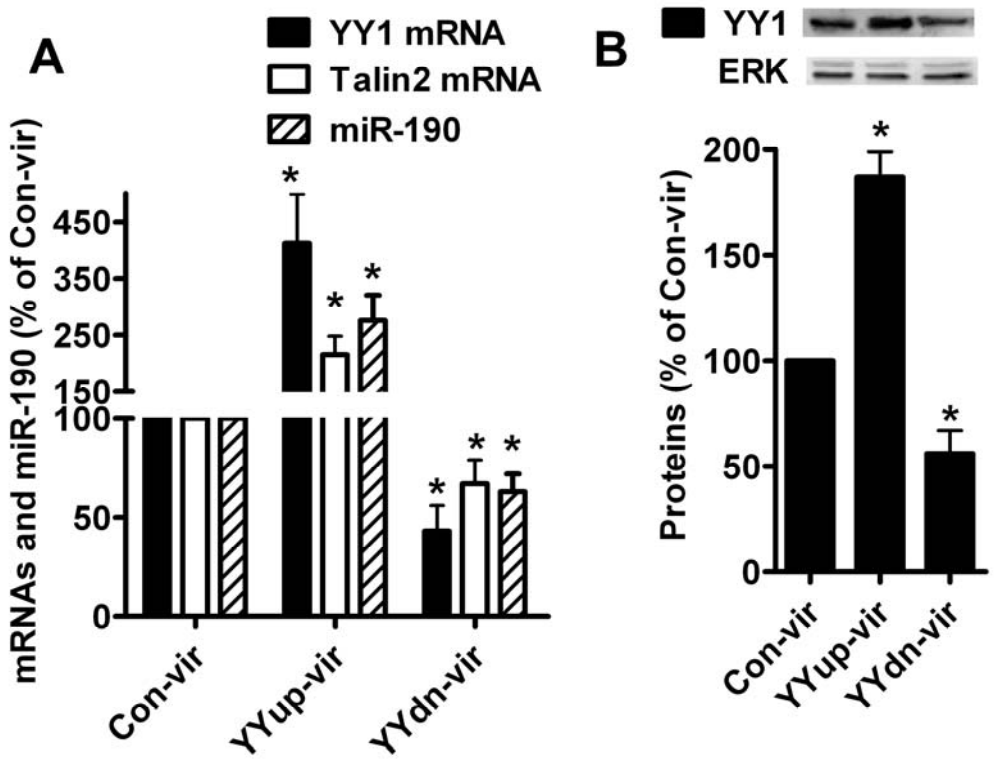

Fig. 4-10 YY1 regulates miR-190 expression

Primary hippocampal cultures from rat were infected with con-vir, YYup-vir and YYdn-vir for three days. The mRNA levels (Talin2, YY1 and NeuroD) and miR-190 were determined in (A). The protein levels of YY1 and NeuroD were measured in nuclear extract (B). The loading controls (ERK) were detected in the whole cell lysis. The results were normalized against those obtained from con-vir-infected cultures in each group.

phosphorylation (187±27% of basal level, n=4), which can be attenuated by U0126 (103±9%, n=4) (Fig. 4-11). However, morphine did not affect YY1 phosphorylation no matter U0126 was used or not. Therefore, YY1 phosphorylation results from fentanyl-induced β-arrestin-mediated ERK phosphorylation.

YY1 phosphorylation has been suggested to modulate its ability to bind DNA (260). The association between YY1 and rat Talin2 promoter was measured by chromatin immunoprecipitation (ChIP). Primers were used to amplify the rat Talin2 promoter in the crosslinked and immunoprecipitated YY1. As indicated in Fig. 4-12, the binding of YY1 to rat Talin2 promoter was reduced after fentanyl treatment in concordant with the increased YY1 phosphorylation, suggesting that YY1 phosphorylation impaired its association with target DNA.

4.3 miR-190 and NeuroD

4.3.1. Fentanyl increases the expression of NeuroD

One of the mechanisms for miRNAs exerting their functions is by destabilizing the mRNA of its targets or inhibiting the translation of the mRNAs. To investigate the functional relevance of reduced miR-190, the targets of miR-190 conserved in human, mouse and rat were predicted by searching the database [http://genome.ewha.ac.kr/miRGator/miRGator.html (261)]. The mRNAs of the presumptive targets were quantified by real-time PCR in rat primary cultures after agonist treatment, because miRNAs frequently destabilize the mRNAs of their target mRNAs (242).

mRNA level of one selected target, neurogenic differentiation 1 (NeuroD), increased after fentanyl (177±22%, n=4, t=9.755, p<0.001), but not morphine (105±7%, n=4, t=0.633, p>0. 05), treatment (Fig. 4-13A). Such fentanyl-specific increase was also observed when rat primary cultures were pretreated with TIPPψ (165±17%, n=4,

Fig. 4-11 Fentanyl induces YY1 phosphorylation

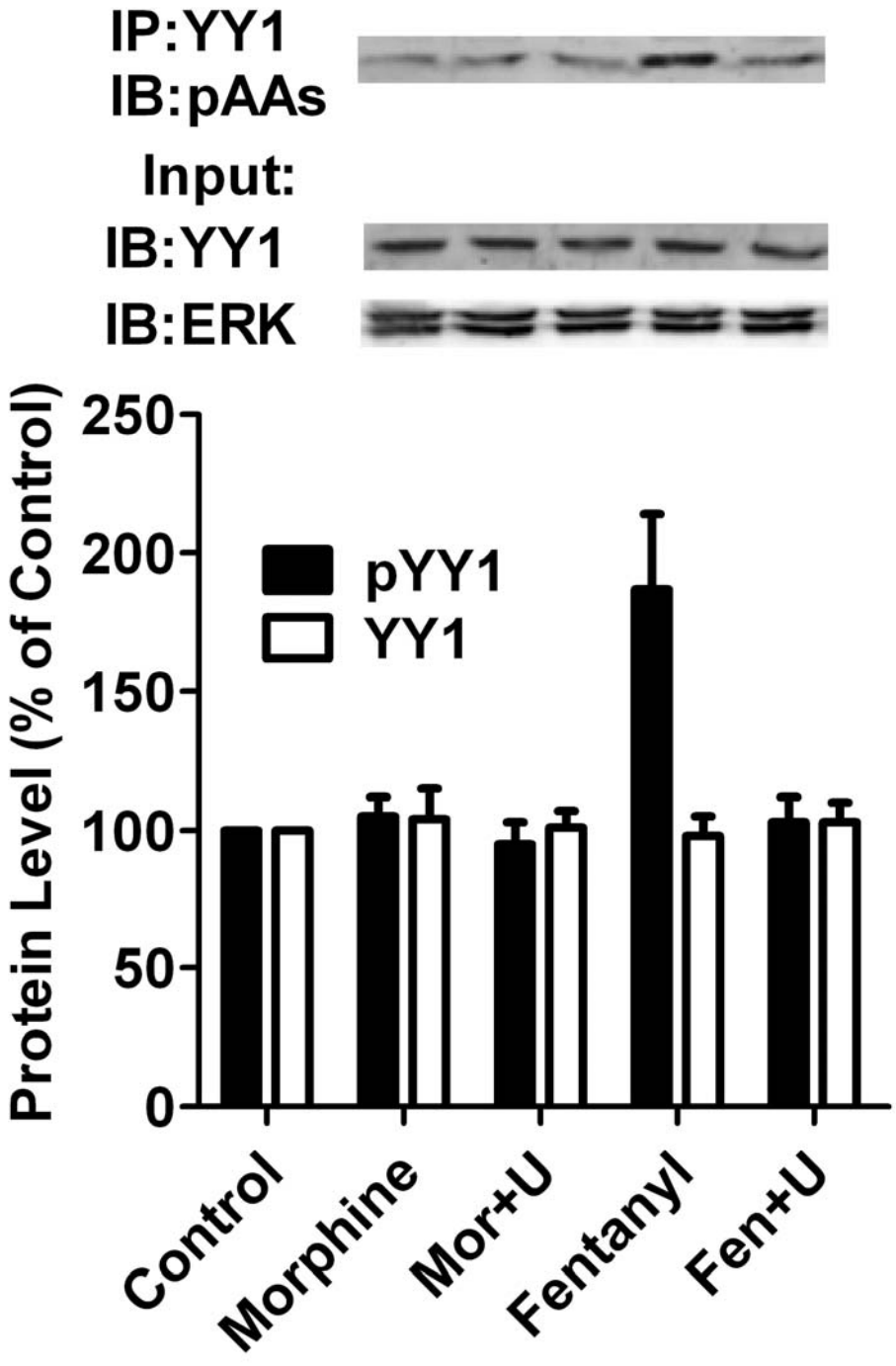

Fig. 4-11 Fentanyl induces YY1 phosphorylation

Primary hippocampal cultures from rat were treated with agonist (1 μM morphine or 10nM fentanyl) for 1 hour with or without a 3-hour pretreatment with 2 μM U0126. The phosphorylated YY1, total YY1 and total ERK were determined. “Mor”, “Fen” and “U” stood for morphine, fentanyl and U0126, respectively.

Fig. 4-12 YY1 phosphorylation inhibits its DNA binding

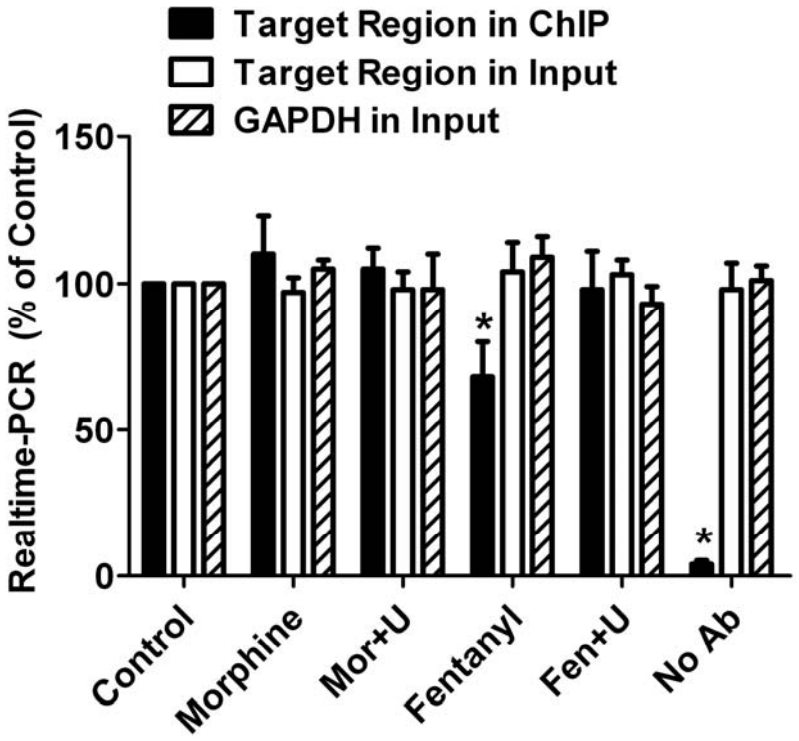

Fig. 4-12 YY1 phosphorylation inhibits its DNA binding

Primary hippocampal cultures from rat were treated with agonist (1 μM morphine or 10nM fentanyl) for 36 hours with or without a 3-hour pretreatment with 2 μM U0126. "Mor", "Fen" and "U" stood for morphine, fentanyl and U0126, respectively. The binding of YY1 to the -288~-138 region on rat Talin2 promoter was determined by real-time PCR after ChIP assay. "No Ab" (without YY1 antibody) was used to confirm the binding is specific to YY1. The real-time PCR performed in the inputs were used to confirm equal amounts of samples were used. The results were normalized against those in control samples in each group.

Fig. 4-13 Fentanyl increases NeuroD expression

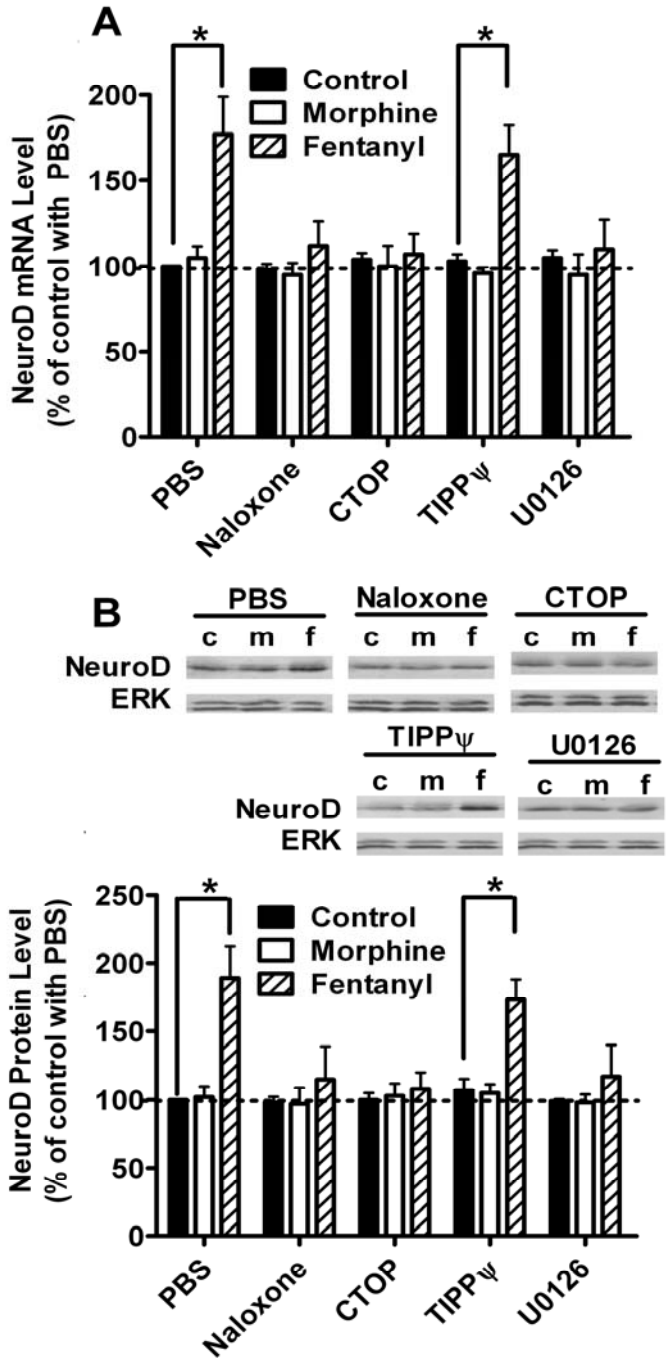

Fig. 4-13 Fentanyl increases NeuroD expression

Rat primary cultures were treated with PBS, 10 μM naloxone, 10 μM CTOP, 10 μM TIPPψ or 2 μM U0126 for three hours. Then the cultures were treated with 1μM morphine or 10nM fentanyl for additional three days. The mRNA levels of NeuroD were determined by real-time PCR (A). The protein levels of NeuroD (B) were determined by immunoblotting after nuclear extraction. The immunoreactivities of NeuroD were normalized against those of total ERK and further normalized against the result obtained from untreated cultures (control) in PBS group. Experiments were repeated for four times. The error bars and "*" presented the standard deviations and significant changes, respectively.

t=8.630, p<0.001), but not observed with naloxone (112±14%, n=4, t=1.520, p>0.05), CTOP (107±12%, n=4, t=0.887, p>0.05) and U0126 (110±17%, n=4, t=1.267, p>0.05), suggesting NeuroD is a possible target of miR-190.

NeuroD protein levels were monitored at the same time. An increase in NeuroD protein level was observed in rat primary cultures treated with fentanyl (189±9%, n=4, t=9.515, p<0.001), but not morphine (102±8%, n=4, t=0.214, p>0.05) (Fig. 4-13B). Such increase was also observed when primary cultures were pretreated with TIPPψ (173±15%, n=4, t=9.421, p<0.001), but not observed with naloxone (115±24%, n=4, t=1.604, p>0.05), CTOP (108±12%, n=4, t=885, p>0.05) and U0126 (117±23%, n=4, t=1.817, p>0.05), which are consistent with the changes on NeuroD mRNA levels.

4.3.2. NeuroD is a target of miR-190

To confirm NeuroD is one of the miR-190 targets, miR-190 mimic and miR-190 inhibitor were purchased and used to transfected the rat primary cultures. As indicated in Fig. 4-14A, miR-190 mimic decreased the mRNA level of NeuroD (72±8%, n=4, q=5.084, p<0.01), while miR-190 inhibitor increased the mRNA level of NeuroD (156±11%, q=10.17, p<0.001). Protein level of NeuroD displayed similar changes, miR-190 mimic decreased it (81±8%, n=4, q=3.981, p<0.01), while miR-190 inhibitor increased it (136±9%, n=4, q=7.983, p<0.001) (Fig. 4-14B).

miR-190 is predicted to bind to nucleotides 521–540 of the 3′-untranslated region (UTR) of rat NeuroD mRNA, which is conserved in human, mouse and rat. To assess the functional interaction between miR-190 and NeuroD mRNA, approximately 300 nucleotides of 3′-UTR of NeuroD (with the predicted miR-190 targeting site in the middle) were inserted into the 3′-UTR of a firefly luciferase reporter mRNA (3UTR). As a control, another luciferase reporter was constructed with miR-190 targeting site mutated (3UTRmu) (Fig. 4-15A). The reporters were then cotransfected with miR-190 mimic or miR-190 inhibitor into HEK293 cells. As expected, miR-190 mimic

Fig. 4-14 miR-190 decreases NeuroD expression

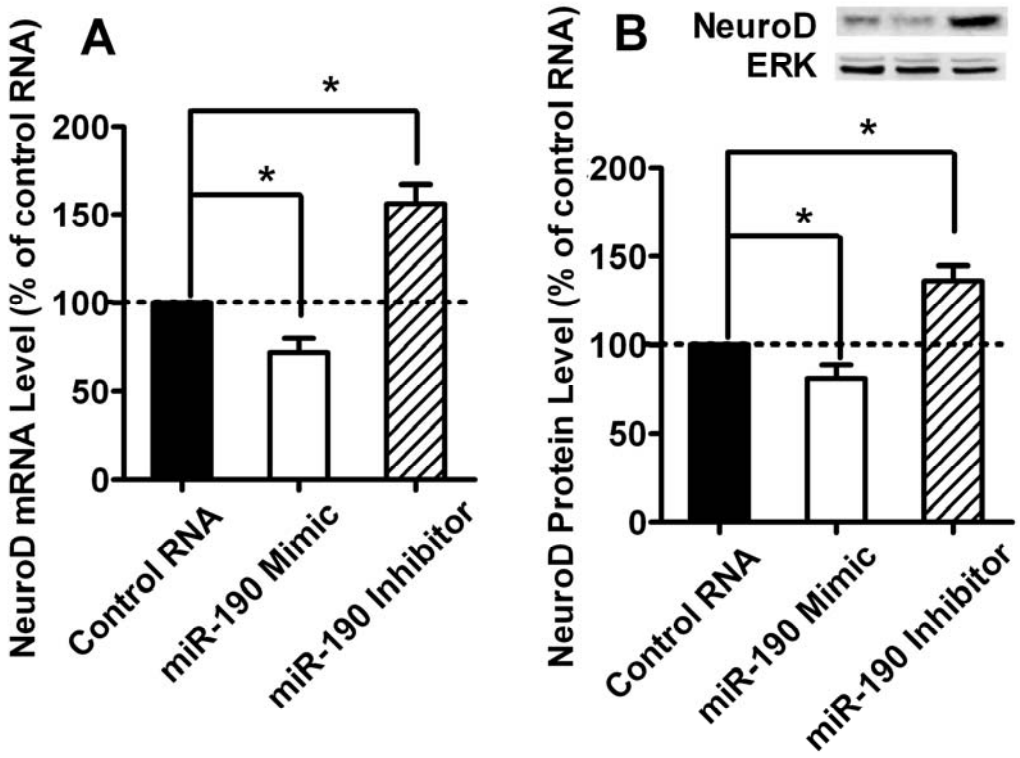

Fig. 4-14 miR-190 decreases NeuroD expression

Rat primary cultures were transfected with control RNA, miR-190 mimic or miR-190 inhibitor by using lipofectamin 2000 (Invitrogen, CA). Two days after transfection, the mRNA (A) and protein (B) levels of NeuroD were determined by real-time PCR and Immunoblotting, respectively. The results were normalized against internal control (β-actin for mRNA and total ERK for protein) and further normalized against the results obtained from cultures transfected with control RNA. Data were analyzed by one-way ANOVA with Dunnett-test as post-hoc test to do comparisons.

Fig. 4-15 NeuroD is a target of miR-190

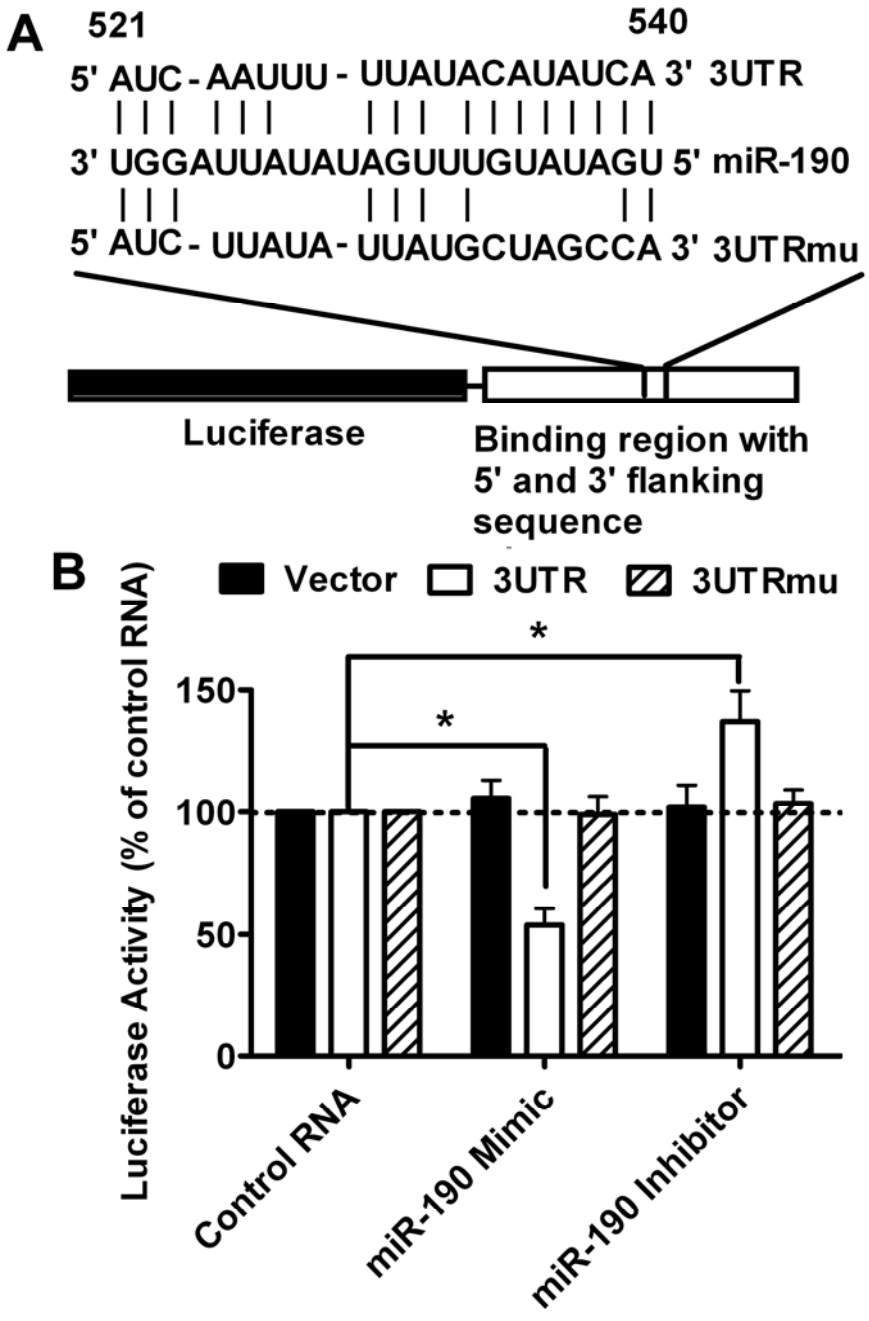

Fig. 4-15 NeuroD is a target of miR-190

(A) Schematics of the 3UTR and 3UTRmu reporters. The first nucleotide after the stop codon of rat NeuroD mRNA is designated as number 1. (B) HEK293 cells were transfected with one of the RNAs, one of the reporters and the luciferase reporter system. RNAs included control RNA, miR-190 mimic and miR-190 inhibitor. Reporters included vector, 3UTR and 3UTRmu. The luciferase expression was determined as described in *Materials and Methods*. The results were normalized against internal control (*Renilla* luciferase) and further normalized against the results obtained from cultures transfected with control RNA in each group. Experiments (A-D) were repeated for four times. The error bars and "*" presented the standard deviations and significant changes, respectively.

suppressed luciferase expression from 3UTR construct (54±7%, n=4, t=9.780, p<0.001), whereas the miR-190 inhibitor enhanced the luciferase expression (137±13%, n=4, t=7.491, p<0.001), presumably by blocking the inhibitory effects of endogenous miR-190 (Fig. 4-15B). In contrast, luciferase expression from 3UTRmu construct was not affected by the miR-190 mimic (99±8%, n=4, t=0.231, p>0.05) or inhibitor (103±6%, n=4, t=0.705, p>0.05) (Fig. 4-15B). These results illustrate a specific interaction between miR-190 and NeuroD mRNA, and support the hypothesis that increased NeuroD level resulted directly from the reduction of miR-190 expression.

4.4 NeuroD activity and spine stability

4.4.1 Agonist-selective regulation on NeuroD activity

4.4.1.1 Fentanyl increases NeuroD expression

Cellular level of NeuroD was determined in primary cultures of rat hippocampal neurons treated with morphine or fentanyl for 3 days. Consistent with previous report, fentanyl, but not morphine, increased the protein level of NeuroD (Fig. 4-16A). Similar modulation was observed on the mRNA level of NeuroD, fentanyl increased the mRNA level of NeuroD, while morphine did not affect it (Fig. 4-16B). NeuroD mRNA is a target of miR-190, and fentanyl regulates NeuroD expression by controlling the expression of miR-190 (Fig. 4-13~4-15). Thus the cellular level of miR-190 was also measured, fentanyl induced a 37±8% (n=4, q=6.142, p<0.001) decrease in miR-190 level, but no decrease was observed after three-day treatment with morphine.

4.4.1.2 Morphine decreases NeuroD activity

Then the activity of NeuroD was determined in agonist-treated samples. Because the phosphorylation of Ser^{336} on NeuroD is essential for its activity (262), the activity of NeuroD was indicated by its phosphorylation, which was determined by measuring the

Fig. 4-16 Agonist-selective regulation on NeuroD activity

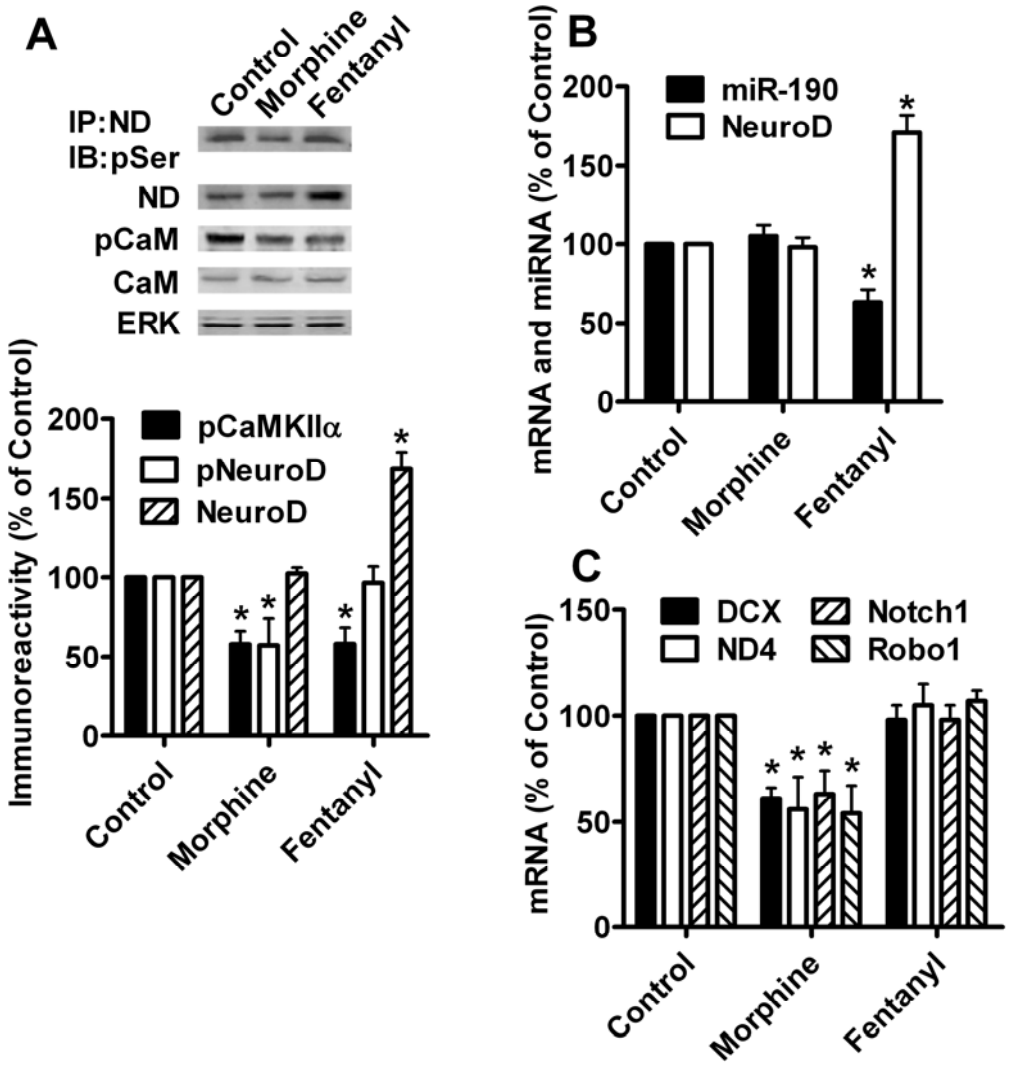

Fig. 4-16 Agonist-selective regulation on NeuroD activity

Primary cultures from rat hippocampal neurons were treated with PBS (control), 1 μM morphine or 10 nM fentanyl for three days.

(A) The amount of phosphorylated serine was determined in the immunoprecipitated NeuroD to indicate the NeuroD phosphorylation. The total NeuroD was measured in the nuclear extraction. The total CaMKIIα, phosphorylated CaMKIIα and total ERK were detected in the whole cell lysis. Total ERK served as internal control. (B) The levels of miR-190 and NeuroD mRNA were measured by real-time PCR. (C) The mRNA levels of DCX, ND4, Notch1 and Robo1 were determined with real-time PCR.

The results were normalized against those in control samples.

phosphorylated serine in the immunoprecipitated NeuroD. The amount of phosphorylated NeuroD decreased after three-day morphine treatment, but was not affected by fentanyl (Fig. 4-16A). To confirm this modulation on NeuroD activity, mRNA levels of several NeuroD targets, doubelcortin (DCX), NeuroD4 (ND4), Notch1 and Robo1, were monitored (263). As indicated in Fig. 4-16C, mRNA levels of these targets decreased after morphine treatment, but not after fentanyl treatment. Thus the status of NeuroD phosphorylation correlated with NeuroD activity, and the activity of NeuroD was regulated differentially by the two agonists.

4.4.1.3 Agonists deactivate CaMKIIα

The effects of agonists on NeuroD activity were different from those on NeuroD expression, suggesting the involvement of other factors. Chronic treatment with morphine attenuates the activity of CaMKIIα, which is a positive regulator of NeuroD (262, 264). Thus the activity of CaMKIIα was measured after agonist treatment by determining the levels of Thr^{286} phosphorylation on CaMKIIα (265)..

Phosphorylation of CaMKIIα was 58±8% (n=4, q=7.901, $p<0.001$) and 57±10% (n=4, q=7.854, $p<0.001$) of basal level after chronic treatment with morphine and fentanyl, respectively (Fig. 4-16A). In addition, two agonists did not modulate the expression of CaMKIIα. Therefore, fentanyl regulated NeuroD activity from two aspects. Fentanyl decreased NeuroD activity by deactivating CaMKIIα, while increased it by decreasing miR-190 level. The two opposite effects counteracted with each other and kept NeuroD activity unchanged. Because morphine does not affect miR-190 level, it decreased NeuroD activity by deactivating CaMKIIα.

4.4.2 Agonist-selective regulation on spine stability

As noted above, morphine decreased the activity of NeuroD and reduced spine stability, while fentanyl kept NeuroD activity constant and did affect spine stability [Fig.

4-17 and (266, 267)]. Thus whether morphine induces spine collapse by decreasing the activity of NeuroD was determined.

Consistent with the observations in Fig. 4-17, when morphine was used to treat the primary cultures for three days, significant decrease was observed in NeuroD activity, as indicated by NeuroD phosphorylation and mRNA levels of NeuroD targets (Fig. 4-17). When NeuroD was over-expressed by using nd-vir, morphine-decreased NeuroD activity was recovered.

One week after plating, a vector encoding DsRed was transfected into primary cultures by using the Lipofectamine 2000. Two weeks later, the primary cultures were subjected for various treatments and monitored for three days. The changes on spine density and total volume of the spines were calculated from the live images to indicate the influence of morphine on the stability of dendritic spines. Consistent with previous report (266, 267), chronic treatment with morphine reduced spine stability, as indicated by spine density and spine volume (Fig. 4-18). When nd-vir was used to infect the primary cultures at the same time with morphine treatment, morphine-induced decrease in spine stability was attenuated. Thus evaluating NeuroD activity recovers morphine-induced decrease in spine stability.

4.5 NeuroD and tolerance

4.5.1 Tolerance

4.5.1.1 Differential Tolerance

The most important difference among agonists is that they can induce the tolerance on analgesia effects to distinct levels (113). Scientists have tried to explain such difference on tolerance development and several concepts have been proposed (6).

Fig. 4-17 Overexpression NeuroD rescues its activity

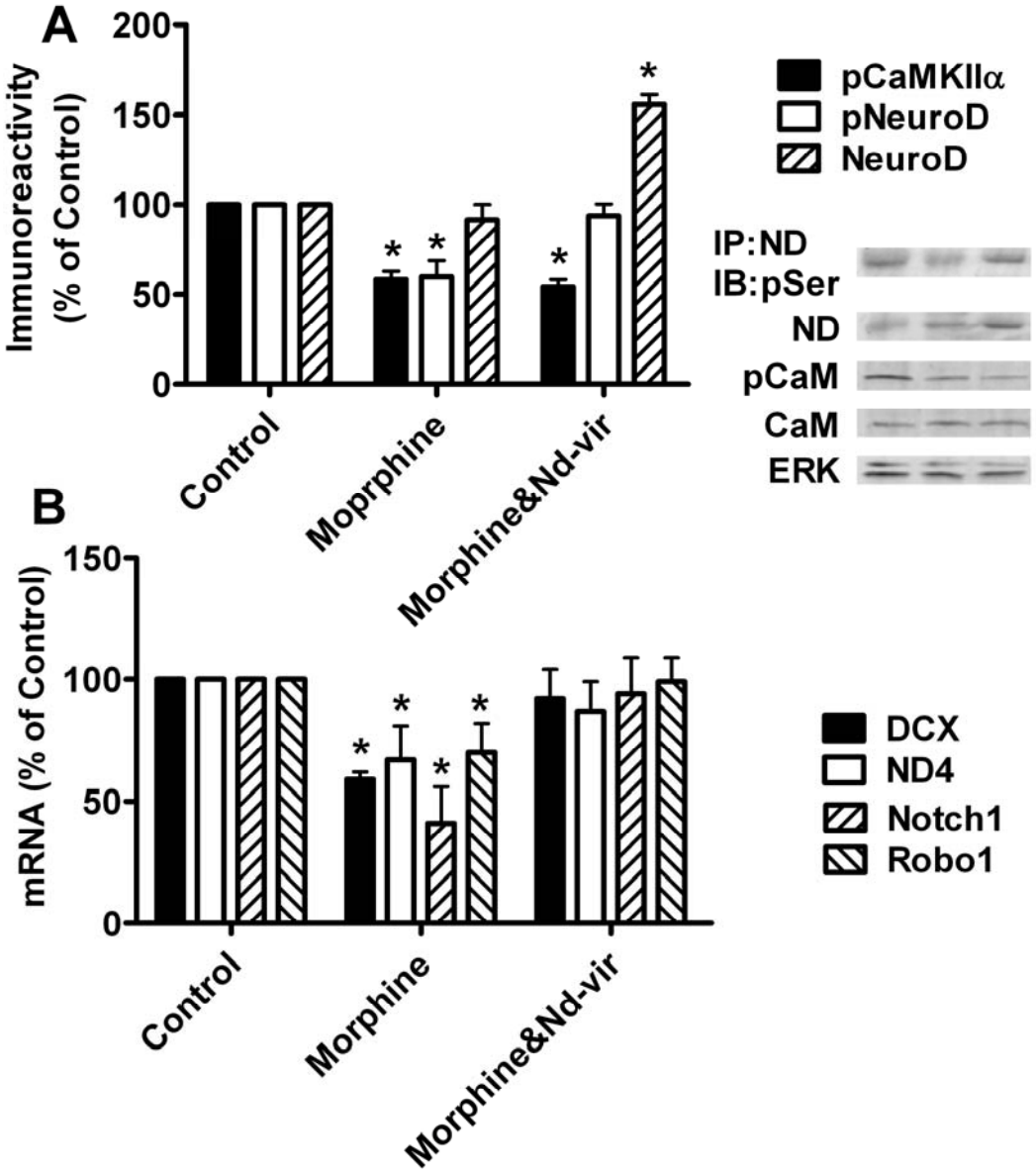

Fig. 4-17 Overexpression NeuroD rescues its activity

Primary cultures were treated with PBS, morphine (1 μM) or morphine (1 μM) plus nd-vir. (A) The amount of phosphorylated NeuroD, total NeuroD, total CaMKIIα, phosphorylated CaMKIIα and total ERK were determined as in Fig. 4-16. (B) The mRNA levels of DCX, ND4, Notch1 and Robo1 were determined with real-time PCR. The results (in A-B) were normalized against those in control samples. Experiments were repeated for four times.

Fig. 4-18 Overexpression NeuroD rescues spine stability

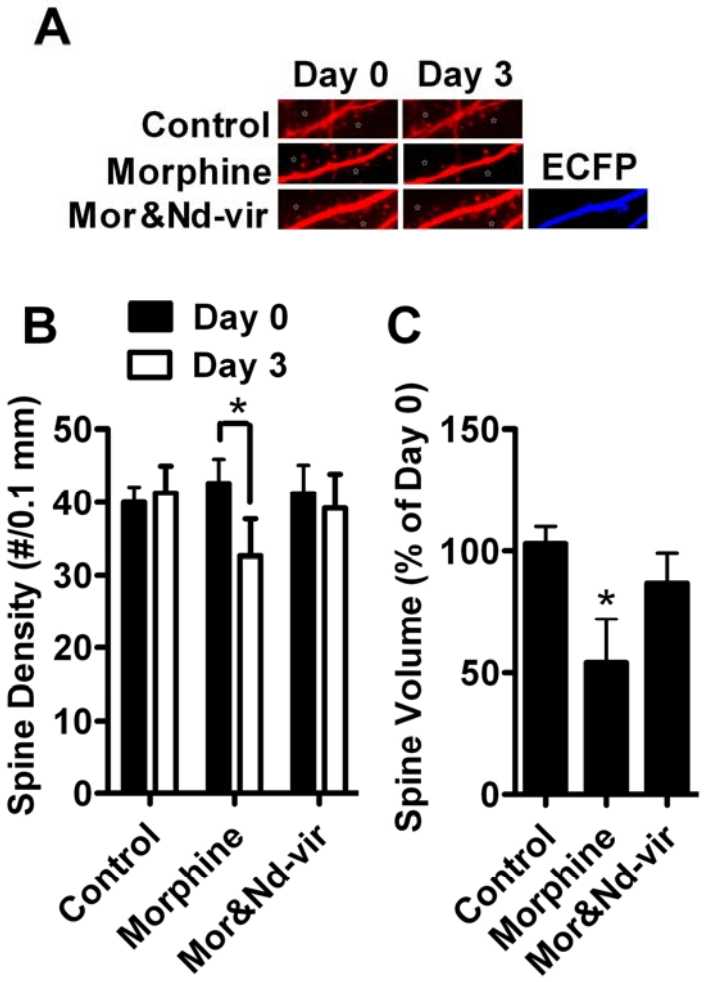

Fig. 4-18 Overexpression NeuroD rescues spine stability

Primary cultures were treated with PBS, morphine (1 μM) and morphine (1 μM) plus nd-vir for 3days. The live images on Day 0 and Day 3 were presented in (A). EGFP and ECFP was used indicated successful infection of con-vir/190-vir and nd-vir, respectively. The densities of spines on Day 0 and Day 3 were presented in (B). The spine volume (indicated by the overall DsRed fluorescence) was calculated by comparing the red fluorescence on dendritic spines on Day 3 to that on Day 0 (C).

4.5.1.2. Tolerance and internalization

Some concepts suggest a correlation between receptor internalization and tolerance development (110). In one theory, the inability of morphine to induce receptor internalization is suggested to keep receptor active on membrane, which promoters more profound adaptation responses and subsequent high tolerance (268). But this theory is not consistent with rapid desensitization induced by morphine (142). In another theory, the inability of morphine to resensitize MOR via receptor internalization leads to the decreased signaling capability of MOR (269). But this theory suggests an inverse correlation between receptor signaling and tolerance development. It fails to explain why decreased adaptation response (lower signaling) can lead to the higher tolerance. In addition, equivalent doses of morphine and methadone induced different receptor internalization but similar tolerance (270, 271). Therefore, the internalization is not a direct answer to the higher tolerance of morphine.

4.5.1.3 Tolerance and agonist-selective signaling

The different levels of tolerance have been hypothesized to be the results of differential gene expression induced by agonist-selective signaling. The effects of agonists on gene expression have been studied for a long time by using microarray and real-time PCR (234). Although the comparison among agonists is rare, the expressional controls on MOR-related factors have been reported. Treatment with etorphine, but not morphine, produces significant increase in protein levels of GRK2, dynamin II and β-arrestin 2 in mouse spinal cord (272).

4.5.2 NeuroD inhibits tolerance development

There is a correlation between the abilities of agonists to inhibit the activity of NeuroD and their abilities to induce tolerance development on analgesia tolerance. This hypothesis is supported by the wide impacts of NeuroD targets in the central nervous

system. In addition, chronic morphine decreases the rate of adult neurogenesis in dentate gyrus, which is highly related to NeuroD functions.

4.5.2.1 Tolerance development assay

To determine the influence of miR-190 and NeuroD on analgesia effect and tolerance development, a sixteen-day experiment was performed with the CD1 mice. To limit the number of mice used in the experiment, up-and-down method was used to determine the ED50s of agonists.

As indicated in Fig. 4-19, on Day 1, ED50s of morphine and fentanyl were assessed by up-and-down method and tail-flick assay. Mice were divided into five groups (30 per group) 4 hrs after test. Each group was injected intracerebroventrically with saline, con-vir, 190-vir, 190-vir-plus-nd-vir, or nd-vir and allowed to rest from Day 2 to Day 7.

On Day 8, the ED50s of morphine and fentanyl were determined in each group. Then each group was further divided into four sub-groups (seven to eight per subgroup): saline-1 saline-2, morphine and fentanyl. The mice in saline subgroups were injected with 0.3 ml saline subcutaneously three times a day for seven days (8:00, 16:00 and 24:00 from Day 9 to Day 15). The mice in morphine/fentanyl subgroup were injected subcutaneously with five folds of ED50 dose of morphine/fentanyl three times a day for seven days. ED50s used for calculation here was the ED50s of each group to which the subgroup belongs determined on Day 8. Thus the same subgroups in different groups will be injected with different amount agonists.

On Day 16, ED50s of morphine were determined in saline-1 and morphine subgroups, and ED50s of fentanyl were determined in saline-2 and fentanyl subgroups separately in each group. Tolerance was calculated by determine the percentage shift of

Fig. 4-19 Schematic of tolerance assay

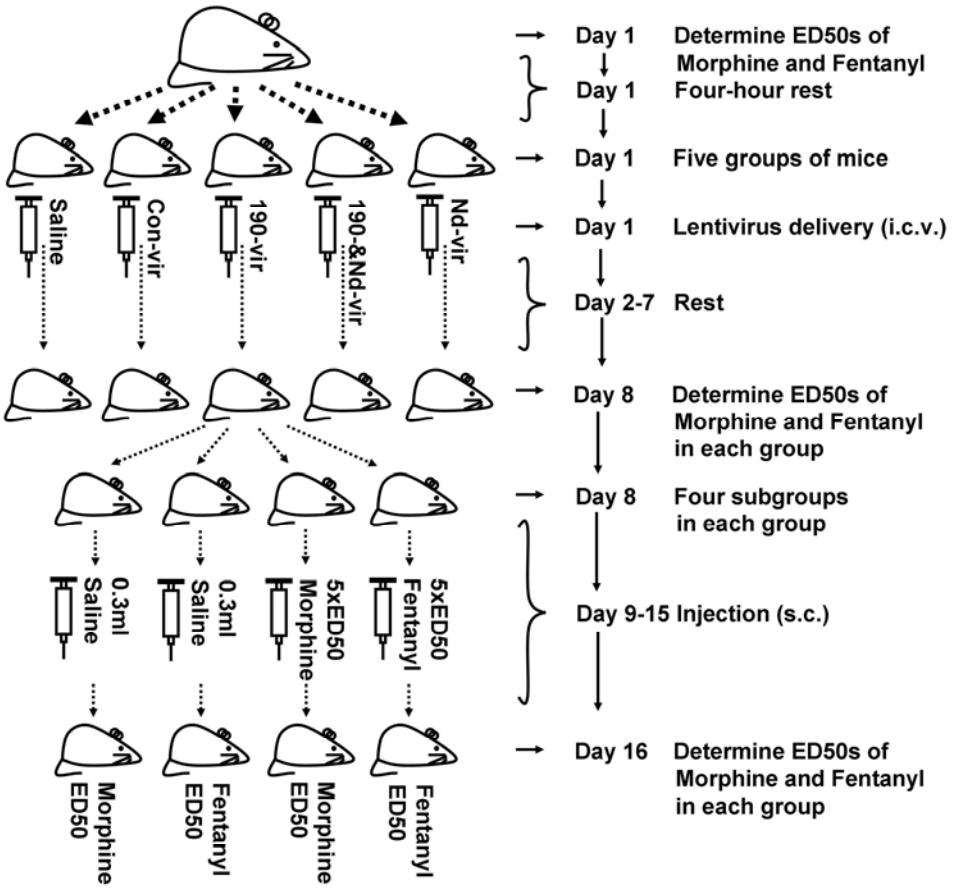

ED50s in each group (e.g. ED50 of morphine in morphine subgroup on Day 16/ ED50 of morphine in the whole group on Day 8-100%).

4.5.2.2 Modulating NeuroD expression affects analgesia

On Day 1 of experiment, the ED50s of morphine and fentanyl were 2.83±0.14 mg/kg and 22.2±1.1 μg/kg respectively in CD1 mice. Then the mice were divided into five groups which received i.c.v. injection of different lentivirus or lentiviruses combination.

ED50s of morphine and fentanyl were assessed again on Day 8 after six-day rest in each group. Mice delivered with saline or con-vir had similar ED50s to those determined on Day 1, suggesting the i.c.v. injection and lentivirus itself does not influence the abilities of agonists to induce analgesia effects (Table 4-2). Infection with 190-vir shifted the ED50 of morphine to 6.80±0.46 mg/kg (about 240% of that on Day 1) and shifted the ED50 of fentanyl to 64.3±3.1 μg/kg (about 290% of that on Day 1). Although nd-vir did not affect the ED50 by itself, it reduced the shift induced by 190-vir. In the mice received both 190-vir and nd-vir, the ED50s of morphine and fentanyl were 4.59±0.22 mg/kg (about 162% of that on Day 1) and 34.8±1.7 μg/kg (about 157% of that on Day 1) respectively (Fig. 4-20). Thus 190-vir influences the analgesia effects by decreasing NeuroD expression.

Moreover, considering the lentivirus system mimicked the effects of morphine and fentanyl, the similar decrease in analgesia effect should be observed after chronic morphine but not fentanyl treatment. If this hypothesis is correct, the higher tolerance induced by morphine than fentanyl will be explained at least partially.

Table 4-2 ED50s of morphine and fentanyl

Day 1					
M (mg/kg)	2.83±0.14				
F(μg/kg)	22.2±1.1				
Day 8					
	Saline	Con-vir	190-vir	190&nd-vir	Nd-vir
M (mg/kg)	3.11±0.15	3.30±0.19	6.80±0.46	4.59±0.22	3.00±0.16
M (% of Day 1)	110	117	240	162	106
F (μg/kg)	22.0±1.1	19.9±1.1	64.3±3.1	34.8±1.7	22.8±1.1
F (% of Day 1)	99	90	290	157	103
Day 16					
	Saline	Con-vir	190-vir	190&nd-vir	Nd-vir
Saline-1					
M (mg/kg)	3.49±0.17	3.48±0.17	7.65±0.73	3.90±0.19	3.35±0.12
M (% of Day 8)	*112*	*105*	*113*	*85*	*112*
Salin-2					
F (μg/kg)	23.6±1.4	21.1±1.4	68.6±4.2	34.8±1.7	22.2±1.1
F (% of Day 8)	*107*	*106*	*107*	*100*	*97*
Morphine					
M (mg/kg)	9.81±0.48	11.82±1.78	12.44±1.67	13.28±1.42	4.63±0.46
M (% of Day 8)	**315**	**358**	**183**	**289**	**203**
Fentanyl					
F (μg/kg)	51.5±2.5	44.2±4.4	68.9±3.4	81.0±3.9	42.2±2.9
F (% of Day 8)	**234**	**222**	**107**	**233**	**185**

Table 4-2 ED50s of morphine and fentanyl

The mice were treated as stated in *Materials and Methods* and Fig. 3A. The ED50s were determined by up-and-down method. The standard errors were provided next to ED50s. ED50s of each group on Day 8 were compared to the ED50s on Day 1 to indicate the influence of miR-190 and NeuroD on analgesia effects. The numbers are underlined. ED50s of each subgroup on Day 16 were compared to the ED50s of the group which the subgroup belongs to on Day 8 to indicate the influence of miR-190 and NeuroD on tolerance development. The shifts in saline subgroups were in *Italic*, while those in agonist subgroups were in **BOLD**. M and F presented morphine and fentanyl respectively.

Fig. 4-20 NeuroD affects analgesia effects

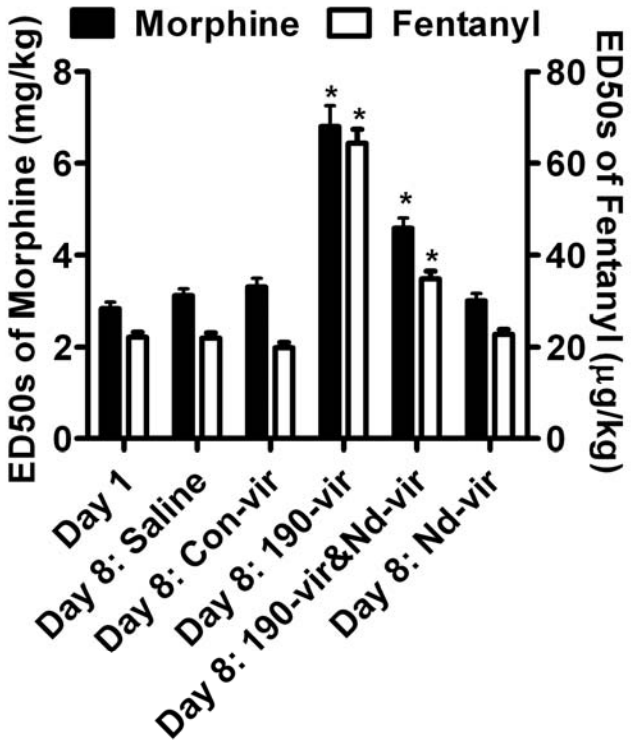

Fig. 4-20 NeuroD affects analgesia effects

The experiments were performed as indicated in Fig. 4-21. The effects of NeuroD and miR-190 on the analgesia effects were summarized.

4.5.2.3 Modulating NeuroD expression affects tolerance

miR-190 and NeuroD modulate analgesia effects. However, the data does not illustrate the influences of miR-190 and NeuroD on agonist-induced tolerance development. Hence, the five groups of mice were subjected to further treatment after determining the ED50s on Day 8. As shown in Fig. 4-21, each group of mice were divided into four subgroups and received s.c. injection with saline or morphine or fentanyl three times a day from Day 9 to Day 15.

Because ED50s are different in different groups, the same subgroups in different groups received different doses of agonists. To make these doses equivalent to each other, the ED50s in each group determined on Day 8 were used for calculation. Take morphine subgroups for instance, the mice received 15.5, 16.5, 32, 23, and 15 mg/kg morphine (500% of ED50 dose) in morphine subgroup of saline, con-vir, 190-vir, 190-vir plus nd-vir, and nd-vir group 21 times within 7 days, respectively. In addition the mice in fentanyl subgroups were injected with 110, 100, 322, 174 and 114 μg/kg respectively 21 times within 7 days. All the mice in saline subgroups (no matter saline-1 or -2) were injected with 0.3 ml saline three times a day for 7 days. Because of the equivalence among these doses, the tolerance or the shift of ED50 should be same if the lentivirus system did not affect the development of tolerance.

ED50s of agonists were determined on Day 16 by using the same procedure and analysis. In each group on Day 16, ED50 of morphine determined in salin-1 subgroup and ED50 of fentanyl determined in salin-2 subgroup were close to those ED50s determined in the same group on Day 8 (Table 4-2). Thus the effects of lentivirus system on analgesia effects reach to status stage before Day 8 and persist at least to Day 16. In addition, the tolerance determined in the experiments should reflect the ability of lentivirus system to modulate tolerance development directly but not the ability to modulate analgesia effect.

Morphine-induced tolerance development in each group was calculated by using the following formula: (morphine's ED50 in morphine subgroup on Day 16 / morphine's ED50 in the same group on Day 8 - 100%). Fentanyl-induced tolerance was calculated similarly except, ED50 of fentanyl and fentanyl subgroups were used. Table 4-2 provided the actually numbers of ED50s and the tolerance development was summarized in Fig. 21. In saline and con-vir, the tolerance were similar: saline (morphine 215%; fentanyl 134%) and con-vir (morphine 258%; fentanyl 122%) (Fig. 4-21). Therefore, lentivirus itself did not affect tolerance. Over-expressing NeuroD with nd-vir, the tolerance induced by morphine and fentanyl were similar (Fig. 4-21), suggesting NeuroD activity is required to maintain the analgesia effects. The decreased NeuroD induced by morphine may contribute to the higher tolerance of morphine than fentanyl.

Fig. 4-21 NeuroD affects tolerance development

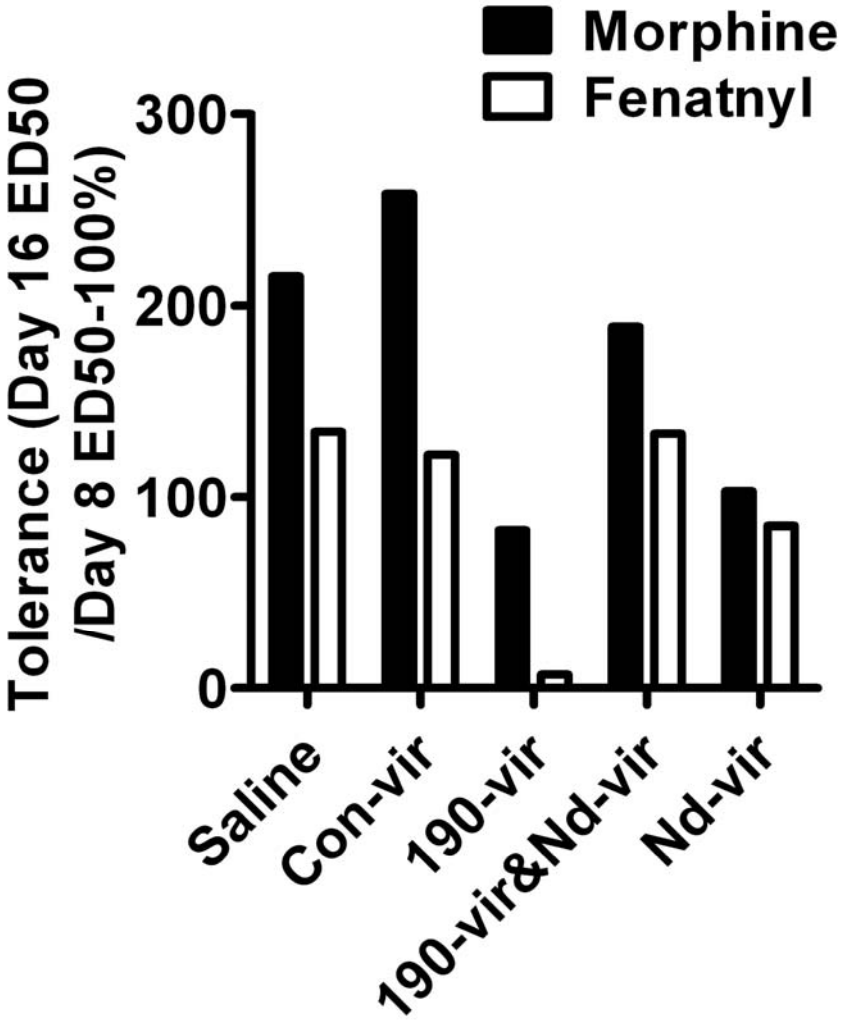

Fig. 4-21 NeuroD affects tolerance development

The experiments were performed as indicated in Fig. 4-19. The effects of NeuroD and miR-190 on the tolerance development were summarized.

5. Summary

As mentioned in the abstract, it is hypothesized that agonist-selective gene regulation may bridge the agonist-selective signaling and the agonist-selective physiological response. During my study, it was demonstrated that agonist-selective regulation on NeuroD and miR-190 bridges agonist-selective ERK phosphorylation and agonist-selective tolerance development.

Morphine induces ERK phosphorylation via PKC pathway and the phosphorylated ERK remains in the cytosol. Etorphine induces ERK phosphorylation via β-arrestin pathway and the phosphorylated ERK translocates into nucleus. The differential location of phosphorylated ERK and the activation of different sets of transcription factors result in agonist-selective regulation on the transcription of *talin2* gene locus and subsequently the cellular content of miR-190. In addition, chronic treatment with both morphine and fentanyl decreases the activity of CaMKIIα. miR-190 decreases the activity of NeuroD by suppressing the expression of NeuroD in a manner similar to most miRNAs. CaMKIIα increases the activity of NeuroD by mediating the phosphorylation on Ser^{336} of NeuroD. These two kinds of effects interact with each other, and the overall influence of agonists on NeuroD activity is that morphine decreases NeuroD activity, while fentanyl keeps it at basal level.

After analyzing the functions of NeuroD, a strong correlation was identified between NeuroD activity and dendritic spine stability. In addition, evaluating the decreased NeuroD activity induced by morphine, morphine-induced decrease in the dendritic spine stability is attenuated. Thus morphine influences spine stability by controlling the activity of NeuroD. The most important agonist-selective physiological response is the different tolerance induced by agonists. My studies have suggested that modulation on NeuroD activity will influence tolerance development; therefore it is possible that the higher level of tolerance induced by morphine results from the decreased NeuroD activity by morphine.

Definitely, there are many problems need further investigation. For example, how NeuroD activity contributes to the spine stability and inhibits the development of tolerance. Although many targets of NeuroD have been suggested to be involved in a variety of biological process in the central nervous system, identification is required. In addition, the ability of fentanyl to control YY1 phosphorylation via ERK phosphorylation has not been elucidated. ERK may lead to the phosphorylation of YY1 by itself or by other targets downstream of it. However, my results provide a possible route from the agonist-selective signaling *in vitro* to the agonist-selective physiological response *in vivo*.

In addition, my studies were not focused on the agonist-NeuroD-tolerance cascade totally. The contribution of MOR-lipid interaction was another topic. Both cholesterol and palmitoylation modulation contribute to the signaling of MOR. Cholesterol stabilizes MOR signaling by supporting the entirety of lipid raft microdomain which functions as an environment for the interaction between MOR and downstream signaling molecules. Palmitoylation stabilizes MOR signaling by maintaining the interaction between MOR and Gαi2 which is essential for Gαi2 activation and signal transduction.

Cholesterol and receptor palmitoylation also communicate with each other as indicated with the crystal structure of β2-adrenergic receptor. Cholesterol stabilizes the crystallization of β2-adrenergic receptor. It interacts with two palmitic acids covalently linked to two β2-adrenergic receptor molecules. Thus the interaction between cholesterol and palmitic acid linked to receptor may stabilize the receptor complex and subsequently contribute to the receptor signaling.

6. Materials and Methods

6.1 Animal studies

Six to eight-week-old CD1 (ICR) or C57/B6 male mice from Charles River (Charles River Laboratories, Portage, MI) were housed in groups of four with access to food and water *ad libitum* in an IACUC-accredited facility at University of Minnesota. All steps were taken to minimize animal suffering and all related procedures were taken in accordance with IACUC policies. Mice were allowed to habituate for one week before experiments.

Tail-flick testing was done between 1:00 and 4:00 p.m. Mice were placed in experimental room 2 h prior, for acclimatization. Mouse tails were placed over an analgesia meter (Columbus Instruments, Columbus) and radiant heat intensity was adjusted for 3 to 5s baseline latency. Cutoff time was 12s to minimize tail damage. Tail-withdrawal response was recorded 30 min after morphine or 15 min after fentanyl injection subcutaneously. Percent of maximum possible effect (%MPE) was calculated by the following formula: (measured latency-baseline latency) *100/(cut-off time-baseline latency). Each dose involved at least 8 mice. ED50 values were generated by using Graphpad Prism 5.0.

For chronic treatment, there are two kinds of procedure. In the first one, mice were anesthetized intraperitoneally (90 mg/kg ketamine and 10 mg/kg xylazine) and implanted with micro-osmotic pump (Alzet Corp., Palo Alto, CA, 1ul/hr 72 hr). The mice were infused with saline, 12μg/hr morphine or 0.31μg/hr fentanyl for three days. 12 μg/hr morphine [1 ED50 dose (2.4 mg/kg)/per 5 hours] and 0.31 μg/hr fentanyl [1 ED50 dose (27 μg/kg)/per 2 hours] were equivalent to each other because the analgesic effect of morphine decreased from 67% to 32% in 30 minutes, while that of fentanyl decreased from 64% to 33% in 15 minutes. In another protocol, the mice were injected with morphine or fentanyl at a dose which is five folds of ED50 three times a day for seven days.

The conditioned place preference (CPP) was separated into four sections. In preconditioning section, each mouse was placed separately into the CPP apparatus for 10 min, with free access to the two compartments. In conditioning section, mice of each treatment group were divided equally. Half of the mice received 5mg/kg morphine or 0.05mg/kg fentanyl subcutaneously in morning session and were placed immediately in the white compartment with green light and round decoration for 30 min. This compartment had been isolated from the other using a removable partition. These mice received equal volume of saline subcutaneously in evening session and were placed immediately in the black compartment with red light night and banding decoration for 30 min. Another half of mice were treated reversely, they received saline in morning session while morphine or fentanyl in evening session. Similar treatment lasted for five days. In the postconditioning section, mouse was placed in the middle of CPP apparatus for 10 min individually, with free access to the two compartments. In the extinguishing section, mouse was placed in the middle of CPP apparatus for 10 min again after six-day rest, with free access to the two compartments. The CPP time is calculated by using the following equation: time spent in the white compartment (drug-paired side) – time spent in black compartment (saline-paired side).

Up-down method described by Dixon and Massey (1969) is also used to determine the ED50 doses of agonists. The first animal was given a dose of drug that was close to the expected ED50 and then evaluated in the tail-flick test. If the %MPE value exceeded 50%, then the dose for the next animal was incrementally decreased (e.g., decreased by log dose of 0.05). Alternatively, if the tail-flick latency did not exceed the 50% MPE criterion, then the dose was incrementally increased (e.g., increased by log dose of 0.05). In general, the test was concluded after six animals (count from the last animal which has similar response to the one before it). The ED50 values and 95% confidence limit were calculated from the appropriate tables given by Dixon.

For intracerebroventricular injection of lentivirus, mouse was anesthetized intraperitoneally (90 mg/kg ketamine and 10 mg/kg xylazine) first. 5 μl of virus (6 X 10^8

TU/ml) were delivered at bregma using hypodermic needle (27 gauge, 1/4 inch). Animals were allowed to rest for 6 days prior to further experiment.

6.2 Cholesterol assay

Cholesterol concentrations were determined using an Amplex Red Cholesterol Assay Kit (Invitrogen). To determine total cellular cholesterol content, cells were homogenized in 0.32 M sucrose and 10 mM HEPES (pH 7.7) and the crude lysis was assayed. Samples were then centrifuged at 1,000g for 10 minutes at 4°C, the supernatant was collected and the pellet was rehomogenized; this process was repeated until the pellet appeared translucent. The collected supernatant was centrifuged at 100,000g for 60 minutes at 4°C. The cholesterol content of cell membranes was determined using the resuspended pellet. The cholesterol content in sucrose gradient fractions (see below) was measured in each fraction immediately after collection. To determine cholesterol incorporation, supernatants from lysed cells were divided into three equal portions. Samples were rotated at 4°C with PBS, HA antibody or FLAG antibody and immunoprecipitated using Protein G beads; the cholesterol concentration in the beads was then assayed.

6.3 Chromatin immunoprecipitation

After washing with cold PBS for three times, cells were fixed with 1% formaldehyde for 15 min at 25 °C. Incubation with glycine at a final concentration of 0.125 M for 5 min at 25 °C was used to stop the fixation. Cells were collected and washed with PBS twice. 400µl (for 100mm dish) CHIP lysis buffer (50 mM HEPES pH 7.5; 140 mM NaCl; 1 % Triton X100; 0.1 % sodium deoxycholate; protease inhibitors) was used to resuspend the cells. Samples were sonicated by using Sonicator Cell Disruptor model W-220F (Heat Systems-Ultrasonic, Inc., Plainview, New York) at output level 6 for 120 sec (15 seconds rest between 15 seconds sonication). After 5 min centrifugation at 13,000 g at 4 °C, the supernatant was added with the antibody against

target protein with 10% saved as input control. Then the samples were rotated in cold room for 6 hours. The Protein G agarose beads with salmon sperm DNA were added to samples, which were then rotated for another 12 hours.

The protein G agarose beads were then washed with CHIP lysis buffer, high salt CHIP lysis buffer (50 mM HEPES pH 7.5; 500 mM NaCl; 1 % Triton X100; 0.1 % sodium deoxycholate; protease inhibitors), CHIP wash buffer (10 mM Tris pH 8.0; 250 mM LiCl; 0.5 % NP-40; 0.5 % sodium deoxycholate; 1 mM EDTA.) and TE buffer (10mM Tris, pH 8.0, 1 mM EDTA), sequentially and twice individually. 75 µl elution buffer (50 mM Tris pH 8.0; 1 % SDS; 10 mM EDTA) was added to the beads and incubated at 65 °C for 10 min. This step was repeated twice and the collected elution buffer was incubated at 65 °C for another 6 hours. The input controls were added with elution buffer to 150 µl and incubated at 65 °C for 6 hours. The DNA was then purified with QIAquick PCR purification kit (Qiagen, CA) and used in further PCR analysis.

6.4 Confocal imaging

Cells were cultured on poly-lysine (sigma, MO) coated–cover slip in 6-well plates. After various treatments, cells were washed twice with PBS at 4ºC twice and fixed with 1% formaldehyde for 20 minutes at room temperature. Then the cells were washed with PBS three times and blocked in blocking buffer (PBS with 5% normal donkey serum). MOR was visualized by staining with mouse monoclonal anti-HA (Convance, 1:1000) and Alexa 488 conjugated goat-anti-mouse antibody (1:1000) (Molecular Probes, OR). Lipid rafts were identified by using lipid raft labeling kits (Molecular Probes, OR). The confocal images were captured with a BD CARV II™ Confocal Imager and a Leica DMIRE2 fluorescence microscope. Colocalization of the fluorescence pixels was calculated with IPlab 4.0 software (BD Biosciences-Bioimage, MD). For live cell imaging, cells were labeled with the same antibodies, but without fixation. After removing the excess antibodies with repeated washings, live cell images were captured with same setup, except that the microscope stage was heated to 37ºC and enclosed with

a chamber in order to control the CO_2 level at 5%. Images of these cells before and 10 minutes after drug treatment were captured and analyzed accordingly.

6.5 Fluorescence flow cytometry

The HA-tagged μ-opioid receptor (HA-MOR) expressed on the plasma membrane was quantified by FACS analysis of the cell surface immunofluoresence. Briefly, HEK293 cells stably expressing HA-MOR were treated under various conditions. After rapidly rinsing twice with PBS at 4 °C, the cells were incubated at 4 °C for 2 hours in PBS with the anti-HA antibody (1:1000 dilution). Afterward, the cells were washed twice with PBS at 4 °C and then incubated with Alexa 488-labeled goat anti-mouse IgG secondary antibody (1:1000) at 4 °C for one additional hour. After washing the cells to remove the excess secondary antibodies, the cells were fixed with 1% formaldehyde in PBS prior to FACS analysis. Receptor immunofluorescence was measured by FACScan (Becton Dickinson, Palo Alto, CA). Fluorescence intensity of 10,000 cells was collected for each sample. Cell Quest software (Becton Dickinson) was used to calculate the mean fluorescence intensity of the cells population.

6.6 Immunoblotting

Following treatments, cells were washed twice with PBS at 4°C. 500 μl of lysis buffer [50 mM Tris-HCl (pH 7.5), 150 mM NaCl, 0.25% sodium deoxycholate, 0.1% Nonidet P-40, 0.5% Triton X-100, 0.1% digitonin (for membrane protein), 50 mM NaF, 1 mM dithiothreitol, 0.5 mM phenylmethylsulfonyl fluoride, 50 mM sodium pyrophosphate, 10 mM sodium vanadate, and 1X protease inhibitor cocktail (Roche Applied Science, IN)] were added to each 100-mm dish. Cells were then incubated for 20 minutes at room temperature. After centrifugation at 13,000g for 5 minutes, the supernatant was transferred to a new tube and mixed with SDS-PAGE sample buffer. Protein concentrations were determined by BCA assay (Pierce, IL) to ensure that equal amounts of protein were loaded onto each lane.

After transferring to a polyvinylidene difluoride membrane, nonspecific binding was blocked by incubating for 1 hour with 10% nonfat milk. Primary antibodies were added and the membranes incubated for another hour at room temperature. Membranes were washed three times with TTBS (0.1% Tween 20, 50 mM Tris-HCl [pH 7.4], and 150 mM NaCl), incubated for 2 hours with AP-conjugated secondary antibody, and washed three times with TTBS. Membranes were developed using ECF substrate (GE Healthcare, Buckinghamshire, UK). The fluorescence intensity of each band was scanned using a Storm 860 system and determined using ImageQuant analysis software (GE Healthcare).

For detecting the phosphorylated YY1 and NeuroD, the cells were separated into three equal aliquots. One of the aliquots was used to prepare the nuclear extract by using the NE-PER Nuclear and Cytoplasmic Extract kit (Pierce). The nuclear extract was mixed with antibody against YY1 for 6 hrs and then with Protein G beads (Invitrogen) overnight at 4°C. The proteins bound to the beads were extracted by using sample buffer after washing the beads with lysis buffer twice. The phosphorylation of YY1 was determined by measuring the amounts of phosphorylated amino acids (pAAs) in the immunoprecipitated YY1. Another aliquot was used to measure the total YY1 and total NeuroD after extracting the nuclear protein. The last aliquot was prepared into whole cell lysis using the same kit, in which the phosphorylated ERK and total ERK were determined. When it is not required to measure the phosphorylated YY1, the cells were only separated into two aliquots equally.

6.7 Immunoprecipitation

Cells treated with proper amount of lysis buffer. The lysis buffer is similar to that used in immunoblotting. NP-40 and sodium deoxycholate are omitted. And digitonin is omitted if the target protein is not membrane protein. After proper extraction (nucleus protein), the sample were centrifuged at 13,000g at 4°C for 10 mins. The supernatant

was added with antibody against target protein. After incubation with rotation for 6 hrs at 4°C, Protein G beads (Invitrogen, CA) were added. Before using the beads were washed with lysis buffer twice. The samples were rotated with the beads overnight at 4°C, washed six times with lysis buffer, and the bound proteins was extracted by using sample buffer.

6.8 Intracellular calcium measurement

One day before assay, CORNING® black with clear flat bottom 96-well-assay plate (Fisher scientific, IL) was coated with poly-L-Lysine (Fisher scientific, IL). The cells were suspended in their grown media at a density of ~3×104 cells/well and seeded into 96-well plate with 150µl media/well. Then the cells were incubated at 37 ºC in a humidified atmosphere of 5% or 10% CO2 at 37 ºC overnight so as to reach an 80~90% confluent cell monolayer before assay.

At the day of assay, 100µl medium/well was removed from plate. To each well, 50µl FLIPR® calcium assay reagent (Molecular Devices Corp) dissolved in 1x reagent buffer (1×HANKs buffer with 20mM HEPES), pH 7.4, with 5mM probenecid was added and the plate was incubated at 37ºC for 1 hour. Agonists, inhibitors and other reagents were dissolved in the assay buffer (HBSS: KCl 5mM, KH2PO4 0.3mM, NaCl 138mM, NaHCO3 4mM, Na2HPO4 0.3mM, D-glucose 5.6mM, with additional 20mM HEPES, 2.5mM probenecid and 13mM CaCl2).

Using a FLEXstation (Molecular Devices Corp.), the intracellular Calcium fluorescence increases after robotic injections of agonists, inhibitors or other reagents were monitored every 1.52 sec intervals with excitation wavelength at 485 nm and with emission wavelength at 525nm. The intracellular calcium release normally reached its maximum 15 sec after agonist injection and returned to baseline within 30 sec after injection.

The intracellular Calcium fluorescence was measured up to 90 sec after agonist injection. Thus a curve of time-course response of intracellular Calcium release was generated. The area under curve (AUC) is then calculated. The baseline was determined by averaging the fluorescence form the time points before agonist injection and after fluorescence returns to basal level. The fluorescence of the time points indicating the intracellular calcium release was added together after subtracting the baseline from them. The result is the AUC.

The AUC from 3 to 4 wells of cells were averaged. For desensitization, the agonist was incubated with cells for indicated times, then ADP was injected to the well to determine the activity of receptor. MOR agonist morphine did not evoke intracellular calcium release alone in HEK293 cells stably expressing HA tagged MOR. Whereas 200nM ADP, a agonist of universally expressed Gq-coupled purinergic P2Y receptor, induced transient but robust intracellular calcium release. In addition, this ADP-induced intracellular calcium release was significantly potentiated by morphine, while MOR antagonist, naloxone, blocked this potentiation. Thus the potentiation of morphine on ADP-induced intracellular calcium release can sever as an indicator of MOR activity.

6.9 Intracellular cAMP

The Amplified Luminescent Proximity Homogenous Assays (AlphaScreen) for cAMP supplied by PerkinElmer Life and Analytical Sciences (Boston, MA) were used. Cells were plated into 96-well plates or 6-well plates (primary neuron). Various concentrations of opioid agonists and antagonists were diluted with KRHB buffer containing 10 μM forskolin and 0.5 mM IBMX. After removal of the growth medium, the 96-well plates were placed on ice, and 100 μl of the drug solution was added to the well.

After sealing the plates with HotSeal (Diversified Biotech, Boston, MA), the plates were incubated at 37°C for 15 min. Reactions were terminated by placing the plates in a

water bath at 85–90°C for 5 min to lyse the cells and release the intracellular cAMP. After centrifuging the plates at 500g for 2 min, the amount of cAMP in 4 μl of the supernatant was determined using the donor beads coated with streptavidin, acceptor beads coated with anti-cAMP antibodies, and biotinylated cAMP in the AlphaScreen assay system. The cAMP concentrations, from 10^{-11} to 10^{-4} M, were used to construct the standard curve. The donor beads (final 20 μg/ml), the acceptor beads (final 15 μg/ml), and biotinylated cAMP (final 10 nM) were diluted in the 1X control buffer [5 mM HEPES, pH 7.4, and 0.3% Tween 20 (60%) and Hanks' buffered salts saline (40%)].

A total of 4 μl of the reaction supernatant or standard cAMP solutions was pipetted into duplicate wells of a 384-well Opti-plate (PerkinElmer Life and Analytical Sciences) with a Biomek 2000 workstation (Beckman Coulter, Fullerton, CA) in a dimly lit room at 4°C. The plate was then sealed with TopSeal adhesive sealing films (PerkinElmer Life and Analytical Sciences) and incubated in the dark at 4°C for 2 h. Then, 12 μl of the donor beads were pipetted into the wells and the mixtures were incubated in the dark at 4°C for 18 to 24 h. After equilibrating to room temperature in the dark (4 h), the content of the cAMP in each well was determined by exciting the donor beads at 680 nm, generating a singlet O2 resulting in the fluorescence emission of the acceptor beads at 520 to 620 nm. The fluorescence of the wells was quantitated with the Fusion (PerkinElmer Life and Analytical Sciences) plate reader, and the amount of cAMP in each sample was extrapolated from the standard curve. For primary neuronal cultures, the cAMP concentration was normalized with the protein concentration because primary cultures are difficult to be plated equally.

6.10 Lipid raft and sucrose gradient

Continuous sucrose gradient was used to separate the microdomains on cell membrane depending on their densities. At the day of assay, cells were collected with 500mM sodium carbonate (pH11, 0.5ml per 150 mm dish) after agonist pretreatment. The cells in Na_2CO_3 were homogenized by passing through 22 gauge, 3-inch needles for

10 times following by sonication using Sonicator Cell Disruptor model W-220F (Heat Systems-Ultrasonic, Inc., Plainview, New York) at output level 4 for 30 sec (10 seconds rest between 10 seconds sonication) . The prepared homogenates were mixed with equal volumes of 80% sucrose [in morpholinoethanesulfonic acid (MES)-buffered saline (MBS), pH 6.8] and placed at the bottom of ultracentrifugation tubes. On top of it, 5% to 30% continuous sucrose gradients, which were formed by the Gradient Station (BioComp), were placed.

Then the gradients were centrifuged at 32,000 rpm for 16 hrs in a SW41 rotor at 4^{o}C, and total 12 fractions were collected with 1ml volume for each sample. To do this assay in mouse hippocampus or primary culture, the cell membrane was concentrated as described in membrane preparation section first. Then the collected cell membrane fractions were subjected for the continuous sucrose gradient. Because MOR expresses relative low in primary culture and mouse hippocampus, the fractions collected form the gradient was further concentrated by supplying the trichloroacetic acid to accomplish a final concentration at 10%. After incubating the samples on ice for 10 min, they were centrifuged at 13,000g at 4^{o}C for 10 min. The pellets were washed with acetone twice followed with 10 min incubation on ice and 10min centrifugation at 13,000g at 4^{o}C. The final pellets were suspended in sample buffer for further analysis.

6.11 Luciferase reporter assays

Elk-1 and CREB activities were measured by using the Elk-1 or CREB driven luciferase reporter system (Stratagene, La Jolla, CA). Briefly, HEK293 cells stably expressing HA-MOR were transfected with GAL4-Elk-1 or GAL4-CREB-1, pFR-luc, and pRL-tk-luc. The GAL4-Elk-1 or GAL-CREB-1 encodes a fusion protein containing the GAL4 DNA binding domain, the transactivation domain of Elk-1 or CREB. pFR-luc encodes the firefly luciferase gene under the control of the GAL4 DNA binding element, and pRL-tk-luc encodes *Renilla* luciferase under the control of the thymidine kinase promoter. One day following transfection, the cells were incubated in serum-free media

overnight. Stimulations with agonists were carried out for 12 hours. Luciferase activities were determined using a dual luciferase assay kit (Promega, Madison, WI). Cells were extracted and assayed sequentially for firefly and *Renilla* luciferase activities. Firefly activities were normalized to *Renilla* luciferase activity.

6.12 Membrane preparation

The cells were resuspended or tissue in appropriate volume (2.5ml per T-75 flask) of homogenizing buffer (10mM HEPES, 0.32M sucrose pH 7.7). Samples were homogenized by using glass Dounce homogenizer (Wheaton, 40ml, pestle A) for 10 strokes. Supernatant was collected after centrifugation at 1,000g for 10 min at 4 ^{o}C. The homogenization and centrifugation were repeated until the pellet appears translucent. The collected supernatant was centrifuged at 100,000g for 60 min. The resulted pellet is the membrane fraction.

6.13 miRNA microarrays

Microarray technique was used to profile miRNA expression at a genome-wide scale. A miRNA probe set was purchased from Invitrogen, designed based on the Sanger miRBase Sequence Database, Release 9.0 (October 2006). The set contains ~1140 oligonucleotides as probes, which are complementary to Caenorhabditis elegans, Drosophila, zebra fish, mouse, rat and human miRNAs, and also include a number of internal and negative control probes. The oligonucleotides were quadruply printed on Corning GAPSII-coated slides by the Microarray Facility at the University ofMinnesota.

For RNA labeling, 25 μg of total RNA was ligated to 0.5 μg of a synthetic linker, pCU-DY547 (Dharmacon, Lafayette, CO). To control the hybridization process, reference DNA oligonucleotides complementary to a subset of mammalian miRNAs were combined and labeled with a ULYSIS Alexa Fluor 647 Kit (Invitrogen). Labeled RNAs and DNAs were then mixed and hybridized to microarray slides. Afterward,

slides were scanned with a ScanArray 5000 machine (Perkin Elmer, Waltham, MA), and BlueFuse (BlueGenome, Cambridge, UK) was used to quantify pixel intensities. Individual spots on the slides were further inspected to exclude abnormal spots from subsequent calculations.

GeneSpring GX 7.3.1 (Agilent Technologies) was used for data normalization based on a percentile method, after background subtraction. Only the miRNAs conserved in human, mouse and rat were subjected for further two-tailed Student's t-test. Microarray data have been deposited into the National Center for Biotechnology Information's Gene Expression Omnibus database under the series GSE14268. Control, morphine-, and fentanyl-treated, rat primary neuronal cultures and mouse hippocampus samples were prepared in triplicates, while mouse cerebellum samples were examined in duplicates. Expression of individual miRNAs as well as mRNAs was quantified by real-time PCR (Qiagen) and normalized to the β-actin mRNA.

6.14 Nuclear extraction

After washing with PBS at 4 ºC twice, 100 µl of lysis buffer (10mM HEPES, pH 7.9, 10mM KCl, 10% 0.1mM EDTA, 0.1mM EGTA, 0.6 % Nonidet P-40, 10mM NaF, 1mM dithiothreitol, 0.5mM phenylmethylsulfonyl fluoride, 50mM sodium pyrophosphate, 10mM sodium vanadate and 1×protease inhibitor cocktail from Roche) was added to the cells in 35 mm dishes and the cells were incubated on ice for 15 minutes. After centrifugation, the supernatant was transferred to a fresh tube and designated as the cytosolic fraction. To fractionate the nuclear proteins further, the nuclear pellet was re-suspended in an extraction buffer (20mM Hepes, pH 7.9, 0.4 M NaCl, 1mM EDTA, 1mM EGTA, 10mM NaF, 1mM dithiothreitol, 0.5mM phenylmethylsulfonyl fluoride, 50mM sodium pyrophosphate, 10mM sodium vanadate and 1×protease inhibitor cocktail from Roche) at 4 ºC. After incubation at 4 ºC for 15 minutes with vigorously shaking, the nuclear extract was centrifuged at 14,000 rpm for 5 minutes and the supernatant was removed and designated as the nucleus fraction. If the

nucleus fraction is not required to be separated from cytosolic fraction, the nucleus protein was extracted by sonication.

6.15 Palmitoylation assay

Palmitoylation of receptors was assayed according to the method of Drisdel et al. (230). Briefly, receptors were immunoprecipitated with MOR antibody other than HA antibody to achieve a higher specificity. The beads were incubated sequentially for 2 hours in lysis buffer containing 50 mM NEM (to block free sulfhydryls), 1 M hydroxylamine (to remove thioester-linked palmitic acid) and 40 μM btn-BMCC (to label free sulfhydryls generated by the hydroxylamine treatment). Extensive washing was included between steps. Covalently linked btn-BMCC was detected using AP-conjugated streptavidin. Receptor loading was controlled based on protein concentration and receptor expression levels.

6.16 PKC subtypes activity assay

Cells were grown in 100mm dishes. At the day of assay, cells were treated with drugs, and then the reaction was ceased by washing with ice-cold PBS twice. Cells were lysed with cell lysis buffer (as used in immunoblotting) at room temperature for 10 min. Then the total cell lysis was centrifuged and the supernatant was collected while the pellet was discarded. To determine the PKC subtypes activity individually, PKCε, PKRα or PKCγ specific antibody (Cell Signaling, MA) was added into the supernatant and mixed in 4ºC for 6hrs. After that, G-protein agarose beads (Invitrogen, CA) 25μl were added into supernatant and antibody mixture; and the mixture was continued to rotate in 4ºC for overnight.

The next day, beads were washed with PBS for 3 times, then the reaction buffer (Cell signaling, MA) with biotinylated PKA substrate peptides (contains the residues surrounding serine 133 of CREB, peptide core sequence: RRPS*YRK) (Cell signaling,

MA) was added together into beads to react with PKC subtypes which were precipitated with G-protein agarose. Reaction was continued for 15min in 37ºC with rotation, and was ceased by adding 120µl (50mM) EDTA. After rotating in 37 ºC for 5 min, the mixture was centrifuged at 13,000rpm for 2min at 4ºC.

Then the supernatant which contained the reacted substrates was collected and 30µl streptavidin linked beads were added. After rotating at 4ºC for 30min, antibody from rabbit specific recognizing phosphor-PKA substrate was added into streptavidin beads (Cell Signaling, MA). Then the streptavidin beads were washed with lysis buffer for three times after rotating at 4ºC overnight. In the next, anti-rabbit-488 in 200µl lysis buffer was added into streptavidin beads as secondary antibody and the beads were continued to be mixed and rotated for 2 hrs at room temperature but without light. In the end, beads which trapped phosphor-substrates and antibodies were washed with lysis buffer for last three times and 500µl lysis buffer was added into beads at the final steps. The beads were mixed and added into 96-well-plate for 100 µl in each well. The PKC subtypes activity level was determined by measuring the antibody fluorescence intensity by α-Fusion plate reader (PerkinElmer Life and Analytical Sciences, Boston, MA).

PKC subtypes' inhibitors were Ordered from Biomatik corporation (Cambridge, Ontraio Canada, www.biomatik.biz): PKCα (Myr-FARKGALRQ-OH), PKCγ (Myr-EAVSLKPT-OH) and PKCε (Myr-CRLVLASC-OH)

6.17 Primary culture

Coverslips were cleaned in 65% HNO_3 for 1 hr or 1%HCl in 75% EtOH overnight. Coverslips or plates were coated with 1mg/50ml Poly-L-Lysine overnight and washed with PBS twice.

Hippocampus or desired brain region were dissected form one-day old rat and plated in Earle's Balanced Salt Solution (EBSS, Invirtogen , CA) with 0.5g/L glucose.

After washing with EBSS twice, the tissue was placed in digestion solution (30mM EDTA, 15mg/ml papain and 132mg/L L-cysteine in EBSS) for 30 min at 37 ºCon. The tissue was mixed every 5 min. After the tissue was settled down at the bottom of tube, digestion inhibition solution (1mg/ml BSA, 1mg/ml ovornucoid, 0.001% DNase in EBSS) was used to replace digestion solution. By using pipette, the tissue was suspended in digestion inhibition solution. After centrifugation at 20,000g at 4 ºC for 10 min, the cells were suspended in plating medium (10% FBS, 5% horse serum, 200μM L-cystine, 10mM sodium pyruvate and antibiotics in MEM). 1.5 million cells were plated in one 35-mm dish with 2ml plating medium.

After 5 hours incubation in 5% CO_2, new plating medium was used to replace the old one. After 24 hours, neuron feeding medium [25% neurobasal media (Invitrogen, CA), 2% horse serum, 2% B27 (Invitrogen, CA), 10mM sodium pyruvate, 0.016 mg/ml 5'Fluoro-2'-deoxy-uridine, 0.032 mg/ml uridine and antibiotics in MEM] was used to replace plating medium. Every week, 0.5 ml conditioned medium from glial cell cultures was added into each 35mm dish. The primary cultures matured after three weeks.

The glial cells were prepared similarly, except glial feeding medium (5% horse serum, 10mM sodium pyruvate and antibotics in MEM) was used instead of neuron feeding medium at the second of plating. Neuron feeding medium without 5'-Fluoro-2'-deoxy-uridine and uridine was used to replace glial feeding medium 7 days after plating. The conditioned medium is collect every three days in the next two weeks. The transfection of primary cultures was done six days after plating. For one 35-mm dish, 0.5 μg plasmid and 30 μl lipofectamine 2000 were mixed in 100 μl MEM individually. After votexing for 5 second and incubating for 5min, the two MEM solutions were combined and votexed for 10 second. Then, 10 min later, the MEM solution was added to primary culture whose medium has been replaced with MEM. The transfection last for 90 min, and neuron feeding medium with 20mg/L d,1-2-amino-5-phosphonopentanoic acid was used to replace MEM at last.

6.18 Radioligand receptor binding assay

Expression of membrane receptors in both stable and transient expressed cells was determined by using radio-labeled receptor ligands in binding assay. Cells were harvested by PBS-EDTA (0.1M NaCl, 0.01M NaH_2PO_4, 0.04% EDTA, pH7.4). Then cells were washed with PBS for twice and re-suspended in 25mM HEPES buffer (pH 7.6). Total binding was determined by co-incubating intact cells with 50,000cpm/ml [^{3}H]-labeled agonists and 5mM $MgCl_2$ at 25^{o}C for 90 min. Non-specific binding was determined by co-incubating cells with 10μM antagonists in addition to [^{3}H]-labeled agonists. Then the cells with radio-ligand binding were collected on Whatman GF/B filters. The protein concentrations were determined by the BCA assay. Then the specific binding was determined by calculating the difference between total and non-specific binding. The receptor concentration was then normalized with protein concentrations.

For receptor binding on cell membrane or in cell lysis, the procedure is similar except the sample preparation. Cell membrane was prepared as stated in the membrane preparation. For cell lysis, the lysis was added with PEG8000 and NaCl to achieve a final concentration at 15% PEG8000 and 150mM NaCl. The sample was incubated on ice for 10 min and then subjected for further experiment.

6.19 Site-direct mutagenesis

The primers used for mutagenesis were designed as mentioned below. The sense primer was generated by flanking 20 nucleotides on each side of the site for mutation. The site of mutation is six nucleotides maximally and have the originated coding sequence been replaced by targeting coding sequence. It is better to have a digestion site in the targeting coding sequence. The antisense primer was generated by complementarily reversing the sense primer. It is also good to have the sense primer 5-7 bp longer or shorter than the anti-sense primer at 3'.

The mutation takes advantage of the PCR techniques. 10ng plasmid containing the coding sequence of un-mutated target gene, 5pmol of the sense and antisense primer, 0.1 mM dNTP and 10 unit Pfu was prepared in 50µl 1XPfu reaction buffer. Another three 50µl reaction mix was prepared similarly but with 10pmol, 15pmol or 20pmol primer. The PCR reaction started from 5 min 95 ^{o}C which was followed with 18 cycles of 90 sec 94 ^{o}C, 90 sec 60 ^{o}C and 10 min 68 ^{o}C. Normally 1kb of the plasmid take 1min for extension and additional two min extension was added to make sure the plasmid was extended fully. The reaction finished with another 10 min 68 ^{o}C.

After collect all the reaction mix in the same tube and 10 unit DpnI was added, it was incubated in 37 ^{o}C for 90 min. After digestion, one volume isopropenol was added and the solution was kept on ice for 10 min. After centrifugation at 13,000g 4 ^{o}C for 10 min, the pellet was washed with 70% ethanol and air dried. 10ul TE was used to re-dissolve the pellet and the resulted solution was used for transformation. The transformed bacterial was cultured in LB medium individually; the plasmids were purified by using Miniprep kit from Qiagen CA. The successful mutation was identified by sequencing or by enzyme digestion if applicable.

6.20 Transfection and infection

Effectene (Qiagen, CA) was used to transfect HEK cells. The procedure followed the instruction of the Effectene kit. Lipofectamine 2000 was also used as described in the instruction from company (Invitrogen, CA)

Infection with adenovirus was used to express MOR or its mutant in MEF (mouse embryonic fibroblast) cells or in primary culture. The titer of the adenovirus was determined to be ~2.5X10^{9} infectious units (IU)/ml. MEF cells were grown in DMEM with 10%FBS at 6-well-plate for 1 days to be about 50% confluent. Then the media was removed; and Ad-MOR virus was diluted in DMEM with 2% FBS and added to the wells. Multiplicity of infection (MOI) was determined by making virus dose and MOR

expression level curve. Desired MOI was used to reach the approximated same receptor expression level. After adding adenovirus and DMEM with 2% FBS for 1 and half hour, DMEM with 10% FBS was added back to the MEF cells, and the cell were incubated at 37^{o}C for 24 hours before the assays were carried out. For primary culture, the virus was titrated before usage. The virus was added to the primary culture directly to achieve a >60 transfection efficiency after three days.

Lentivirus was constructed by using using the Lentiviral miR RNAi Expression System (Invitrogen, CA). The lentivirus expressing miRNA was generated by insert the oligo-nucleotides into the designed point of pLenti6/V5-GW/EmGFP. The resulted construct was recombinated with pDONR221 and V5-DEST to get the final plasmid. The plasmid was transfected with pLP1, pLP2 and pLP/VSVG (Invitrogen, CA) into 293FT (Invitrogen, CA) according to the instruction. The culture medium was collected in the two days following transfection. After filtering the medium with 0.45 μm filter, the medium was centrifuged in 100,000 g at 4 ^{o}C for 2 hours. The pellet was resuspended in the MEM and used for infection. The lentivirus for normal protein was generated by inserting the cDNA or antisense cDNA of target gene into between the SpeI and XhoI sites of V5-DEST (Invitrogen). ECFP (with its own CMV promoter) from ECFP-N1 (Clontech) was inserted in the XbaI site of the same plasmid. Titers of the viruses (~1.2 × 10^{6} TU/ml) were determined in neuroblastoma N2A cells. Infection efficiency was more than 60%. The virus used for animal work was further concentrated by centrifuging in 24,000 g at 4 ^{o}C for 2 hours to achieve a high titer (6 × 10^{8} TU/ml).

6. 21 TUNEL assay

TUNEL assays (TdT-dUTP terminus nick-end labeling assays) were carried out with ApopTag In Situ Apoptosis Detection kit (Chemicon), and cells were counterstained with DAPI (Santa Cruz). As a positive control, cells were treated with 1 μM staurosporin for 24 hours to induce apoptosis.

6.22 Statistic

The comparison between two groups was performed by using the two tailed t-test. The comparison between multiple groups was performed by using the one-way ANOVA test with Dunnett-test as post-hoc test, or two-way ANOVA-test with Bonferroni-test as post-hoc test.

7. Reference

1. Ferguson, S. S. (2001) Evolving concepts in G protein-coupled receptor endocytosis: the role in receptor desensitization and signaling. *Pharmacol Rev* **53,** 1-24.
2. Fredriksson, R. & Schioth, H. B. (2005) The repertoire of G-protein-coupled receptors in fully sequenced genomes. *Mol Pharmacol* **67,** 1414-25.
3. Neer, E. J. (1995) Heterotrimeric G proteins: organizers of transmembrane signals. *Cell* **80,** 249-57.
4. Neves, S. R., Ram, P. T. & Iyengar, R. (2002) G protein pathways. *Science* **296,** 1636-9.
5. Violin, J. D. & Lefkowitz, R. J. (2007) Beta-arrestin-biased ligands at seven-transmembrane receptors. *Trends Pharmacol Sci* **28,** 416-22.
6. Borgland, S. L. (2001) Acute opioid receptor desensitization and tolerance: is there a link? *Clin Exp Pharmacol Physiol* **28,** 147-54.
7. Ahn, S., Maudsley, S., Luttrell, L. M., Lefkowitz, R. J. & Daaka, Y. (1999) Src-mediated tyrosine phosphorylation of dynamin is required for beta2-adrenergic receptor internalization and mitogen-activated protein kinase signaling. *J Biol Chem* **274,** 1185-8.
8. DeWire, S. M., Ahn, S., Lefkowitz, R. J. & Shenoy, S. K. (2007) Beta-arrestins and cell signaling. *Annu Rev Physiol* **69,** 483-510.
9. Shenoy, S. K. & Lefkowitz, R. J. (2003) Multifaceted roles of beta-arrestins in the regulation of seven-membrane-spanning receptor trafficking and signalling. *Biochem J* **375,** 503-15.
10. Luttrell, L. M. & Lefkowitz, R. J. (2002) The role of beta-arrestins in the termination and transduction of G-protein-coupled receptor signals. *J Cell Sci* **115,** 455-65.
11. Kohout, T. A., Nicholas, S. L., Perry, S. J., Reinhart, G., Junger, S. & Struthers, R. S. (2004) Differential desensitization, receptor phosphorylation, beta-arrestin recruitment, and ERK1/2 activation by the two endogenous ligands for the CC chemokine receptor 7. *J Biol Chem* **279,** 23214-22.

12. Lohse, M. J., Andexinger, S., Pitcher, J., Trukawinski, S., Codina, J., Faure, J. P., Caron, M. G. & Lefkowitz, R. J. (1992) Receptor-specific desensitization with purified proteins. Kinase dependence and receptor specificity of beta-arrestin and arrestin in the beta 2-adrenergic receptor and rhodopsin systems. *J Biol Chem* **267,** 8558-64.

13. Ma, L. & Pei, G. (2007) beta-arrestin signaling and regulation of transcription. *J Cell Sci* **120,** 213-8.

14. Xiao, K., McClatchy, D. B., Shukla, A. K., Zhao, Y., Chen, M., Shenoy, S. K., Yates, J. R., 3rd & Lefkowitz, R. J. (2007) Functional specialization of beta-arrestin interactions revealed by proteomic analysis. *Proc Natl Acad Sci U S A* **104,** 12011-6.

15. Zhou, L. F. & Zhu, Y. P. (2006) Changes of CREB in rat hippocampus, prefrontal cortex and nucleus accumbens during three phases of morphine induced conditioned place preference in rats. *J Zhejiang Univ Sci B* **7,** 107-13.

16. Hughes, J., Smith, T. W., Kosterlitz, H. W., Fothergill, L. A., Morgan, B. A. & Morris, H. R. (1975) Identification of two related pentapeptides from the brain with potent opiate agonist activity. *Nature* **258,** 577-80.

17. Kosterlitz, H. W. & Waterfield, A. A. (1975) In vitro models in the study of structure-activity relationships of narcotic analgesics. *Annu Rev Pharmacol* **15,** 29-47.

18. Pert, C. B. & Snyder, S. H. (1973) Opiate receptor: demonstration in nervous tissue. *Science* **179,** 1011-4.

19. Simon, E. J., Hiller, J. M. & Edelman, I. (1973) Stereospecific binding of the potent narcotic analgesic (3H) Etorphine to rat-brain homogenate. *Proc Natl Acad Sci U S A* **70,** 1947-9.

20. Terenius, L. (1973) Stereospecific interaction between narcotic analgesics and a synaptic plasm a membrane fraction of rat cerebral cortex. *Acta Pharmacol Toxicol (Copenh)* **32,** 317-20.

21. Evans, C. J., Keith, D. E., Jr., Morrison, H., Magendzo, K. & Edwards, R. H. (1992) Cloning of a delta opioid receptor by functional expression. *Science* **258,** 1952-5.

22. Hawkins, K. N., Knapp, R. J., Gehlert, D. R., Lui, G. K., Yamamura, M. S., Roeske, L. C., Hruby, V. J. & Yamamura, H. I. (1988) Quantitative autoradiography of [3H]CTOP binding to mu opioid receptors in rat brain. *Life Sci* **42,** 2541-51.

23. Kieffer, B. L., Befort, K., Gaveriaux-Ruff, C. & Hirth, C. G. (1992) The delta-opioid receptor: isolation of a cDNA by expression cloning and pharmacological characterization. *Proc Natl Acad Sci U S A* **89,** 12048-52.

24. Fukuda, K., Kato, S., Mori, K., Nishi, M. & Takeshima, H. (1993) Primary structures and expression from cDNAs of rat opioid receptor delta- and mu-subtypes. *FEBS Lett* **327,** 311-4.

25. Chen, Y., Mestek, A., Liu, J. & Yu, L. (1993) Molecular cloning of a rat kappa opioid receptor reveals sequence similarities to the mu and delta opioid receptors. *Biochem J* **295 (Pt 3),** 625-8.

26. Yasuda, K., Raynor, K., Kong, H., Breder, C. D., Takeda, J., Reisine, T. & Bell, G. I. (1993) Cloning and functional comparison of kappa and delta opioid receptors from mouse brain. *Proc Natl Acad Sci U S A* **90,** 6736-40.

27. Meng, F., Xie, G. X., Thompson, R. C., Mansour, A., Goldstein, A., Watson, S. J. & Akil, H. (1993) Cloning and pharmacological characterization of a rat kappa opioid receptor. *Proc Natl Acad Sci U S A* **90,** 9954-8.

28. Li, S., Zhu, J., Chen, C., Chen, Y. W., Deriel, J. K., Ashby, B. & Liu-Chen, L. Y. (1993) Molecular cloning and expression of a rat kappa opioid receptor. *Biochem J* **295 (Pt 3),** 629-33.

29. Law, P. Y. & Loh, H. H. (1999) Regulation of opioid receptor activities. *J Pharmacol Exp Ther* **289,** 607-24.

30. Law, P. Y., Wong, Y. H. & Loh, H. H. (2000) Molecular mechanisms and regulation of opioid receptor signaling. *Annu Rev Pharmacol Toxicol* **40,** 389-430.

31. Walker, J. M., Bowen, W. D., Walker, F. O., Matsumoto, R. R., De Costa, B. & Rice, K. C. (1990) Sigma receptors: biology and function. *Pharmacol Rev* **42,** 355-402.

32. Martin, W. R., Eades, C. G., Thompson, J. A., Huppler, R. E. & Gilbert, P. E. (1976) The effects of morphine- and nalorphine- like drugs in the nondependent and morphine-dependent chronic spinal dog. *J Pharmacol Exp Ther* **197,** 517-32.

33. Mollereau, C., Parmentier, M., Mailleux, P., Butour, J. L., Moisand, C., Chalon, P., Caput, D., Vassart, G. & Meunier, J. C. (1994) ORL1, a novel member of the opioid receptor family. Cloning, functional expression and localization. *FEBS Lett* **341,** 33-8.

34. Fukuda, K., Kato, S., Mori, K., Nishi, M., Takeshima, H., Iwabe, N., Miyata, T., Houtani, T. & Sugimoto, T. (1994) cDNA cloning and regional distribution of a novel member of the opioid receptor family. *FEBS Lett* **343,** 42-6.

35. Chen, Y., Fan, Y., Liu, J., Mestek, A., Tian, M., Kozak, C. A. & Yu, L. (1994) Molecular cloning, tissue distribution and chromosomal localization of a novel member of the opioid receptor gene family. *FEBS Lett* **347,** 279-83.

36. Johnson, P. S., Wang, J. B., Wang, W. F. & Uhl, G. R. (1994) Expressed mu opiate receptor couples to adenylate cyclase and phosphatidyl inositol turnover. *Neuroreport* **5,** 507-9.

37. Bunzow, J. R., Saez, C., Mortrud, M., Bouvier, C., Williams, J. T., Low, M. & Grandy, D. K. (1994) Molecular cloning and tissue distribution of a putative member of the rat opioid receptor gene family that is not a mu, delta or kappa opioid receptor type. *FEBS Lett* **347,** 284-8.

38. Lachowicz, J. E., Shen, Y., Monsma, F. J., Jr. & Sibley, D. R. (1995) Molecular cloning of a novel G protein-coupled receptor related to the opiate receptor family. *J Neurochem* **64,** 34-40.

39. Prenzel, N., Zwick, E., Daub, H., Leserer, M., Abraham, R., Wallasch, C. & Ullrich, A. (1999) EGF receptor transactivation by G-protein-coupled receptors requires metalloproteinase cleavage of proHB-EGF. *Nature* **402,** 884-8.

40. Farooqui, M., Geng, Z. H., Stephenson, E. J., Zaveri, N., Yee, D. & Gupta, K. (2006) Naloxone acts as an antagonist of estrogen receptor activity in MCF-7 cells. *Mol Cancer Ther* **5,** 611-20.

41. Meis, S. (2003) Nociceptin/orphanin FQ: actions within the brain. *Neuroscientist* **9,** 158-68.

42. New, D. C. & Wong, Y. H. (2002) The ORL1 receptor: molecular pharmacology and signalling mechanisms. *Neurosignals* **11,** 197-212.

43. Calo, G., Guerrini, R., Rizzi, A., Salvadori, S. & Regoli, D. (2000) Pharmacology of nociceptin and its receptor: a novel therapeutic target. *Br J Pharmacol* **129,** 1261-83.

44. Taylor, F. & Dickenson, A. (1998) Nociceptin/orphanin FQ. A new opioid, a new analgesic? *Neuroreport* **9,** R65-70.

45. Polastron, J., Meunier, J. C. & Jauzac, P. (1994) Chronic morphine induces tolerance and desensitization of mu-opioid receptor but not down-regulation in rabbit. *Eur J Pharmacol* **266,** 139-46.

46. Mogil, J. S. & Pasternak, G. W. (2001) The molecular and behavioral pharmacology of the orphanin FQ/nociceptin peptide and receptor family. *Pharmacol Rev* **53,** 381-415.

47. Matthes, H. W., Smadja, C., Valverde, O., Vonesch, J. L., Foutz, A. S., Boudinot, E., Denavit-Saubie, M., Severini, C., Negri, L., Roques, B. P., Maldonado, R. & Kieffer, B. L. (1998) Activity of the delta-opioid receptor is partially reduced, whereas activity of the kappa-receptor is maintained in mice lacking the mu-receptor. *J Neurosci* **18,** 7285-95.

48. Kitanaka, N., Sora, I., Kinsey, S., Zeng, Z. & Uhl, G. R. (1998) No heroin or morphine 6beta-glucuronide analgesia in mu-opioid receptor knockout mice. *Eur J Pharmacol* **355,** R1-3.

49. Loh, H. H., Liu, H. C., Cavalli, A., Yang, W., Chen, Y. F. & Wei, L. N. (1998) mu Opioid receptor knockout in mice: effects on ligand-induced analgesia and morphine lethality. *Brain Res Mol Brain Res* **54,** 321-6.

50. Abdelhamid, E. E., Sultana, M., Portoghese, P. S. & Takemori, A. E. (1991) Selective blockage of delta opioid receptors prevents the development of morphine tolerance and dependence in mice. *J Pharmacol Exp Ther* **258,** 299-303.

51. Fundytus, M. E., Schiller, P. W., Shapiro, M., Weltrowska, G. & Coderre, T. J. (1995) Attenuation of morphine tolerance and dependence with the highly selective delta-opioid receptor antagonist TIPP[psi]. *Eur J Pharmacol* **286,** 105-8.

52. Zhu, Y., King, M. A., Schuller, A. G., Nitsche, J. F., Reidl, M., Elde, R. P., Unterwald, E., Pasternak, G. W. & Pintar, J. E. (1999) Retention of supraspinal delta-like analgesia and loss of morphine tolerance in delta opioid receptor knockout mice. *Neuron* **24,** 243-52.

53. Filliol, D., Ghozland, S., Chluba, J., Martin, M., Matthes, H. W., Simonin, F., Befort, K., Gaveriaux-Ruff, C., Dierich, A., LeMeur, M., Valverde, O., Maldonado, R. & Kieffer, B. L. (2000) Mice deficient for delta- and mu-opioid receptors exhibit opposing alterations of emotional responses. *Nat Genet* **25,** 195-200.

54. Roberts, A. J., Gold, L. H., Polis, I., McDonald, J. S., Filliol, D., Kieffer, B. L. & Koob, G. F. (2001) Increased ethanol self-administration in delta-opioid receptor knockout mice. *Alcohol Clin Exp Res* **25,** 1249-56.

55. Gaveriaux-Ruff, C. & Kieffer, B. L. (2002) Opioid receptor genes inactivated in mice: the highlights. *Neuropeptides* **36,** 62-71.

56. Massotte, D., Brillet, K., Kieffer, B. & Milligan, G. (2002) Agonists activate Gi1 alpha or Gi2 alpha fused to the human mu opioid receptor differently. *J Neurochem* **81,** 1372-82.

57. Simonin, F., Valverde, O., Smadja, C., Slowe, S., Kitchen, I., Dierich, A., Le Meur, M., Roques, B. P., Maldonado, R. & Kieffer, B. L. (1998) Disruption of the kappa-opioid receptor gene in mice enhances sensitivity to chemical visceral pain, impairs pharmacological actions of the selective kappa-agonist U-50,488H and attenuates morphine withdrawal. *Embo J* **17,** 886-97.

58. McLaughlin, J. P., Marton-Popovici, M. & Chavkin, C. (2003) Kappa opioid receptor antagonism and prodynorphin gene disruption block stress-induced behavioral responses. *J Neurosci* **23,** 5674-83.

59. Hsia, J. A., Moss, J., Hewlett, E. L. & Vaughan, M. (1984) ADP-ribosylation of adenylate cyclase by pertussis toxin. Effects on inhibitory agonist binding. *J Biol Chem* **259,** 1086-90.

60. Wong, Y. H., Demoliou-Mason, C. D. & Barnard, E. A. (1989) Opioid receptors in magnesium-digitonin-solubilized rat brain membranes are tightly coupled to a pertussis toxin-sensitive guanine nucleotide-binding protein. *J Neurochem* **52,** 999-1009.

61. Sanchez-Blazquez, P., Garcia-Espana, A. & Garzon, J. (1995) In vivo injection of antisense oligodeoxynucleotides to G alpha subunits and supraspinal analgesia evoked by mu and delta opioid agonists. *J Pharmacol Exp Ther* **275,** 1590-6.

62. Sanchez-Blazquez, P., Juarros, J. L., Martinez-Pena, Y., Castro, M. A. & Garzon, J. (1993) Gx/z and Gi2 transducer proteins on mu/delta opioid-mediated supraspinal antinociception. *Life Sci* **53,** PL381-6.

63. Standifer, K. M., Rossi, G. C. & Pasternak, G. W. (1996) Differential blockade of opioid analgesia by antisense oligodeoxynucleotides directed against various G protein alpha subunits. *Mol Pharmacol* **50,** 293-8.

64. Garzon, R., Pichiorri, F., Palumbo, T., Iuliano, R., Cimmino, A., Aqeilan, R., Volinia, S., Bhatt, D., Alder, H., Marcucci, G., Calin, G. A., Liu, C. G., Bloomfield, C. D., Andreeff, M. & Croce, C. M. (2006) MicroRNA fingerprints during human megakaryocytopoiesis. *Proc Natl Acad Sci U S A* **103,** 5078-83.

65. Tallent, M., Dichter, M. A., Bell, G. I. & Reisine, T. (1994) The cloned kappa opioid receptor couples to an N-type calcium current in undifferentiated PC-12 cells. *Neuroscience* **63,** 1033-40.

66. Piros, E. T., Prather, P. L., Law, P. Y., Evans, C. J. & Hales, T. G. (1996) Voltage-dependent inhibition of Ca2+ channels in GH3 cells by cloned mu- and delta-opioid receptors. *Mol Pharmacol* **50,** 947-56.

67. Piros, E. T., Prather, P. L., Loh, H. H., Law, P. Y., Evans, C. J. & Hales, T. G. (1995) Ca2+ channel and adenylyl cyclase modulation by cloned mu-opioid receptors in GH3 cells. *Mol Pharmacol* **47,** 1041-9.

68. Charles, A. C., Piros, E. T., Evans, C. J. & Hales, T. G. (1999) L-type Ca2+ channels and K+ channels specifically modulate the frequency and amplitude of spontaneous Ca2+ oscillations and have distinct roles in prolactin release in GH3 cells. *J Biol Chem* **274,** 7508-15.

69. Henry, D. J., Grandy, D. K., Lester, H. A., Davidson, N. & Chavkin, C. (1995) Kappa-opioid receptors couple to inwardly rectifying potassium channels when coexpressed by Xenopus oocytes. *Mol Pharmacol* **47,** 551-7.

70. Audet, N., Paquin-Gobeil, M., Landry-Paquet, O., Schiller, P. W. & Pineyro, G. (2005) Internalization and Src activity regulate the time course of ERK activation by delta opioid receptor ligands. *J Biol Chem* **280,** 7808-16.

71. Belcheva, M. M., Clark, A. L., Haas, P. D., Serna, J. S., Hahn, J. W., Kiss, A. & Coscia, C. J. (2005) Mu and kappa opioid receptors activate ERK/MAPK via different protein kinase C isoforms and secondary messengers in astrocytes. *J Biol Chem* **280,** 27662-9.

72. Hawes, B. E., van Biesen, T., Koch, W. J., Luttrell, L. M. & Lefkowitz, R. J. (1995) Distinct pathways of Gi- and Gq-mediated mitogen-activated protein kinase activation. *J Biol Chem* **270,** 17148-53.

73. Hawes, B. E., Luttrell, L. M., van Biesen, T. & Lefkowitz, R. J. (1996) Phosphatidylinositol 3-kinase is an early intermediate in the G beta gamma-mediated mitogen-activated protein kinase signaling pathway. *J Biol Chem* **271,** 12133-6.

74. Rodriguez-Fernandez, J. L. & Rozengurt, E. (1996) Bombesin, bradykinin, vasopressin, and phorbol esters rapidly and transiently activate Src family tyrosine kinases in Swiss 3T3 cells. Dissociation from tyrosine phosphorylation of p125 focal adhesion kinase. *J Biol Chem* **271,** 27895-901.

75. Simonson, M. S., Wang, Y. & Herman, W. H. (1996) Nuclear signaling by endothelin-1 requires Src protein-tyrosine kinases. *J Biol Chem* **271,** 77-82.

76. Luttrell, D. K. & Luttrell, L. M. (2004) Not so strange bedfellows: G-protein-coupled receptors and Src family kinases. *Oncogene* **23,** 7969-78.

77. Okamoto, Y., Tsuneto, S., Matsuda, Y., Inoue, T., Tanimukai, H., Tazumi, K., Ono, Y., Kurokawa, N. & Uejima, E. (2007) A retrospective chart review of the antiemetic effectiveness of risperidone in refractory opioid-induced nausea and vomiting in advanced cancer patients. *J Pain Symptom Manage* **34,** 217-22.

78. Zheng, H., Zeng, Y., Zhang, X., Chu, J., Loh, H. H. & Law, P. Y. (2009) {micro}-Opioid Receptor Agonists Differentially Regulate the Expression of miR-190 and NeuroD. *Mol Pharmacol* **Epub ahead of print**.

79. Kramer, H. K. & Simon, E. J. (2000) mu and delta-opioid receptor agonists induce mitogen-activated protein kinase (MAPK) activation in the absence of receptor internalization. *Neuropharmacology* **39,** 1707-19.

80. Williams, J. T., Christie, M. J. & Manzoni, O. (2001) Cellular and synaptic adaptations mediating opioid dependence. *Physiol Rev* **81,** 299-343.

81. Avidor-Reiss, T., Nevo, I., Levy, R., Pfeuffer, T. & Vogel, Z. (1996) Chronic opioid treatment induces adenylyl cyclase V superactivation. Involvement of Gbetagamma. *J Biol Chem* **271,** 21309-15.

82. Bie, B. & Pan, Z. Z. (2005) Increased glutamate synaptic transmission in the nucleus raphe magnus neurons from morphine-tolerant rats. *Mol Pain* **1,** 7.

83. Thompson, R. C., Mansour, A., Akil, H. & Watson, S. J. (1993) Cloning and pharmacological characterization of a rat mu opioid receptor. *Neuron* **11,** 903-13.

84. Wang, J. B., Imai, Y., Eppler, C. M., Gregor, P., Spivak, C. E. & Uhl, G. R. (1993) mu opiate receptor: cDNA cloning and expression. *Proc Natl Acad Sci U S A* **90,** 10230-4.

85. Zimprich, A., Simon, T. & Hollt, V. (1995) Cloning and expression of an isoform of the rat mu opioid receptor (rMOR1B) which differs in agonist induced desensitization from rMOR1. *FEBS Lett* **359,** 142-6.

86. Pan, Y. X., Xu, J., Bolan, E., Chang, A., Mahurter, L., Rossi, G. & Pasternak, G. W. (2000) Isolation and expression of a novel alternatively spliced mu opioid receptor isoform, MOR-1F. *FEBS Lett* **466,** 337-40.

87. Abbadie, C., Rossi, G. C., Orciuolo, A., Zadina, J. E. & Pasternak, G. W. (2002) Anatomical and functional correlation of the endomorphins with mu opioid receptor splice variants. *Eur J Neurosci* **16,** 1075-82.

88. Furchgott, R. (1966) The use of haloalkylamines in the differentiation of receptors and in the determination of dissciationof receptor-agonist complexes. *Adv Drug Res (Harper NJ and Simmonds AB eds)* **3,** 21-55.

89. Kenakin, T. (1995) Agonist-receptor efficacy. I: Mechanisms of efficacy and receptor promiscuity. *Trends Pharmacol Sci* **16,** 188-92.

90. Urban, J. D., Clarke, W. P., von Zastrow, M., Nichols, D. E., Kobilka, B., Weinstein, H., Javitch, J. A., Roth, B. L., Christopoulos, A., Sexton, P. M., Miller, K. J., Spedding, M. & Mailman, R. B. (2007) Functional selectivity and classical concepts of quantitative pharmacology. *J Pharmacol Exp Ther* **320,** 1-13.

91. Kenakin, T. (1995) Agonist-receptor efficacy. II. Agonist trafficking of receptor signals. *Trends Pharmacol Sci* **16,** 232-8.

92. Shenoy, S. K., Drake, M. T., Nelson, C. D., Houtz, D. A., Xiao, K., Madabushi, S., Reiter, E., Premont, R. T., Lichtarge, O. & Lefkowitz, R. J. (2006) beta-arrestin-dependent, G protein-independent ERK1/2 activation by the beta2 adrenergic receptor. *J Biol Chem* **281,** 1261-73.

93. Gesty-Palmer, D., Chen, M., Reiter, E., Ahn, S., Nelson, C. D., Wang, S., Eckhardt, A. E., Cowan, C. L., Spurney, R. F., Luttrell, L. M. & Lefkowitz, R. J. (2006) Distinct beta-arrestin- and G protein-dependent pathways for parathyroid hormone receptor-stimulated ERK1/2 activation. *J Biol Chem* **281,** 10856-64.

94. Azzi, M., Charest, P. G., Angers, S., Rousseau, G., Kohout, T., Bouvier, M. & Pineyro, G. (2003) Beta-arrestin-mediated activation of MAPK by inverse agonists reveals distinct active conformations for G protein-coupled receptors. *Proc Natl Acad Sci U S A* **100,** 11406-11.

95. Zheng, H., Loh, H. H. & Law, P. Y. (2008) {beta}-Arrestin-Dependent {micro}-Opioid Receptor-Activated Extracellular Signal-Regulated Kinases (ERKs)

Translocate to Nucleus in Contrast to G Protein-Dependent ERK Activation. *Mol Pharmacol* **73,** 178-90.

96. Tohgo, A., Choy, E. W., Gesty-Palmer, D., Pierce, K. L., Laporte, S., Oakley, R. H., Caron, M. G., Lefkowitz, R. J. & Luttrell, L. M. (2003) The stability of the G protein-coupled receptor-beta-arrestin interaction determines the mechanism and functional consequence of ERK activation. *J Biol Chem* **278,** 6258-67.
97. Tohgo, A., Pierce, K. L., Choy, E. W., Lefkowitz, R. J. & Luttrell, L. M. (2002) beta-Arrestin scaffolding of the ERK cascade enhances cytosolic ERK activity but inhibits ERK-mediated transcription following angiotensin AT1a receptor stimulation. *J Biol Chem* **277,** 9429-36.
98. Kobayashi, H., Narita, Y., Nishida, M. & Kurose, H. (2005) Beta-arrestin2 enhances beta2-adrenergic receptor-mediated nuclear translocation of ERK. *Cell Signal* **17,** 1248-53.
99. Kang, J., Shi, Y., Xiang, B., Qu, B., Su, W., Zhu, M., Zhang, M., Bao, G., Wang, F., Zhang, X., Yang, R., Fan, F., Chen, X., Pei, G. & Ma, L. (2005) A nuclear function of beta-arrestin1 in GPCR signaling: regulation of histone acetylation and gene transcription. *Cell* **123,** 833-47.
100. Felder, C. C., Kanterman, R. Y., Ma, A. L. & Axelrod, J. (1990) Serotonin stimulates phospholipase A2 and the release of arachidonic acid in hippocampal neurons by a type 2 serotonin receptor that is independent of inositolphospholipid hydrolysis. *Proc Natl Acad Sci U S A* **87,** 2187-91.
101. Hoyer, D., Clarke, D. E., Fozard, J. R., Hartig, P. R., Martin, G. R., Mylecharane, E. J., Saxena, P. R. & Humphrey, P. P. (1994) International Union of Pharmacology classification of receptors for 5-hydroxytryptamine (Serotonin). *Pharmacol Rev* **46,** 157-203.
102. Polakiewicz, R. D., Schieferl, S. M., Gingras, A. C., Sonenberg, N. & Comb, M. J. (1998) mu-Opioid receptor activates signaling pathways implicated in cell survival and translational control. *J Biol Chem* **273,** 23534-41.

103. Stout, B. D., Clarke, W. P. & Berg, K. A. (2002) Rapid desensitization of the serotonin(2C) receptor system: effector pathway and agonist dependence. *J Pharmacol Exp Ther* **302,** 957-62.

104. Harizi, H., Corcuff, J. B. & Gualde, N. (2008) Arachidonic-acid-derived eicosanoids: roles in biology and immunopathology. *Trends Mol Med* **14,** 461-9.

105. Meves, H. (2008) Arachidonic acid and ion channels: an update. *Br J Pharmacol* **155,** 4-16.

106. Mottola, D. M., Kilts, J. D., Lewis, M. M., Connery, H. S., Walker, Q. D., Jones, S. R., Booth, R. G., Hyslop, D. K., Piercey, M., Wightman, R. M., Lawler, C. P., Nichols, D. E. & Mailman, R. B. (2002) Functional selectivity of dopamine receptor agonists. I. Selective activation of postsynaptic dopamine D2 receptors linked to adenylate cyclase. *J Pharmacol Exp Ther* **301,** 1166-78.

107. Kilts, J. D., Connery, H. S., Arrington, E. G., Lewis, M. M., Lawler, C. P., Oxford, G. S., O'Malley, K. L., Todd, R. D., Blake, B. L., Nichols, D. E. & Mailman, R. B. (2002) Functional selectivity of dopamine receptor agonists. II. Actions of dihydrexidine in D2L receptor-transfected MN9D cells and pituitary lactotrophs. *J Pharmacol Exp Ther* **301,** 1179-89.

108. Keith, D. E., Murray, S. R., Zaki, P. A., Chu, P. C., Lissin, D. V., Kang, L., Evans, C. J. & von Zastrow, M. (1996) Morphine activates opioid receptors without causing their rapid internalization. *J Biol Chem* **271,** 19021-4.

109. Zhang, J., Ferguson, S. S., Barak, L. S., Bodduluri, S. R., Laporte, S. A., Law, P. Y. & Caron, M. G. (1998) Role for G protein-coupled receptor kinase in agonist-specific regulation of mu-opioid receptor responsiveness. *Proc Natl Acad Sci U S A* **95,** 7157-62.

110. Koch, T., Widera, A., Bartzsch, K., Schulz, S., Brandenburg, L. O., Wundrack, N., Beyer, A., Grecksch, G. & Hollt, V. (2005) Receptor endocytosis counteracts the development of opioid tolerance. *Mol Pharmacol* **67,** 280-7.

111. Haberstock-Debic, H., Kim, K. A., Yu, Y. J. & von Zastrow, M. (2005) Morphine promotes rapid, arrestin-dependent endocytosis of mu-opioid receptors in striatal neurons. *J Neurosci* **25,** 7847-57.

112. Zhao, H., Loh, H. H. & Law, P. Y. (2006) Adenylyl cyclase superactivation induced by long-term treatment with opioid agonist is dependent on receptor localized within lipid rafts and is independent of receptor internalization. *Mol Pharmacol* **69,** 1421-32.

113. Duttaroy, A. & Yoburn, B. C. (1995) The effect of intrinsic efficacy on opioid tolerance. *Anesthesiology* **82,** 1226-36.

114. Paronis, C. A. & Holtzman, S. G. (1992) Development of tolerance to the analgesic activity of mu agonists after continuous infusion of morphine, meperidine or fentanyl in rats. *J Pharmacol Exp Ther* **262,** 1-9.

115. Li, L. Y. & Chang, K. J. (1996) The stimulatory effect of opioids on mitogen-activated protein kinase in Chinese hamster ovary cells transfected to express mu-opioid receptors. *Mol Pharmacol* **50,** 599-602.

116. Ferguson, S. S., Barak, L. S., Zhang, J. & Caron, M. G. (1996) G-protein-coupled receptor regulation: role of G-protein-coupled receptor kinases and arrestins. *Can J Physiol Pharmacol* **74,** 1095-110.

117. Ferguson, S. S., Zhang, J., Barak, L. S. & Caron, M. G. (1996) G-protein-coupled receptor kinases and arrestins: regulators of G-protein-coupled receptor sequestration. *Biochem Soc Trans* **24,** 953-9.

118. Lefkowitz, R. J. (1993) G protein-coupled receptor kinases. *Cell* **74,** 409-12.

119. Bohn, L. M., Gainetdinov, R. R., Lin, F. T., Lefkowitz, R. J. & Caron, M. G. (2000) Mu-opioid receptor desensitization by beta-arrestin-2 determines morphine tolerance but not dependence. *Nature* **408,** 720-3.

120. Kozasa, T. & Gilman, A. G. (1996) Protein kinase C phosphorylates G12 alpha and inhibits its interaction with G beta gamma. *J Biol Chem* **271,** 12562-7.

121. Li, J., Xiang, B., Su, W., Zhang, X., Huang, Y. & Ma, L. (2003) Agonist-induced formation of opioid receptor-G protein-coupled receptor kinase (GRK)-G beta gamma complex on membrane is required for GRK2 function in vivo. *J Biol Chem* **278,** 30219-26.

122. Metaye, T., Gibelin, H., Perdrisot, R. & Kraimps, J. L. (2005) Pathophysiological roles of G-protein-coupled receptor kinases. *Cell Signal* **17,** 917-28.

123. Kovoor, A., Nappey, V., Kieffer, B. L. & Chavkin, C. (1997) Mu and delta opioid receptors are differentially desensitized by the coexpression of beta-adrenergic receptor kinase 2 and beta-arrestin 2 in xenopus oocytes. *J Biol Chem* **272,** 27605-11.

124. Appleyard, S. M., Patterson, T. A., Jin, W. & Chavkin, C. (1997) Agonist-induced phosphorylation of the kappa-opioid receptor. *J Neurochem* **69,** 2405-12.

125. McLaughlin, J. P., Myers, L. C., Zarek, P. E., Caron, M. G., Lefkowitz, R. J., Czyzyk, T. A., Pintar, J. E. & Chavkin, C. (2004) Prolonged kappa opioid receptor phosphorylation mediated by G-protein receptor kinase underlies sustained analgesic tolerance. *J Biol Chem* **279,** 1810-8.

126. Appleyard, S. M., Celver, J., Pineda, V., Kovoor, A., Wayman, G. A. & Chavkin, C. (1999) Agonist-dependent desensitization of the kappa opioid receptor by G protein receptor kinase and beta-arrestin. *J Biol Chem* **274,** 23802-7.

127. Deng, H. B., Yu, Y., Wang, H., Guang, W. & Wang, J. B. (2001) Agonist-induced mu opioid receptor phosphorylation and functional desensitization in rat thalamus. *Brain Res* **898,** 204-14.

128. Chavkin, C., McLaughlin, J. P. & Celver, J. P. (2001) Regulation of opioid receptor function by chronic agonist exposure: constitutive activity and desensitization. *Mol Pharmacol* **60,** 20-5.

129. Johnson, E. E., Christie, M. J. & Connor, M. (2005) The role of opioid receptor phosphorylation and trafficking in adaptations to persistent opioid treatment. *Neurosignals* **14,** 290-302.

130. Schulz, S., Mayer, D., Pfeiffer, M., Stumm, R., Koch, T. & Hollt, V. (2004) Morphine induces terminal micro-opioid receptor desensitization by sustained phosphorylation of serine-375. *Embo J* **23,** 3282-9.

131. Wess, J. (1997) G-protein-coupled receptors: molecular mechanisms involved in receptor activation and selectivity of G-protein recognition. *Faseb J* **11,** 346-54.

132. Cen, B., Xiong, Y., Ma, L. & Pei, G. (2001) Direct and differential interaction of beta-arrestins with the intracellular domains of different opioid receptors. *Mol Pharmacol* **59,** 758-64.

133. DeGraff, J. L., Gurevich, V. V. & Benovic, J. L. (2002) The third intracellular loop of alpha 2-adrenergic receptors determines subtype specificity of arrestin interaction. *J Biol Chem* **277,** 43247-52.

134. Han, M., Gurevich, V. V., Vishnivetskiy, S. A., Sigler, P. B. & Schubert, C. (2001) Crystal structure of beta-arrestin at 1.9 A: possible mechanism of receptor binding and membrane Translocation. *Structure* **9,** 869-80.

135. Lan, H., Liu, Y., Bell, M. I., Gurevich, V. V. & Neve, K. A. (2009) A dopamine D2 receptor mutant capable of G protein-mediated signaling but deficient in arrestin binding. *Mol Pharmacol* **75,** 113-23.

136. Macey, T. A., Liu, Y., Gurevich, V. V. & Neve, K. A. (2005) Dopamine D1 receptor interaction with arrestin3 in neostriatal neurons. *J Neurochem* **93,** 128-34.

137. Lefkowitz, R. J., Pitcher, J., Krueger, K. & Daaka, Y. (1998) Mechanisms of beta-adrenergic receptor desensitization and resensitization. *Adv Pharmacol* **42,** 416-20.

138. Palmer, T. M., Benovic, J. L. & Stiles, G. L. (1996) Molecular basis for subtype-specific desensitization of inhibitory adenosine receptors. Analysis of a chimeric A1-A3 adenosine receptor. *J Biol Chem* **271,** 15272-8.

139. Roth, A., Kreienkamp, H. J., Meyerhof, W. & Richter, D. (1997) Phosphorylation of four amino acid residues in the carboxyl terminus of the rat somatostatin receptor subtype 3 is crucial for its desensitization and internalization. *J Biol Chem* **272,** 23769-74.

140. Hasbi, A., Polastron, J., Allouche, S., Stanasila, L., Massotte, D. & Jauzac, P. (1998) Desensitization of the delta-opioid receptor correlates with its phosphorylation in SK-N-BE cells: involvement of a G protein-coupled receptor kinase. *J Neurochem* **70,** 2129-38.

141. Schulz, R., Wehmeyer, A. & Schulz, K. (2002) Opioid receptor types selectively cointernalize with G protein-coupled receptor kinases 2 and 3. *J Pharmacol Exp Ther* **300,** 376-84.

142. Johnson, E. A., Oldfield, S., Braksator, E., Gonzalez-Cuello, A., Couch, D., Hall, K. J., Mundell, S. J., Bailey, C. P., Kelly, E. & Henderson, G. (2006) Agonist-selective mechanisms of mu-opioid receptor desensitization in human embryonic kidney 293 cells. *Mol Pharmacol* **70,** 676-85.

143. Bohn, L. M., Lefkowitz, R. J. & Caron, M. G. (2002) Differential mechanisms of morphine antinociceptive tolerance revealed in (beta)arrestin-2 knock-out mice. *J Neurosci* **22,** 10494-500.

144. Bohn, L. M., Lefkowitz, R. J., Gainetdinov, R. R., Peppel, K., Caron, M. G. & Lin, F. T. (1999) Enhanced morphine analgesia in mice lacking beta-arrestin 2. *Science* **286,** 2495-8.

145. Terman, G. W., Jin, W., Cheong, Y. P., Lowe, J., Caron, M. G., Lefkowitz, R. J. & Chavkin, C. (2004) G-protein receptor kinase 3 (GRK3) influences opioid analgesic tolerance but not opioid withdrawal. *Br J Pharmacol* **141,** 55-64.

146. Whistler, J. L. & von Zastrow, M. (1998) Morphine-activated opioid receptors elude desensitization by beta-arrestin. *Proc Natl Acad Sci U S A* **95,** 9914-9.

147. Bohn, L. M., Dykstra, L. A., Lefkowitz, R. J., Caron, M. G. & Barak, L. S. (2004) Relative opioid efficacy is determined by the complements of the G protein-coupled receptor desensitization machinery. *Mol Pharmacol* **66,** 106-12.

148. Chu, J., Zheng, H., Loh, H. H. & Law, P. Y. (2008) Morphine-induced mu-opioid receptor rapid desensitization is independent of receptor phosphorylation and beta-arrestins. *Cell Signal* **20,** 1616-24.

149. Mellor, H. & Parker, P. J. (1998) The extended protein kinase C superfamily. *Biochem J* **332 (Pt 2),** 281-92.

150. Newton, A. C. (2001) Protein kinase C: structural and spatial regulation by phosphorylation, cofactors, and macromolecular interactions. *Chem Rev* **101,** 2353-64.

151. Parker, P. J. & Murray-Rust, J. (2004) PKC at a glance. *J Cell Sci* **117,** 131-2.

152. Nishizuka, Y. (1995) Protein kinase C and lipid signaling for sustained cellular responses. *Faseb J* **9,** 484-96.

153. Yoon, S. H., Jin, W., Spencer, R. J., Loh, H. H. & Thayer, S. A. (1998) Desensitization of delta-opioid-induced mobilization of Ca2+ stores in NG108-15 cells. *Brain Res* **802,** 9-18.

154. Song, S. L. & Chueh, S. H. (1999) Phosphorylation promotes the desensitization of the opioid-induced Ca2+ increase in NG108-15 cells. *Brain Res* **818,** 316-25.

155. Bailey, C. P., Kelly, E. & Henderson, G. (2004) Protein kinase C activation enhances morphine-induced rapid desensitization of mu-opioid receptors in mature rat locus ceruleus neurons. *Mol Pharmacol* **66,** 1592-8.

156. Cao, J. L., Ding, H. L., He, J. H., Zhang, L. C., Wang, J. K. & Zeng, Y. M. (2005) [Different roles of the spinal protein kinase C alpha and gamma in morphine dependence and naloxone-precipitated withdrawal.]. *Sheng Li Xue Bao* **57,** 161-8.

157. Sweitzer, S. M., Wong, S. M., Peters, M. C., Mochly-Rosen, D., Yeomans, D. C. & Kendig, J. J. (2004) Protein kinase C epsilon and gamma: involvement in formalin-induced nociception in neonatal rats. *J Pharmacol Exp Ther* **309,** 616-25.

158. Cerezo, M., Laorden, M. L. & Milanes, M. V. (2002) Inhibition of protein kinase C but not protein kinase A attenuates morphine withdrawal excitation of rat hypothalamus-pituitary-adrenal axis. *Eur J Pharmacol* **452,** 57-66.

159. Narita, M., Aoki, T., Ozaki, S., Yajima, Y. & Suzuki, T. (2001) Involvement of protein kinase Cgamma isoform in morphine-induced reinforcing effects. *Neuroscience* **103,** 309-14.

160. Umlauf, E., Csaszar, E., Moertelmaier, M., Schuetz, G. J., Parton, R. G. & Prohaska, R. (2004) Association of stomatin with lipid bodies. *J Biol Chem* **279,** 23699-709.

161. Smith, F. L., Javed, R., Elzey, M. J., Welch, S. P., Selley, D., Sim-Selley, L. & Dewey, W. L. (2002) Prolonged reversal of morphine tolerance with no reversal of dependence by protein kinase C inhibitors. *Brain Res* **958,** 28-35.

162. Newton, P. M., Kim, J. A., McGeehan, A. J., Paredes, J. P., Chu, K., Wallace, M. J., Roberts, A. J., Hodge, C. W. & Messing, R. O. (2007) Increased response to morphine in mice lacking protein kinase C epsilon. *Genes Brain Behav* **6,** 329-38.

163. Mao, J., Price, D. D., Phillips, L. L., Lu, J. & Mayer, D. J. (1995) Increases in protein kinase C gamma immunoreactivity in the spinal cord of rats associated with tolerance to the analgesic effects of morphine. *Brain Res* **677,** 257-67.

164. Kavaliers, M., Ossenkopp, K. P. & Tysdale, D. M. (1991) Evidence for the involvement of protein kinase C in the modulation of morphine-induced 'analgesia' and the inhibitory effects of exposure to 60-Hz magnetic fields in the snail, Cepaea nemoralis. *Brain Res* **554,** 65-71.

165. Smith, F. L., Gabra, B. H., Smith, P. A., Redwood, M. C. & Dewey, W. L. (2007) Determination of the role of conventional, novel and atypical PKC isoforms in the expression of morphine tolerance in mice. *Pain* **127,** 129-39.

166. Lindgren, M., Hallbrink, M., Prochiantz, A. & Langel, U. (2000) Cell-penetrating peptides. *Trends Pharmacol Sci* **21,** 99-103.

167. Fawell, S., Seery, J., Daikh, Y., Moore, C., Chen, L. L., Pepinsky, B. & Barsoum, J. (1994) Tat-mediated delivery of heterologous proteins into cells. *Proc Natl Acad Sci U S A* **91,** 664-8.

168. Cherezov, V., Rosenbaum, D. M., Hanson, M. A., Rasmussen, S. G., Thian, F. S., Kobilka, T. S., Choi, H. J., Kuhn, P., Weis, W. I., Kobilka, B. K. & Stevens, R. C. (2007) High-resolution crystal structure of an engineered human beta2-adrenergic G protein-coupled receptor. *Science* **318,** 1258-65.

169. Palczewski, K., Kumasaka, T., Hori, T., Behnke, C. A., Motoshima, H., Fox, B. A., Le Trong, I., Teller, D. C., Okada, T., Stenkamp, R. E., Yamamoto, M. & Miyano, M. (2000) Crystal structure of rhodopsin: A G protein-coupled receptor. *Science* **289,** 739-45.

170. Prather, P. L., Song, L., Piros, E. T., Law, P. Y. & Hales, T. G. (2000) delta-Opioid receptors are more efficiently coupled to adenylyl cyclase than to L-type Ca(2+) channels in transfected rat pituitary cells. *J Pharmacol Exp Ther* **295,** 552-62.

171. Dang, V. C. & Williams, J. T. (2005) Morphine-Induced mu-opioid receptor desensitization. *Mol Pharmacol* **68,** 1127-32.

172. Zheng, H., Chu, J., Qiu, Y., Loh, H. H. & Law, P. Y. (2008) Agonist-selective signaling is determined by the receptor location within the membrane domains. *Proc Natl Acad Sci U S A* **105,** 9421-6.

173. Wilden, U., Wust, E., Weyand, I. & Kuhn, H. (1986) Rapid affinity purification of retinal arrestin (48 kDa protein) via its light-dependent binding to phosphorylated rhodopsin. *FEBS Lett* **207,** 292-5.

174. Benovic, J. L., Kuhn, H., Weyand, I., Codina, J., Caron, M. G. & Lefkowitz, R. J. (1987) Functional desensitization of the isolated beta-adrenergic receptor by the beta-adrenergic receptor kinase: potential role of an analog of the retinal protein arrestin (48-kDa protein). *Proc Natl Acad Sci U S A* **84,** 8879-82.

175. Lohse, M. J., Benovic, J. L., Codina, J., Caron, M. G. & Lefkowitz, R. J. (1990) beta-Arrestin: a protein that regulates beta-adrenergic receptor function. *Science* **248,** 1547-50.

176. Lefkowitz, R. J. & Whalen, E. J. (2004) beta-arrestins: traffic cops of cell signaling. *Curr Opin Cell Biol* **16,** 162-8.

177. Lefkowitz, R. J. (1998) G protein-coupled receptors. III. New roles for receptor kinases and beta-arrestins in receptor signaling and desensitization. *J Biol Chem* **273,** 18677-80.

178. Aragay, A. M., Ruiz-Gomez, A., Penela, P., Sarnago, S., Elorza, A., Jimenez-Sainz, M. C. & Mayor, F., Jr. (1998) G protein-coupled receptor kinase 2 (GRK2): mechanisms of regulation and physiological functions. *FEBS Lett* **430,** 37-40.

179. Pitcher, J. A., Inglese, J., Higgins, J. B., Arriza, J. L., Casey, P. J., Kim, C., Benovic, J. L., Kwatra, M. M., Caron, M. G. & Lefkowitz, R. J. (1992) Role of beta gamma subunits of G proteins in targeting the beta-adrenergic receptor kinase to membrane-bound receptors. *Science* **257,** 1264-7.

180. Zhai, P., Yamamoto, M., Galeotti, J., Liu, J., Masurekar, M., Thaisz, J., Irie, K., Holle, E., Yu, X., Kupershmidt, S., Roden, D. M., Wagner, T., Yatani, A.,

Vatner, D. E., Vatner, S. F. & Sadoshima, J. (2005) Cardiac-specific overexpression of AT1 receptor mutant lacking G alpha q/G alpha i coupling causes hypertrophy and bradycardia in transgenic mice. *J Clin Invest* **115,** 3045-56.

181. Zuo, Z. (2005) The role of opioid receptor internalization and beta-arrestins in the development of opioid tolerance. *Anesth Analg* **101,** 728-34, table of contents.
182. Ribas, C., Penela, P., Murga, C., Salcedo, A., Garcia-Hoz, C., Jurado-Pueyo, M., Aymerich, I. & Mayor, F., Jr. (2007) The G protein-coupled receptor kinase (GRK) interactome: role of GRKs in GPCR regulation and signaling. *Biochim Biophys Acta* **1768,** 913-22.
183. Bradbury, F. A., Zelnik, J. C. & Traynor, J. R. (2009) G protein independent phosphorylation and internalization of the delta-opioid receptor. *J Neurochem* **109,** 1526-35.
184. Tolkovsky, A. M. & Levitzki, A. (1978) Mode of coupling between the beta-adrenergic receptor and adenylate cyclase in turkey erythrocytes. *Biochemistry* **17,** 3795.
185. Gales, C., Van Durm, J. J., Schaak, S., Pontier, S., Percherancier, Y., Audet, M., Paris, H. & Bouvier, M. (2006) Probing the activation-promoted structural rearrangements in preassembled receptor-G protein complexes. *Nat Struct Mol Biol* **13,** 778-86.
186. Oldham, W. M. & Hamm, H. E. (2008) Heterotrimeric G protein activation by G-protein-coupled receptors. *Nat Rev Mol Cell Biol* **9,** 60-71.
187. Gripentrog, J. M. & Miettinen, H. M. (2005) Activation and nuclear translocation of ERK1/2 by the formyl peptide receptor is regulated by G protein and is not dependent on [beta]-arrestin translocation or receptor endocytosis. *Cellular Signalling* **17,** 1300-1311.
188. Alves, I. D., Salgado, G. F., Salamon, Z., Brown, M. F., Tollin, G. & Hruby, V. J. (2005) Phosphatidylethanolamine enhances rhodopsin photoactivation and transducin binding in a solid supported lipid bilayer as determined using plasmon-waveguide resonance spectroscopy. *Biophys J* **88,** 198-210.

189. Alves, I. D., Salamon, Z., Varga, E., Yamamura, H. I., Tollin, G. & Hruby, V. J. (2003) Direct observation of G-protein binding to the human delta-opioid receptor using plasmon-waveguide resonance spectroscopy. *J Biol Chem* **278,** 48890-7.

190. Zhang, L., Tetrault, J., Wang, W., Loh, H. H. & Law, P. Y. (2006) Short- and long-term regulation of adenylyl cyclase activity by delta-opioid receptor are mediated by Galphai2 in neuroblastoma N2A cells. *Mol Pharmacol* **69,** 1810-9.

191. Chini, B. & Parenti, M. (2004) G-protein coupled receptors in lipid rafts and caveolae: how, when and why do they go there? *J Mol Endocrinol* **32,** 325-38.

192. Foster, L. J., De Hoog, C. L. & Mann, M. (2003) Unbiased quantitative proteomics of lipid rafts reveals high specificity for signaling factors. *Proc Natl Acad Sci U S A* **100,** 5813-8.

193. Nebl, T., Pestonjamasp, K. N., Leszyk, J. D., Crowley, J. L., Oh, S. W. & Luna, E. J. (2002) Proteomic analysis of a detergent-resistant membrane skeleton from neutrophil plasma membranes. *J Biol Chem* **277,** 43399-409.

194. MacLellan, D. L., Steen, H., Adam, R. M., Garlick, M., Zurakowski, D., Gygi, S. P., Freeman, M. R. & Solomon, K. R. (2005) A quantitative proteomic analysis of growth factor-induced compositional changes in lipid rafts of human smooth muscle cells. *Proteomics* **5,** 4733-42.

195. Macdonald, J. L. & Pike, L. J. (2005) A simplified method for the preparation of detergent-free lipid rafts. *J Lipid Res* **46,** 1061-7.

196. Janes, P. W., Ley, S. C. & Magee, A. I. (1999) Aggregation of lipid rafts accompanies signaling via the T cell antigen receptor. *J Cell Biol* **147,** 447-61.

197. Simon, M. I., Strathmann, M. P. & Gautam, N. (1991) Diversity of G proteins in signal transduction. *Science* **252,** 802-8.

198. Gilman, A. G. (1987) G proteins: transducers of receptor-generated signals. *Annu Rev Biochem* **56,** 615-49.

199. Chaipatikul, V., Loh, H. H. & Law, P. Y. (2003) Ligand-selective activation of mu-oid receptor: demonstrated with deletion and single amino acid mutations of third intracellular loop domain. *J Pharmacol Exp Ther* **305,** 909-18.

200. Herrlich, A., Daub, H., Knebel, A., Herrlich, P., Ullrich, A., Schultz, G. & Gudermann, T. (1998) Ligand-independent activation of platelet-derived growth factor receptor is a necessary intermediate in lysophosphatidic, acid-stimulated mitogenic activity in L cells. *Proc Natl Acad Sci U S A* **95,** 8985-90.

201. Wess, J. (1998) Molecular basis of receptor/G-protein-coupling selectivity. *Pharmacol Ther* **80,** 231-64.

202. Gurevich, V. V. & Gurevich, E. V. (2006) The structural basis of arrestin-mediated regulation of G-protein-coupled receptors. *Pharmacol Ther* **110,** 465-502.

203. Pierce, K. L. & Lefkowitz, R. J. (2001) Classical and new roles of beta-arrestins in the regulation of G-protein-coupled receptors. *Nat Rev Neurosci* **2,** 727-33.

204. Claing, A., Laporte, S. A., Caron, M. G. & Lefkowitz, R. J. (2002) Endocytosis of G protein-coupled receptors: roles of G protein-coupled receptor kinases and beta-arrestin proteins. *Prog Neurobiol* **66,** 61-79.

205. Daaka, Y., Luttrell, L. M. & Lefkowitz, R. J. (1997) Switching of the coupling of the beta2-adrenergic receptor to different G proteins by protein kinase A. *Nature* **390,** 88-91.

206. Okamoto, T., Murayama, Y., Hayashi, Y., Inagaki, M., Ogata, E. & Nishimoto, I. (1991) Identification of a Gs activator region of the beta 2-adrenergic receptor that is autoregulated via protein kinase A-dependent phosphorylation. *Cell* **67,** 723-30.

207. Digby, G. J., Lober, R. M., Sethi, P. R. & Lambert, N. A. (2006) Some G protein heterotrimers physically dissociate in living cells. *Proc Natl Acad Sci U S A* **103,** 17789-94.

208. El Kouhen, R., Burd, A. L., Erickson-Herbrandson, L. J., Chang, C. Y., Law, P. Y. & Loh, H. H. (2001) Phosphorylation of Ser363, Thr370, and Ser375 residues within the carboxyl tail differentially regulates mu-opioid receptor internalization. *J Biol Chem* **276,** 12774-80.

209. Gombos, I., Kiss, E., Detre, C., Laszlo, G. & Matko, J. (2006) Cholesterol and sphingolipids as lipid organizers of the immune cells' plasma membrane: their

impact on the functions of MHC molecules, effector T-lymphocytes and T-cell death. *Immunol Lett* **104,** 59-69.

210. DeBose-Boyd, R. A. (2008) Feedback regulation of cholesterol synthesis: sterol-accelerated ubiquitination and degradation of HMG CoA reductase. *Cell Res* **18,** 609-21.
211. Cohen, D. E. (2008) Balancing Cholesterol Synthesis and Absorption in the Gastrointestinal Tract. *J Clin Lipidol* **2,** S1-S3.
212. Rodal, S. K., Skretting, G., Garred, O., Vilhardt, F., van Deurs, B. & Sandvig, K. (1999) Extraction of cholesterol with methyl-beta-cyclodextrin perturbs formation of clathrin-coated endocytic vesicles. *Mol Biol Cell* **10,** 961-74.
213. Quan, G., Xie, C., Dietschy, J. M. & Turley, S. D. (2003) Ontogenesis and regulation of cholesterol metabolism in the central nervous system of the mouse. *Brain Res Dev Brain Res* **146,** 87-98.
214. Nicholas, H. J. (1961) Cholesterol. The metabolism of cholesterol in the central nervous system. *J Kans Med Soc* **62,** 358-61.
215. Dietschy, J. M. & Turley, S. D. (2004) Thematic review series: brain Lipids. Cholesterol metabolism in the central nervous system during early development and in the mature animal. *J Lipid Res* **45,** 1375-97.
216. Dietschy, J. M. & Turley, S. D. (2002) Control of cholesterol turnover in the mouse. *J Biol Chem* **277,** 3801-4.
217. Roth, B. L., Willins, D. L. & Kroeze, W. K. (1998) G protein-coupled receptor (GPCR) trafficking in the central nervous system: relevance for drugs of abuse. *Drug Alcohol Depend* **51,** 73-85.
218. Duane, W. C., Hunninghake, D. B., Freeman, M. L., Pooler, P. A., Schlasner, L. A. & Gebhard, R. L. (1988) Simvastatin, a competitive inhibitor of HMG-CoA reductase, lowers cholesterol saturation index of gallbladder bile. *Hepatology* **8,** 1147-50.
219. Lullman-Rauch, R. (1976) Letter: Cholesterol biosynthesis inhibitor AY9944. *Lab Invest* **34,** 537.

220. Chini, B. & Parenti, M. (2009) G-protein coupled receptors, cholesterol and palmitoylation: facts about fats. *J Mol Endocrinol*.

221. Probst, W. C., Snyder, L. A., Schuster, D. I., Brosius, J. & Sealfon, S. C. (1992) Sequence alignment of the G-protein coupled receptor superfamily. *DNA Cell Biol* **11,** 1-20.

222. Chen, C., Shahabi, V., Xu, W. & Liu-Chen, L. Y. (1998) Palmitoylation of the rat mu opioid receptor. *FEBS Lett* **441,** 148-52.

223. Hawtin, S. R., Tobin, A. B., Patel, S. & Wheatley, M. (2001) Palmitoylation of the vasopressin V1a receptor reveals different conformational requirements for signaling, agonist-induced receptor phosphorylation, and sequestration. *J Biol Chem* **276,** 38139-46.

224. Escriba, P. V., Wedegaertner, P. B., Goni, F. M. & Vogler, O. (2007) Lipid-protein interactions in GPCR-associated signaling. *Biochim Biophys Acta* **1768,** 836-52.

225. Wei, H., Ahn, S., Shenoy, S. K., Karnik, S. S., Hunyady, L., Luttrell, L. M. & Lefkowitz, R. J. (2003) Independent beta-arrestin 2 and G protein-mediated pathways for angiotensin II activation of extracellular signal-regulated kinases 1 and 2. *Proc Natl Acad Sci U S A* **100,** 10782-7.

226. Jin, H., Xie, Z., George, S. R. & O'Dowd, B. F. (1999) Palmitoylation occurs at cysteine 347 and cysteine 351 of the dopamine D(1) receptor. *Eur J Pharmacol* **386,** 305-12.

227. Hayashi, M. K. & Haga, T. (1997) Palmitoylation of muscarinic acetylcholine receptor m2 subtypes: reduction in their ability to activate G proteins by mutation of a putative palmitoylation site, cysteine 457, in the carboxyl-terminal tail. *Arch Biochem Biophys* **340,** 376-82.

228. Kennedy, M. E. & Limbird, L. E. (1993) Mutations of the alpha 2A-adrenergic receptor that eliminate detectable palmitoylation do not perturb receptor-G-protein coupling. *J Biol Chem* **268,** 8003-11.

229. O'Dowd, B. F., Hnatowich, M., Caron, M. G., Lefkowitz, R. J. & Bouvier, M. (1989) Palmitoylation of the human beta 2-adrenergic receptor. Mutation of

Cys341 in the carboxyl tail leads to an uncoupled nonpalmitoylated form of the receptor. *J Biol Chem* **264,** 7564-9.

230. Drisdel, R. C., Alexander, J. K., Sayeed, A. & Green, W. N. (2006) Assays of protein palmitoylation. *Methods* **40,** 127-34.
231. Ahn, S., Shenoy, S. K., Wei, H. & Lefkowitz, R. J. (2004) Differential kinetic and spatial patterns of beta-arrestin and G protein-mediated ERK activation by the angiotensin II receptor. *J Biol Chem* **279,** 35518-25.
232. Whitmarsh, A. J. & Davis, R. J. (1999) Signal transduction by MAP kinases: regulation by phosphorylation-dependent switches. *Sci STKE* **1999,** PE1.
233. Przewlocki, R. (2004) Opioid abuse and brain gene expression. *Eur J Pharmacol* **500,** 331-49.
234. Ammon, S., Mayer, P., Riechert, U., Tischmeyer, H. & Hollt, V. (2003) Microarray analysis of genes expressed in the frontal cortex of rats chronically treated with morphine and after naloxone precipitated withdrawal. *Brain Res Mol Brain Res* **112,** 113-25.
235. Janknecht, R., Zinck, R., Ernst, W. H. & Nordheim, A. (1994) Functional dissection of the transcription factor Elk-1. *Oncogene* **9,** 1273-8.
236. Aplin, A. E., Stewart, S. A., Assoian, R. K. & Juliano, R. L. (2001) Integrin-mediated adhesion regulates ERK nuclear translocation and phosphorylation of Elk-1. *J Cell Biol* **153,** 273-82.
237. Gille, H., Kortenjann, M., Thomae, O., Moomaw, C., Slaughter, C., Cobb, M. H. & Shaw, P. E. (1995) ERK phosphorylation potentiates Elk-1-mediated ternary complex formation and transactivation. *Embo J* **14,** 951-62.
238. Shoda, T., Fukuda, K., Uga, H., Mima, H. & Morikawa, H. (2001) Activation of mu-opioid receptor induces expression of c-fos and junB via mitogen-activated protein kinase cascade. *Anesthesiology* **95,** 983-9.
239. Dudley, D. T., Pang, L., Decker, S. J., Bridges, A. J. & Saltiel, A. R. (1995) A synthetic inhibitor of the mitogen-activated protein kinase cascade. *Proc Natl Acad Sci U S A* **92,** 7686-9.

240. Frodin, M. & Gammeltoft, S. (1999) Role and regulation of 90 kDa ribosomal S6 kinase (RSK) in signal transduction. *Mol Cell Endocrinol* **151,** 65-77.

241. Sheffler, D. J., Kroeze, W. K., Garcia, B. G., Deutch, A. Y., Hufeisen, S. J., Leahy, P., Bruning, J. C. & Roth, B. L. (2006) p90 ribosomal S6 kinase 2 exerts a tonic brake on G protein-coupled receptor signaling. *Proc Natl Acad Sci U S A* **103,** 4717-22.

242. Bartel, D. P. (2004) MicroRNAs: genomics, biogenesis, mechanism, and function. *Cell* **116,** 281-97.

243. Tsuchiya, S., Okuno, Y. & Tsujimoto, G. (2006) MicroRNA: biogenetic and functional mechanisms and involvements in cell differentiation and cancer. *J Pharmacol Sci* **101,** 267-70.

244. Valencia-Sanchez, M. A., Liu, J., Hannon, G. J. & Parker, R. (2006) Control of translation and mRNA degradation by miRNAs and siRNAs. *Genes Dev* **20,** 515-24.

245. Kosik, K. S. (2006) The neuronal microRNA system. *Nat Rev Neurosci* **7,** 911-20.

246. Schratt, G. M., Tuebing, F., Nigh, E. A., Kane, C. G., Sabatini, M. E., Kiebler, M. & Greenberg, M. E. (2006) A brain-specific microRNA regulates dendritic spine development. *Nature* **439,** 283-9.

247. Arvidsson, U., Riedl, M., Chakrabarti, S., Lee, J. H., Nakano, A. H., Dado, R. J., Loh, H. H., Law, P. Y., Wessendorf, M. W. & Elde, R. (1995) Distribution and targeting of a mu-opioid receptor (MOR1) in brain and spinal cord. *J Neurosci* **15,** 3328-41.

248. Kalscheuer, S., Zhang, X., Zeng, Y. & Upadhyaya, P. (2008) Differential expression of microRNAs in early-stage neoplastic transformation in the lungs of F344 rats chronically treated with the tobacco carcinogen 4-(methylnitrosamino)-1-(3-pyridyl)-1-butanone. *Carcinogenesis* **29,** 2394-9.

249. Favata, M. F., Horiuchi, K. Y., Manos, E. J., Daulerio, A. J., Stradley, D. A., Feeser, W. S., Van Dyk, D. E., Pitts, W. J., Earl, R. A., Hobbs, F., Copeland, R. A., Magolda, R. L., Scherle, P. A. & Trzaskos, J. M. (1998) Identification of a

novel inhibitor of mitogen-activated protein kinase kinase. *J Biol Chem* **273,** 18623-32.

250. Jin, W., Lo, T. M., Loh, H. H. & Thayer, S. A. (1994) U73122 inhibits phospholipase C-dependent calcium mobilization in neuronal cells. *Brain Res* **642,** 237-43.

251. Muid, R. E., Dale, M. M., Davis, P. D., Elliott, L. H., Hill, C. H., Kumar, H., Lawton, G., Twomey, B. M., Wadsworth, J., Wilkinson, S. E. & et al. (1991) A novel conformationally restricted protein kinase C inhibitor, Ro 31-8425, inhibits human neutrophil superoxide generation by soluble, particulate and post-receptor stimuli. *FEBS Lett* **293,** 169-72.

252. Nam, J. S., Ino, Y., Sakamoto, M. & Hirohashi, S. (2002) Src family kinase inhibitor PP2 restores the E-cadherin/catenin cell adhesion system in human cancer cells and reduces cancer metastasis. *Clin Cancer Res* **8,** 2430-6.

253. Cullen, B. R. (2004) Transcription and processing of human microRNA precursors. *Mol Cell* **16,** 861-5.

254. Zeng, Y. (2006) Principles of micro-RNA production and maturation. *Oncogene* **25,** 6156-62.

255. Rodriguez, A., Griffiths-Jones, S., Ashurst, J. L. & Bradley, A. (2004) Identification of mammalian microRNA host genes and transcription units. *Genome Res* **14,** 1902-10.

256. Griffiths-Jones, S., Saini, H. K., van Dongen, S. & Enright, A. J. (2008) miRBase: tools for microRNA genomics. *Nucleic Acids Res* **36,** D154-8.

257. Monkley, S. J., Pritchard, C. A. & Critchley, D. R. (2001) Analysis of the mammalian talin2 gene TLN2. *Biochem Biophys Res Commun* **286,** 880-5.

258. Donohoe, M. E., Zhang, X., McGinnis, L., Biggers, J., Li, E. & Shi, Y. (1999) Targeted disruption of mouse Yin Yang 1 transcription factor results in peri-implantation lethality. *Mol Cell Biol* **19,** 7237-44.

259. He, Y. & Casaccia-Bonnefil, P. (2008) The Yin and Yang of YY1 in the nervous system. *J Neurochem* **106,** 1493-502.

260. Becker, K. G., Jedlicka, P., Templeton, N. S., Liotta, L. & Ozato, K. (1994) Characterization of hUCRBP (YY1, NF-E1, delta): a transcription factor that binds the regulatory regions of many viral and cellular genes. *Gene* **150,** 259-66.

261. Nam, S., Kim, B., Shin, S. & Lee, S. (2008) miRGator: an integrated system for functional annotation of microRNAs. *Nucleic Acids Res* **36,** D159-64.

262. Gaudilliere, B., Konishi, Y., de la Iglesia, N., Yao, G. & Bonni, A. (2004) A CaMKII-NeuroD signaling pathway specifies dendritic morphogenesis. *Neuron* **41,** 229-41.

263. Seo, S., Lim, J. W., Yellajoshyula, D., Chang, L. W. & Kroll, K. L. (2007) Neurogenin and NeuroD direct transcriptional targets and their regulatory enhancers. *Embo J* **26,** 5093-108.

264. Lou, L., Zhou, T., Wang, P. & Pei, G. (1999) Modulation of Ca2+/calmodulin-dependent protein kinase II activity by acute and chronic morphine administration in rat hippocampus: differential regulation of alpha and beta isoforms. *Mol Pharmacol* **55,** 557-63.

265. Colbran, R. J. & Brown, A. M. (2004) Calcium/calmodulin-dependent protein kinase II and synaptic plasticity. *Curr Opin Neurobiol* **14,** 318-27.

266. Liao, D., Grigoriants, O. O., Loh, H. H. & Law, P. Y. (2007) Agonist-dependent postsynaptic effects of opioids on miniature excitatory postsynaptic currents in cultured hippocampal neurons. *J Neurophysiol* **97,** 1485-94.

267. Liao, D., Lin, H., Law, P. Y. & Loh, H. H. (2005) Mu-opioid receptors modulate the stability of dendritic spines. *Proc Natl Acad Sci U S A* **102,** 1725-30.

268. Whistler, J. L., Chuang, H. H., Chu, P., Jan, L. Y. & von Zastrow, M. (1999) Functional dissociation of mu opioid receptor signaling and endocytosis: implications for the biology of opiate tolerance and addiction. *Neuron* **23,** 737-46.

269. Koch, T., Schulz, S., Schroder, H., Wolf, R., Raulf, E. & Hollt, V. (1998) Carboxyl-terminal splicing of the rat mu opioid receptor modulates agonist-mediated internalization and receptor resensitization. *J Biol Chem* **273,** 13652-7.

270. Hong, O., Young, G. & Khazan, N. (1986) Differential cross-tolerance among morphine, methadone, and ethylketocyclazocine--EEG and behavior. *NIDA Res Monogr* **67,** 170-6.

271. Neil, A. (1982) Morphine- and methadone-tolerant mice differ in cross-tolerance to other opiates. Heterogeneity in opioid mechanisms indicated. *Naunyn Schmiedebergs Arch Pharmacol* **320,** 50-3.

272. Narita, M., Suzuki, M., Narita, M., Niikura, K., Nakamura, A., Miyatake, M., Yajima, Y. & Suzuki, T. (2006) mu-Opioid receptor internalization-dependent and -independent mechanisms of the development of tolerance to mu-opioid receptor agonists: Comparison between etorphine and morphine. *Neuroscience* **138,** 609-19.

8. Copyright Information

8.1 Molecular Pharmacology

9650 Rockville Pike
Bethesda, MD 20814-3995

Phone: (301) 634-7060
Fax: (301) 634-7061

info@aspet.org
www.aspet.org

November 24, 2009

Hui Zheng
Dept. of Pharmacology
University of Minnesota
6-120 Jackson Hall
321 Church St., SE
Minneapolis, MN 55455

Email: zhen0091@umn.edu

Dear Mr. Zheng:

This is to grant you permission to republish the following figures in your Ph.D. dissertation entitled, "Agonist-selective signaling and MOR":

> Figures 1, 2B, 3A-B, 4A-B, 5B,6 and 9A from Hui Zheng, Horace H. Loh. and Ping-Yee Law, β-Arrestin-Dependent μ-Opioid Receptor-Activated Extracellular Signal-Regulated Kinases (ERKs) Translocate to Nucleus in Contrast to G Protein-Dependent ERK Activation. *Mol Pharmacol* January 2008 73:178-190
>
> Figures 2-3, 5-6 and table 1 from Hui Zheng, Yan Zeng, Xiaoxiao Zhang, Ji Chu, Horace H. Loh, and Ping-Yee Law, μ-Opioid Receptor Agonists Differentially Regulate the Expression of miR-190 and NeuroD *Mol Pharmacol* mol.109.060848

Permission to reproduce the figure is granted for worldwide use in all languages, translations, and editions, and in any format or medium including print and electronic. The authors and the source of the materials must be cited in full, including the article title, journal title, volume, year, and page numbers.

Sincerely yours,

Richard Dodenhoff
Journals Director

8.2 PNAS

As a PNAS author, you and your employing institution or company retain extensive rights for use of your materials and intellectual property. You retain these rights and permissions without having to obtain explicit permission from PNAS, provided that you cite the original source:

1. The right to post a PDF of your article on your web site or that of your employer's institution (provided that the institution is nonprofit).
2. The right to make electronic or hard copies of articles for your personal use, including classroom use, or for the personal use of colleagues, provided those copies are not for sale and are not distributed in a systematic way outside of your employing institution.
3. The right to post and update a preprint version of your article on a public electronic server such as the Web. See the information on electronic preprints below.
4. The right to permit others to use your original figures or tables published in PNAS for noncommercial and educational use (i.e., in a review article, in a book that is not for sale), provided that the original source is cited. Third parties need not ask PNAS for permission to use figures and tables for such use.
5. The right, after publication in PNAS, to use all or part of your article in a printed compilation of your own works, such as collected writings or lecture notes.
6. If your article is a "work for hire" made within the scope of your employment, your employer may use all or part of the information in your article for intracompany use.
7. **The right to include your article in your thesis or dissertation.**
8. The right to present all or part of your paper at a meeting or conference, including ones that are webcast, and to give copies of your paper to meeting attendees before or after publication in PNAS. For interactions with the media prior to publication, see the PNAS Policy on Media Coverage.
9. The right to publish a new or extended version of your paper provided that it is sufficiently different to be considered a new work.
10. The right to expand your article into book-length form for publication.

11. The right to reuse your original figures and tables in your future works.

12. Patent and trademark rights or rights to any process or procedure described in your article.

Please refer to: http://www.pnas.org/content/101/34/12399.full

http://www.pnas.org/site/misc/authorfaq.shtml